Analytical Calculation of Velocity-Dependent Relative Permeability from Well Test Data in Gas-Condensate Reservoirs, and its Applications

by

Ibrahim Mohammed Alabdulwahab

Submitted for the degree of Doctor of Philosophy

Heriot-Watt University

School of Energy, Geoscience, Infrastructure and Society,

Institute of Petroleum Engineering

February 2019

Abstract

Well testing analysis is a valuable tool that has evolved to become a tool that can be used to estimate formation permeability, skin, wellbore storage and reservoir pressure. The aim of the study presented in this thesis is to propose a set of techniques that utilise well test pressure buildup data to better characterise and manage gas-condensate (GC) reservoirs. The thesis starts by investigating the ability to calculate the pressure versus radius profile from the pressure versus time well test data under various condensate richness conditions using the probe radius concept proposed previously for single-phase oil conditions. First, the technique is validated in single-phase oil and single-phase gas systems before applying it to a more complex two-phase GC system. The results show how the pressure profile can be used to estimate the radial extent of the condensate bank. Then, the study proposes a method to analytically calculate the relative permeabilities (k_r) affected by pressure and velocity due to coupling and inertia in single-rate and multi-rate tests using Darcy's law and the aforementioned pressure profile. The results highlight the importance of velocity effects in the calculated k_r data and show that ignoring such effects could drastically distort the estimation of reservoir parameters. The validity of these calculations is verified by comparing the results with the output from a numerical simulator based on a single-layer single-well radial reservoir model. Moreover, the importance of data treatment, such as smoothing, in order to obtain a reasonable and usable results is discussed. The study then explores other applications of the analytically obtained velocity-dependent k_r data, more specifically for production data analysis based on the type-curve technique. In addition, the thesis suggests a new method to estimate the formation permeability of GC reservoirs by combining both methods, the k_r calculation from well test data with the two-phase analysis of the production data, through an iterative process. The iterative method produced excellent permeability estimation within 5% margin of error. This can be beneficial in the case where reservoir permeability is unknown.

Dedication

To the two pillars I stand on,

my beloved wife, Noha, for her unconditional love and support.

my daughter, Yasmeen, for her curiosity that inspires me.

To my parents,

Mohammed and Nawal for their love and support.

To my brother and sisters,

Othman, Norah, Hend, Nouf, Lena and Lama, for their love and support.

Acknowledgments

All praise to God.

I would like to express my sincere gratitude and appreciation to all those who supported me during my study.

My deepest gratitude and thanks to my supervisor, Prof. Mahmoud Jamiolahmady for his continues support, expertise, advice and his invaluable input throughout the years.

I would also like to thank Tim Whittle, Prof. Dugald Duncan, and Dr. Heiko Gimperlein for their support and valuable feedback.

Special thanks to my office colleagues and friends: Abdulelah Nasief, Badr Jan, Caroline Johnson, Hamid Reza Nasriani, Hosien Doryanidaryuni, Ifeanyi Seteyeobot, Mojtaba Moradi and Yasser Aldulaij for their friendship, support and coffee breaks.

I would also like to thank Saudi Aramco for their financial sponsorship to pursue my PhD degree. Special thanks to the Reservoir Description and Simulation (RDSD) Management, in particular my managers, Khaled Alsubaie and Khaled Zainalabedin, and my supervisors and mentors, Faisal Al-Thawad, Saud Bin Akresh, Abdulhakim Al-Nahdi and Anisur Rahman for their trust and continues support throughout my career and studies.

I would also like to thank my examiners for dedicating the time to evaluate my work. My appreciation is also extended to Heriot-Watt University, the EGIS computer support group, and IPE staff.

ACADEMIC REGISTRY
Research Thesis Submission

Name*:*	Ibrahim Mohammed I. Alabdulwahab		
School:	EGIS - IPE		
Version: *(i.e. First, Resubmission, Final)*	Final	Degree Sought:	PhD

Declaration

In accordance with the appropriate regulations I hereby submit my thesis and I declare that:

1) the thesis embodies the results of my own work and has been composed by myself
2) where appropriate, I have made acknowledgement of the work of others and have made reference to work carried out in collaboration with other persons
3) the thesis is the correct version of the thesis for submission and is the same version as any electronic versions submitted*.
4) my thesis for the award referred to, deposited in the Heriot-Watt University Library, should be made available for loan or photocopying and be available via the Institutional Repository, subject to such conditions as the Librarian may require
5) I understand that as a student of the University I am required to abide by the Regulations of the University and to conform to its discipline.
6) I confirm that the thesis has been verified against plagiarism via an approved plagiarism detection application e.g. Turnitin.

* *Please note that it is the responsibility of the candidate to ensure that the correct version of the thesis is submitted.*

Signature of Candidate*:*	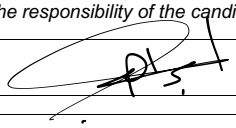	Date:	05/03/2018

Submission

Submitted By *(name in capitals):*	IBRAHIM MOHAMMED I. ALABDULWAHAB
Signature of Individual Submitting:	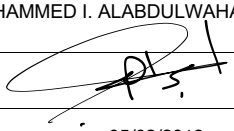
Date Submitted:	05/03/2018

For Completion in the Student Service Centre (SSC)

Received in the SSC by *(name in capitals):*			
Method of Submission *(Handed in to SSC; posted through internal/external mail):*			
*E-thesis Submitted (**mandatory for final theses**)*			
Signature:		Date:	

Please note this form should be bound into the submitted thesis.
Academic Registry/Version (1) August 2016

Table of Contents

List of Tables

List of Figures

Nomenclature

α_1 = unit conversion to oilfield units, 0.007082

A = Area, ft^2

B_g = Gas formation volume factor, lb/Mscf

B_o = Oil formation volume factor, lb/STB

c_t = total compressibility, 1/psi

c_g = gas compressibility, 1/psi

c_{tp} = two-phase compressibility, 1/psi

c_f = formation compressibility, 1/psi

h = reservoir thickness, ft

k = permeability, mD

k_{eff} = effective permeability, fraction

k_r = relative permeability, fraction

k_{rg} = gas relative permeability, fraction

k_{ro} = oil relative permeability, fraction

m_T = total mass rate, lb/D

N_c = capillary number

N_{cn} = ratio of capillary number

P_c = capillary pressure, psia

p = pressure, psia

p_e = entry capillary pressure, psia

$p_p(p)$ = pseudo-pressure, psi^2/cp

$p_p(p')$ = pseudo-pressure derivative, psi^2/cp

q_g = gas flow rate, Mscf/D

q_o = oil flow rate, STB/D

r = radius, ft

r_m = probe radius, ft

S = saturation, fraction

t = time, hours

t_p = producing time at constant rate, hours

T = reservoir temperature, °R

v_g = gas velocity, ft/sec

x = liquid mass fraction, fraction

z = gas compressibility factor, fraction

α_1 = unit conversion factor for oilfield unit system, 0.007082

λ = mobility, mD/cp

λ_g = gas mobility, mD/cp

μ = viscosity, cp

μ_g = gas viscosity, cp

μ_o = oil viscosity, cp

μ_{tp} = equivalent-two-phase viscosity, cp

ρ = density, lb/ft^3

ρ_g = gas density, lb/ft^3

ρ_o = oil density, lb/ft^3

ϕ = porosity, fraction

σ_{gc} = gas/condensate interfacial tension, dyne/cm

λ = pore size distribution index

Δp = pressure differential, psia

Δt_e = equivalent shut-in time, hours

List of Publications

The research material in this thesis was part of the research program of a joint industry project (JIP) referred to as "Unconventional Gas & Gas-Condensate Recovery Studies". The results of this research have been reported, presented and discussed every six months in the corresponding steering committee meetings during November 2014 to November 2016.

Furthermore, parts of the results of this study have been submitted as technical papers and presentations in the following conferences:

Paper: Alabdulwahab et al. Calculation of Relative Permeability using Well Test Data in Gas-Condensate Reservoirs at SPE Europec featured at 80th EAGE Conference & Exhibition. SPE-190878-MS.

Poster & Presentation: Obtaining Relative Permeability Data Analytically from Well Test Data, and its Potential Benefits at DEVEX 2018 Aberdeen.

In addition, the following paper titled "Application of Relative Permeability Calculated Analytically from Well Test Data in Production Analysis" is being prepared to be submitted for an SPE peer-reviewed journal.

Chapter 1

Introduction

1.1 Purpose of this Chapter

The purpose of this chapter is to communicate concisely the objectives of this study and describe the layout and the content of each chapter. In addition, a brief highlight will be given on why gas-condensate reservoirs are important and hence need improved tools to better understand and manage their fluid-flow interaction and flow behaviour, followed by a brief overview on available methods to obtain relative permeabilities.

1.2 Why Gas-Condensate Reservoirs are Valuable

Demand for energy is continually increasing (**Figure 1.1**), the International Energy Agency reports that global energy demand grew by 2.1% in 2017, more than twice the growth rate in 2016, even though the price for oil was increasing. Fossil fuels met over 70% of the growth in energy demand, and natural gas demand increased the most, reaching a record share of 22% in total energy demands (International Energy Agency 2018).

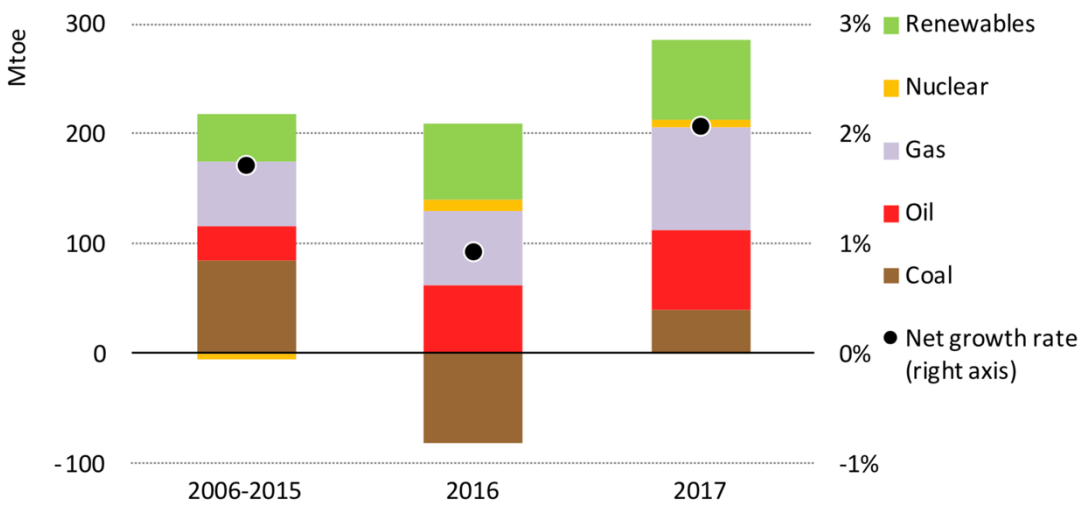

Figure 1.1—Average annual growth in energy demand by fuel. © OECD/IEA 2018

Discoveries of new conventional oil fields are becoming scarce and have been reduced massively due to recent oil price volatility. The International Energy Agency (2017) reports that oil fields discoveries have fallen to 2.4 billion barrels, a record low in 2016, compared to an average of 9 billion barrels per year over the past 15 years (**Figure 1.2**). Stable gas production and less volatile prices coupled with high demand make natural gas production an attractive prospect.

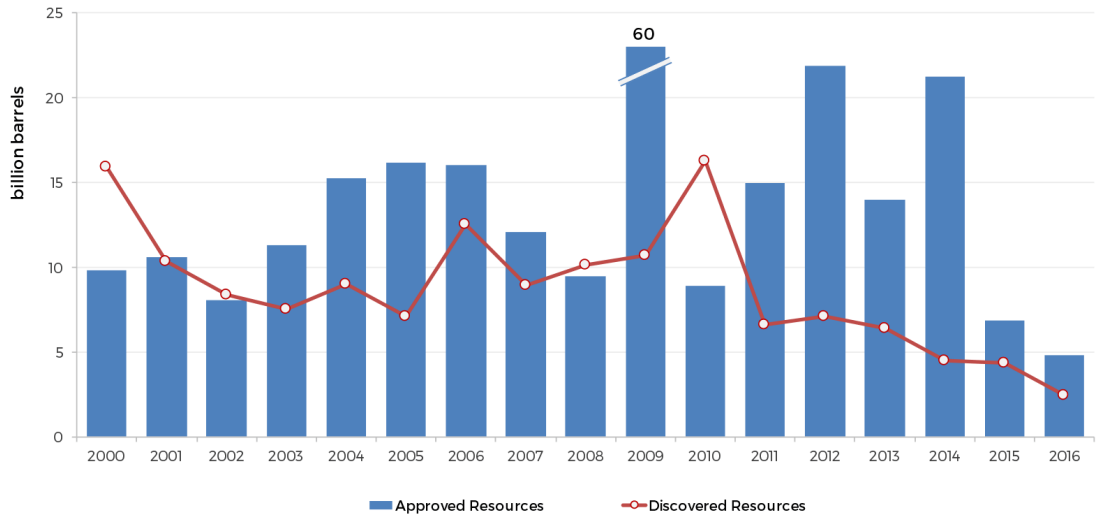

Figure 1.2—Conventional crude oil resources discovered. © IEA

Gas-condensate reservoirs are gas fields with high condensate gas ratio (CGR). Condensate is a very light oil when examined using the crude oil API gravity scale (light oils have an API gravity of 31.1^{o} or above), thus making it extremely valuable. It does not require as much refining as crude oil, which makes it an attractive hydrocarbon. However, such reservoirs are complex in terms of their behaviour as two-phase flow can develop around the wellbore (more details can be found in Chapter 2), but they can be attractive to develop and produce especially if the complexities are dealt with and adequately analysed and evaluated.

1.3 Available Models for the Calculation of Relative Permeability

Relative permeability data are of significant importance when it comes to two-phase flow. Two-phase analysis techniques for gas-condensate reservoirs require the calculation of pseudo-variables, which require relative permeability data to be available and to be a function of pressure.

Several methods are available to obtain relative permeabilities for gas-condensate system, such as direct measurements from core-flooding experiments–which are expensive and complex to conduct. On the other hand, several mathematical models have been developed to approximate relative permeabilities due to the difficulty of conducting experimental measurements (Li and Horne 2006). Many works have proposed mathematical models for the calculation of relative permeabilities from capillary pressure data (Purcell, 1949; Burdine, 1953; Corey, 1954; Corey and Brooks, 1966)—more on this in section 2.2.2.

Li and Horne (2006) have shown a comparison between relative permeabilities obtained experimentally and those calculated using the correlation models of Purcell (1949), Corey (1954) and Corey and Brooks (1966). Their results indicate that the Purcell model is the best fit to the experimental data of the

wetting-phase relative permeability, but not a good fit for the nonwetting-phase. In addition, they found that using Corey's model gave very similar results to Corey and Brooks model, but both cases were different from the measured data.

Using of such models can approximate relative permeability as a function of saturation. They require capillary pressure values to be available, but most importantly, the calculated data would lack any additional relative permeability effects observed in gas-condensate reservoirs due to low interfacial tension and high velocity (as will be discussed in sections 2.2.4 and 3.5). Furthermore, relative permeabilities as a function of saturation would need to be correlated to pressure using steady-state assumption (as will be discussed in section 2.2.5), in order to compute two-phase pseudo-variables, that are needed for the two-phase analysis techniques.

In this thesis, one of the main goals is to fill this gap by analytically calculating relative permeabilities data from well test data.

1.4 Aim of the Research

The study in this thesis aims to provide a sound theoretical framework using a handful of techniques for better gas-condensate characterisation and analysis—more specifically in the areas of well test and production data analysis. It takes into consideration the near wellbore rate effects unique to gas-condensate reservoirs. These are the dependency of gas-condensate relative permeability on velocity and pressure, which are explained in more detail in sections 2.2.4 and 3.5.

In order to achieve the above objective, an investigation was first carried out on the capabilities of calculating pressure versus radius profile from well test transient pressure versus time data in gas-condensate reservoirs. The well test transient pressure data were generated using numerical simulation, which allowed the investigation of the individual or combined impact of relevant

parameters to verify the reliability of the approach. The main technique considered is based on the probe radius concept first developed for single-phase systems. Initially, it was established that the probe radius concept could determine the flowing reservoir pressure within the reservoir at the end of the drawdown period before the shut-in using the buildup data, for single-phase oil and single-phase gas systems. Once the results were verified, the concept was extended to two-phase gas-condensate systems, where both oil and gas coexisted and were flowing. The pressure versus radius profile can then be utilised to determine condensate bank extent, and more importantly, to analytically calculate relative permeability data. That is, one of the main milestones in this thesis was to evaluate the application of using the pressure versus distance derivative to determine dynamic (inclusive of velocity effects) relative permeability data in the vicinity of the well within the reservoir.

Having velocity-dependent relative permeability data will help in both improving well test and production data analysis employing the two-phase pseudo-pressure approach as well as using such valuable data for other reservoir description and management purposes. The reliability of the proposed technique was also examined for multi-rate testing which has shorter test times and variable flow rates compared to single-rate testing. The other important application examined in the thesis is the use of analytically calculated relative permeability for improved production analysis using an equivalent-phase approach where two-phase pseudo-variables were used. Furthermore, a method to estimate formation permeability, when absolute permeability is unknown, using both well test and production data via an iterative procedure is proposed.

In these exercises, the emphasis is on the effects of coupling and inertia and how to account for them, which will improve the design and interpretation of reservoir data in gas-condensate reservoirs.

1.5 Thesis Layout

The thesis starts with an introduction to well testing and gas-condensate reservoirs followed by details of reservoir, rock and fluid models used in the study. Then the method of calculating pressure versus radius profile from well test data is described followed by the application of calculating velocity-dependent relative permeability data analytically from the gradient of the obtained pressure versus radius profile. Later, the results of various single-rate and multi-rate testing are presented followed by the application of using the relative permeability data in two-phase production data analysis.

Chapter 1—Introduction

This chapter is the introduction to the thesis, giving the reader an overview of what will be discussed and the purpose of each chapter.

Chapter 2—Literature Review

In this chapter, there is a brief discussion on the importance of pressure versus time transient data obtained during well test operations in reservoir characterisation with an emphasis on buildup data being more reliable. This is followed by an introduction to gas condensate reservoirs, their fluid and flow behaviours and particularly the dependency of their relative permeability on pressure and velocity due to coupling (an increase in relative permeability when IFT decreases or velocity increases) and inertia (a decrease in relative permeability when velocity increases). In addition, the last section will discuss the application of well testing in gas-condensate reservoirs, and existing published research in terms of single-phase versus two-phase solutions.

Chapter 3—Data Summary and Simulation Models

In this chapter, the basics of the reservoir models built, using the ECLIPSE 300 commercial numerical simulator, for this study is explained. In addition, details of the rock data and fluids composition are also discussed including the

use of the velocity-dependent model in the ECLIPSE simulator. This chapter is to be used as a reference for subsequent chapters.

Chapter 4—Pressure Versus Distance Profile for Well Testing Buildup Data

In this chapter, the focus is on the calculation of the pressure versus radius profile from well test buildup data. The underlying concept used for this method and the calculation procedure are explained. It also highlights the benefits of the calculated pressure profile and explores the application of the pressure profile for single-phase and two-phase systems.

Chapter 5—Velocity-Dependent Two-Phase Relative Permeability from Well Test Data

In this chapter, an analytical method for calculating velocity-dependent relative permeability using well test data is described. The calculation relies on gradient of the pressure versus radius profile described in Chapter 4. Due to nature of gradient calculation, a discussion on the resultant numerical dispersion observed in the data and how to reduce the noise in the data is thoroughly investigated. Then smoothing solutions are discussed and recommended to be applied to the procedure resulting in practically acceptable noise-free relative permeability data. Finally, in this chapter, the process of calculating the relative permeability data is linked to the results of Chapter 4.

Chapter 6—Pressure Profile and Relative Permeability in Multi-Rate Testing

This chapter first briefly discusses the importance of multi-rate testing for gas-condensate reservoirs. Then the reliability of the methods explained in Chapters 4 and 5 are examined for multi-rate testing data. It also showcases how the proposed methods work for special cases with varying flow rates and shorter test duration.

Chapter 7—Two-Phase Production Data Analysis Using Velocity-Dependent Relative Permeability

In this chapter, one of the main applications of the results of the proposed well test data analysis technique is discussed. That is, how the pressure transient data can provide data that can be applied for improved production data analysis. More specifically the method of analysing the production data using a two-phase approach with analytically calculated velocity-dependent relative permeability data is described, and example cases are discussed showing good results. In addition, a new iterative process is suggested using both two-phase well test and production data to obtain permeability.

Chapter 8—Conclusions and Future Work

A summary of the conclusions of this work is given, in this chapter with a discussion on the practical implication and future work.

Chapter 2

Literature Review

In the first section of this chapter, a brief introduction to well testing, the role it plays in reservoir characterisation, and one of its main concepts used in this study, is given. In the next section, an introduction on gas-condensate reservoirs is discussed with an overview on the two-phase fluid behaviour and what the published research has suggested to tackle the condensate banking problem, which occurs when pressure drops below dew point and the valuable condensate with its low mobility hinders gas flow. In addition, the vital role of relative permeability in gas-condensate reservoirs is discussed including the impact of coupling and inertia that affects the behaviour of relative permeability and the available models to predict relative permeabilities. Furthermore, the chapter concludes with the applications of well test analysis in gas-condensate reservoirs.

2.1 Introduction to Well Testing

The objective of well test analysis is to describe an unknown system (well and reservoir) through indirect measurements (pressure and flow rate), which makes it an inverse problem, that usually does not have a unique solution (Gringarten et al. 1979). In other words, a solution model for the well test data could describe multiple formation characteristics. The non-uniqueness of the inverse problem can be reduced by integrating other sources of information, such as production or formation logs, static geological model, or even other tests in the

same reservoir. This integration approach is crucial in improved understanding of the well test data.

2.1.1 Importance of Well Testing in Reservoir Characterisation

Well testing analysis is a valuable tool that has advanced significantly since its first inception, becoming more powerful and faster to perform. It began just as a tool to determine well quality by estimating producing rates at different producing pressures; then it evolved to become a tool that can be used to obtain formation permeability, skin, wellbore storage and reservoir pressure (Ramey 1992); all these data help to better understand and characterise the reservoir. The reservoir parameters and well performance data obtained from the interpretation of well test data can help to manage the field properly (Stewart & Jamiolahmady 2016).

Interacting with a subsurface asset is challenging, especially concerning data acquisition. Raw data collection is limited; wells are the main gateway to get an insight of the reservoir, however, many of the data collected through wells are local measured-points that lack a bigger picture and dynamic characteristics (Bourdet 2002). That is where well test analysis comes into play; with the ability to see more of the reservoir from observing pressure and rate over time to the ability to estimate reservoir parameters, and characterising anomalies (such as faults, channels, water-fronts, and fractures). Well testing analysis provides more depth and dynamic view of the reservoir compared to other available engineering tools.

The advantage of well testing is that it captures data transient through the reservoir, beyond just the immediate vicinity around the wells, shedding light on reservoir and fluids characteristics away from the wellbore. Well testing techniques have become a requirement in both the exploration and development phases of field appraisals (Stewart 2011).

2.1.2 Reliability of Pressure Buildup Tests

Generally, well tests consist of a period of production at a constant flow rate—drawdown, where the pressure at the well is decreasing followed by a period of shut-in—buildup, where the pressure at the well starts to increase (**Figure 2.1**).

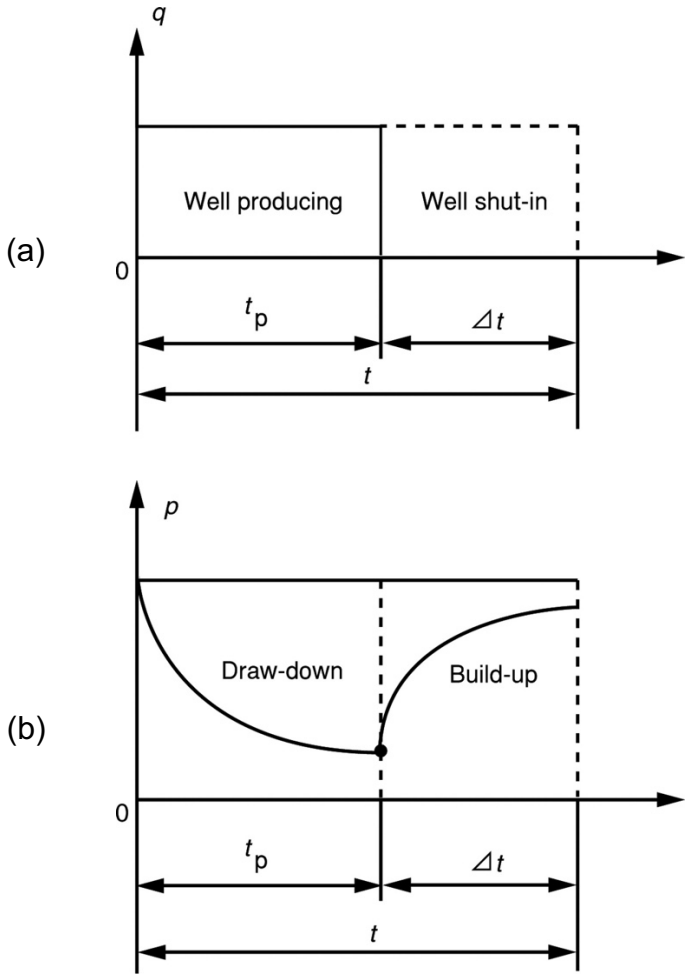

Figure 2.1—A schematic example of pressure drawdown followed by buildup tests showing (a) the flow rate, q, applied to the well and (b) the pressure response, p, measured at the well as a function of time (Corbett et al. 2012).

Well test analysis concepts were first developed for drawdown tests, as they are the first response from the well. Pressure response of the system is then recorded and analysed. However, the challenge in analysing drawdown data is in keeping the production rate constant. Without a constant flow rate, the

analysis result becomes erroneous. As it is difficult to produce at a constant flow rate without any fluctuation and interruption for the test duration, the buildup response is usually used and is considered to be more reliable, as the flow rate is known to be zero when the well is shut-in. However, the principle of superposition is then required to develop the solution for a buildup test, which consists of a rate change, i.e. a shut-in after a flow period (Horner, 1951; Matthews, 1961). Although the disadvantage of buildup tests is the production loss, due to the well being shut for a period of time; however, this can be managed strategically (e.g. when other wells are maintaining the production quota or taking advantage of periods of time where shut-in is needed for well or facility maintenances). For these reasons, in this study, the well test data utilised are buildup tests.

2.2 Introduction to Gas-Condensate Reservoirs

2.2.1 Gas Condensate Behaviour

The state of a reservoir (gas or liquid, or both) can be identified based on its initial pressure and temperature on a pressure-temperature phase envelope plot (Coskuner 1999), as in **Figure 2.2**. Bubble point curve, dew point curve and critical point make a bounding area where two-phase (liquid and gas) exist in equilibrium. Outside of the two-phase envelope, a single-phase condition exists. The lines inside the bounded area indicate the liquid volume as a percentage of the total fluid.

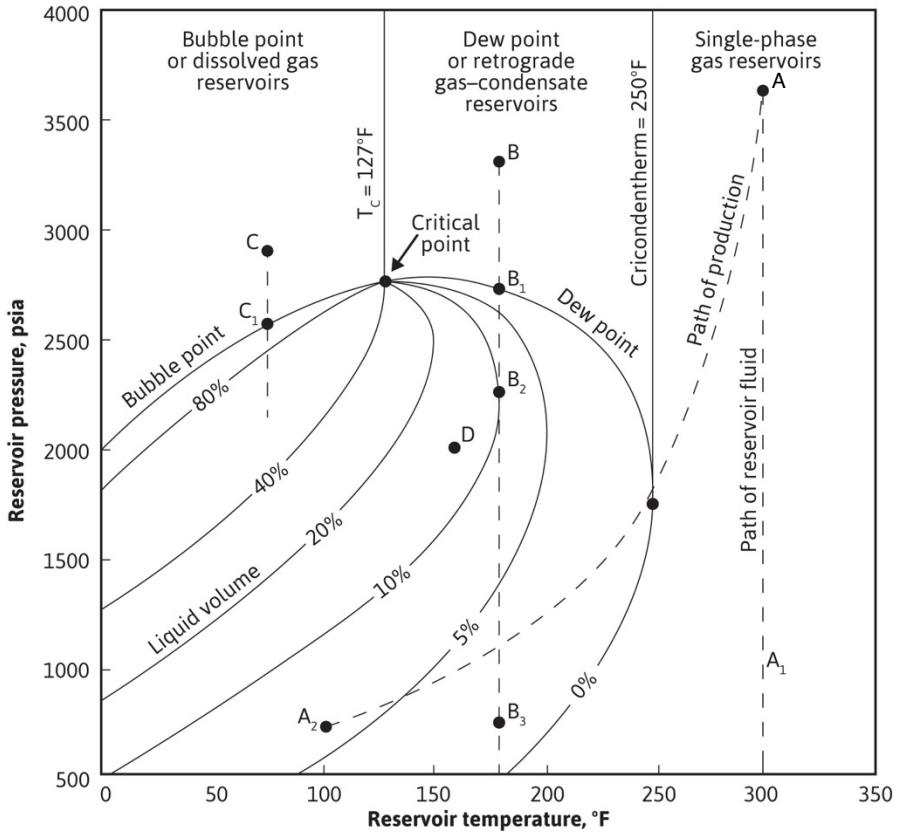

Figure 2.2—PT plot showing the single-phase regions and the two-phase envelope where point (A) represent single-phase gas reservoir dropping in pressure to A1 and remain single-phase. Point (B) represent gas-condensate reservoirs initially in single-phase conditions, once it drops below dew point (B1) the fluid will become two-phase (B2, B3). The third is the undersaturated reservoirs at point (C), once the pressure drops below the bubble point, gas starts to appear (C1). (Terry & Rogers 2014).

A gas-condensate reservoir is initially a single-phase gas reservoir at high-pressure point (pressure above dew point). It is mainly composed of methane, C1, and other short-chained hydrocarbons, but it also contains long-chain hydrocarbons called intermediate/heavy-ends (Fan et al. 2005). When pressure and temperature conditions change, the reservoir's fluid will become two phases, gas and condensate (also called retrograde condensation). As reservoir temperature usually does not change much, pressure can change drastically based on wells production. Once the bottomhole pressure of a producing well

drops below the dew point pressure (p_d), the condensate starts to form around the wellbore with an increase in the condensate up to a maximum level as pressure continues to drop, after which the condensation will start to re-evaporate as pressure continues to drop. The loss of heavy-end components around the wellbore is referred to as condensate banking. It is unlikely to disappear even after shutting-in the well, and it can adversely affect the productivity of the well (**Figure 2.3**), by restricting the flow of gas. The condensate liquid is also very valuable which is not desirable to be lost in the reservoir due to condensate banking. Productivity reduction have been reported in the literature to be a factor of 2 to 4 (Fussell 1973; Afidick et al. 1994; Barnum et al. 1995; Wheaton & Zhang 2000; Smits et al. 2001; Kumar et al. 2006). Some studies indicate that most productivity reduction occurs in wells with a flow capacity (kh) of less than 1000 mD.ft (Barnum et al. 1995).

Initially, the condensate that is dropping out of gas, away from the wellbore, is immobile, due to its saturation being below critical saturation (S_c)–the saturation point after which the phase starts to flow. Such condensate has a negligible effect on gas mobility. Closer to the wellbore, however, when the saturation of the condensate reaches a critical value, which allows the condensate to flow, the condensate is mobile, and it has a significant effect on gas mobility, lowering its relative gas permeability (Thomas et al. 2009)–more on this in section 2.2.2. However, (Danesh et al. 1988; Danesh et al. 1991) has shown that S_c is close to zero in gas-condensate reservoirs (more on that in section 2.2.3). In that region, near the wellbore, the pseudo steady-state regime may be assumed to be describing the near-wellbore flow (Danesh 1998).

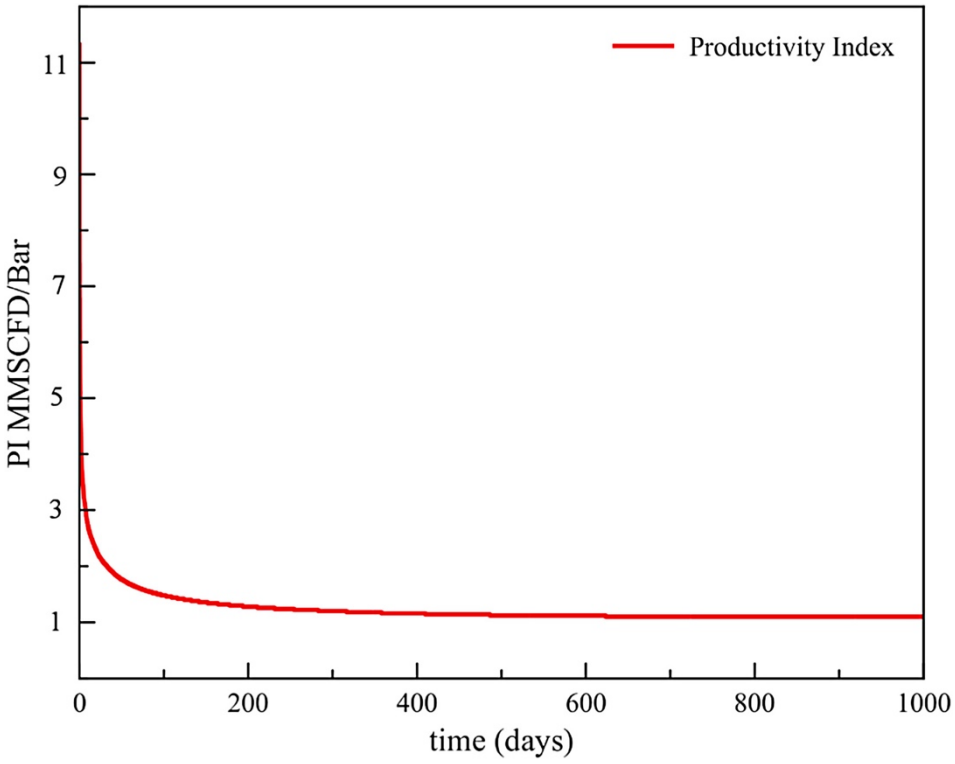

Figure 2.3—A schematic example of a reduction of productivity index (PI) in gas-condensate reservoirs (Rahimzadeh et al. 2016).

The amount of the condensate that develops around the well depends not only on how far the reservoir condition is below the dew point but also on fluid composition. A richer fluid composition has more of the heavy components that ends up forming a bigger condensate bank than leaner fluid composition which have fewer heavy components and hence does not become as challenging as richer fluids (**Figure 2.4** shows a maximum liquid drop-out of about 25% for the rich fluid, and about 2% for the lean fluid). Productivity in gas-condensate reservoirs declines even in moderately rich reservoirs due to the effect of condensate buildup around the wellbore (Mokhtari et al. 2013). In addition, research have shown that lean gas condensate can significantly reduce productivity over time, as shown in Arun field (Afidick et al. 1994) and in other published work, where a lean gas condensate with maximum liquid dropout of only 2% can still hinder production by 5% (Huerta Quinones et al. 2012). In contrast, dry gas has no heavy components to generate the liquid drop-out.

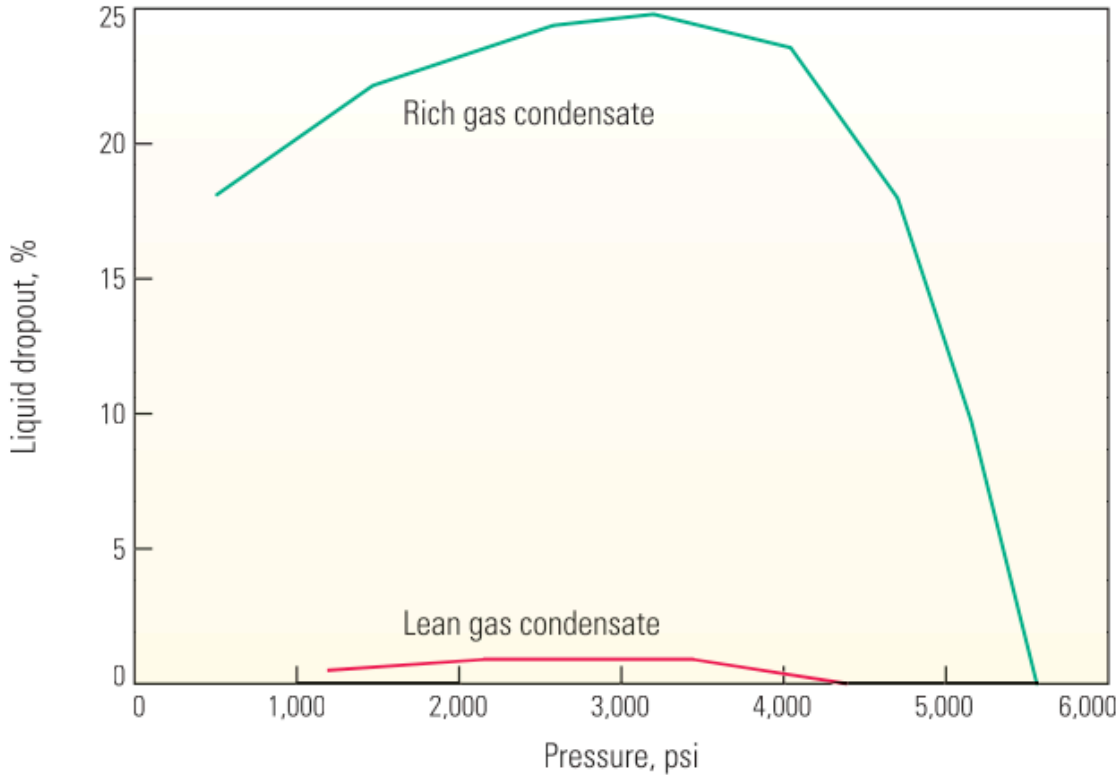

Figure 2.4—Amount of potential liquid dropout in lean versus rich gas condensate (Fan et al. 2005).

Gas-condensate reservoirs are complex in terms of data analysis due to two-phase physics, and in terms of operation and reservoir management due to condensate development around the wellbore, causing restriction to gas flow (Fan et al. 2005). The combination of two-phase flow and their unique relative permeability characteristics around the wellbore, as described in the next section, present a difficulty for reservoir data analysis, such as well test or production analysis.

In conclusion, condensate blockage or banking, can cause severe productivity loss, could kill the well, and pose a complex challenge for the data analyst. Gas-condensate reservoirs are costly and risky to develop; hence the need for better characterisation tools.

2.2.2 Relative Permeability in Gas-Condensate Reservoirs

The flow behaviour of both gas and condensate is governed by relative permeability curves which traditionally varies for different rocks. The presence of condensate causes the gas relative permeability (k_{rg}) to decrease sharply. It is however not made up by the oil relative permeability (k_{ro}), which remains low. Additionally, these relative permeability data are shown to be affected by the production rate and pressure. Hence, predicting production from gas-condensate reservoirs need accurate relative permeability data, primarily when the condensate bank is formed.

Availability of representative relative permeability data for gas-condensate reservoirs can be challenging, due to their dependency on velocity and pressure. Several analytical models have been developed to predict relative permeability as a function of saturation (Purcell 1949; Burdine 1953; Corey 1954; Corey & Brooks 1966). The models developed by Corey (1954) and Corey and Brooks (1966) are an extension of the work of Burdine (1953). In the method by Corey and Brooks (1966), they adjusted Corey's (1954) method by modifying the representation of capillary pressure function to a more general form:

$$P_c = p_e(S_w^*)^{-1/\lambda} \tag{2.1}$$

where p_e is the entry capillary pressure, λ is the pore size distribution index and S_w^* the normalised wetting-phase saturation.

They derived the wetting and nonwetting-phase relative permeabilities as following:

$$k_{rw} = (S_w^*)^{\frac{2+3\lambda}{\lambda}} \tag{2.2}$$

$$k_{rnw} = (1 - S_w^*)^2 \left[1 - (S_w^*)^{\frac{2+\lambda}{\lambda}}\right] \tag{2.3}$$

Such methods are limited in their application. For gas-condensate conditions that are examined in this thesis, such as low IFT and high velocity, it is needed that additional effect are accounted for in the relative permeability calculation.

The model by Corey and Brooks (1966) above would only approximate relative permeabilities to base curves, without honouring any effects related to velocity and pressure. Furthermore, the obtained relative permeabilities using the above models would give relative permeability as a function of saturation, and not pressure–which is needed for pseudo-variables calculation.

2.2.3 Gas Condensate Fluid Regions

In theory, gas-condensate reservoirs can be divided into three fluid regions (Fevang & Whitson 1996), although in some situations not all three regions are observed (**Figure 2.5**).

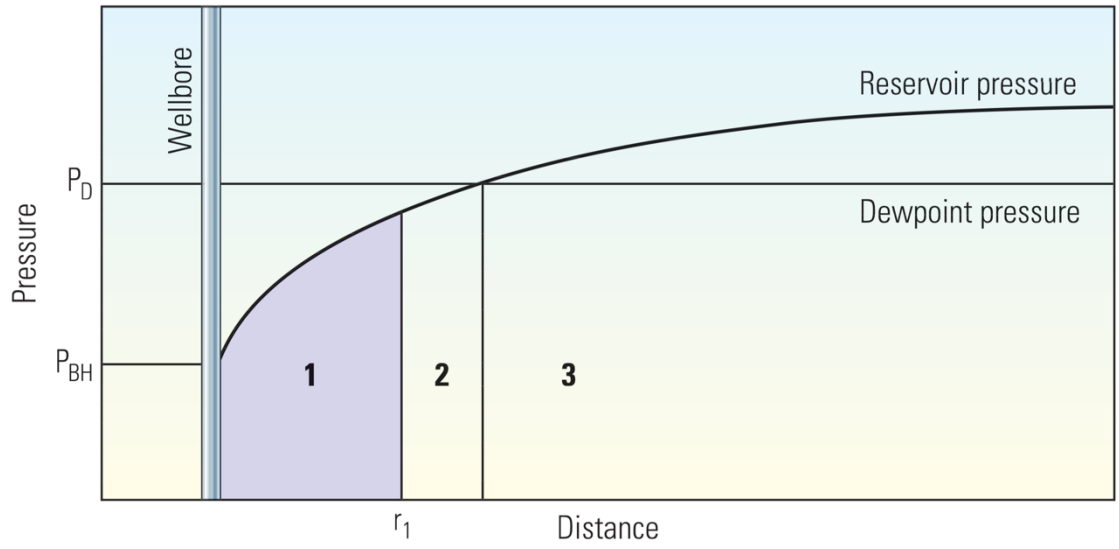

Figure 2.5—Possible three fluid regions for a gas-condensate reservoir (Fan et al. (2005). (3) where reservoir pressure is above dewpoint; (2) where pressure dropped below dewpoint, but condensation has not reached S_c; (1) is where condensate has reached S_c, and both gas and condensate are assumed to be flowing.

When the bottom-hole pressure goes below the dewpoint pressure of the fluid, region-1 and region-2 can exist. Whereas, region-3 exists only when the reservoir pressure is above the dewpoint, which means that the phase at region-3 is single-phase gas.

In region-1, both gas and condensate are flowing, and the condensate saturation is higher than the critical condensate saturation. This region ranges in size from tens of feet for lean condensates to hundreds of feet for rich condensate; the size of this region depends on the amount of produced gas and the percentage of liquid dropout. It surrounds the wellbore and could extend further from the well for reservoirs with high permeability. Condensate bank blockage can be significant even for leaner gas-condensate fluids; as capillary forces can retain a condensate that accumulates with time.

In region-2, both gas and condensate exist, but condensate is assumed to be immobile, due to its saturation being below the critical condensate saturation (S_c). The condensate saturation increases, and the gas phase becomes leaner as gas flows towards the wellbore. However, the Heriot-Watt Gas-Condensate Recovery (HW-GCR) research team has shown that critical saturation in gas-condensate reservoirs is much lower than for conventional gas-oil systems due to efficient condensate film flow in these low IFT systems (Danesh et al. 1988; Danesh et al. 1991). Thus, this region is not considered significant in this thesis, when considering the proposed analytical approach which will be discussed in detail later in Chapters 4 and 5, and two phases are assumed to be flowing. It should be noted that the low mobility of condensate has been shown in many fields to result in accumulation of condensate with time due to gravity which cannot be described by a zero mobility when high S_c is considered.

In region-3, the pressure is above dewpoint and only single-phase gas exist. This region is the furthest away from the wellbore, and it includes most of the reservoir. However, as the well keeps producing, and pressure dropping below the dewpoint keeps propagating further, it shrinks, and eventually the whole reservoir could become two-phase when the reservoir pressure is below dewpoint everywhere.

2.2.4 Velocity Effects

Additional relative permeability effects are occurring around the wellbore due to viscous, capillary and inertial forces. It is well known that at high velocities, a reduction in gas relative permeability occur due to inertial flow (Forchheimer 1914). The effect of interfacial tension (IFT) on relative permeability data at low IFT values has been shown to improve the gas relative permeability (Bardon & Longeron 1980). HWU-GCR team was the first to report the positive effect of velocity on gas relative permeability at high rates (**Figure 2.6**), calling it "positive velocity dependency" or "positive coupling" (Danesh et al. 1994) which was later proved by many researches (Chen et al. 1995; Henderson et al. 1997; Ali et al. 1997; Henderson et al. 1998; Blom et al. 2000; Henderson et al. 2001). The main reason for this unique behaviour was explained by Jamiolahmady et al. (2000) and Jamiolahmady et al. (2003) following a mechanistic modelling approach at the pore level for a single and network of pores. The dominant effect of coupling has also been demonstrated in numerical simulations of flow around horizontal wells where geometry can influence the flow towards the wellbore (Ghahri et al. 2010; Ghahri et al. 2011) and in perforated regions (Jamiolahmady et al. 2007).

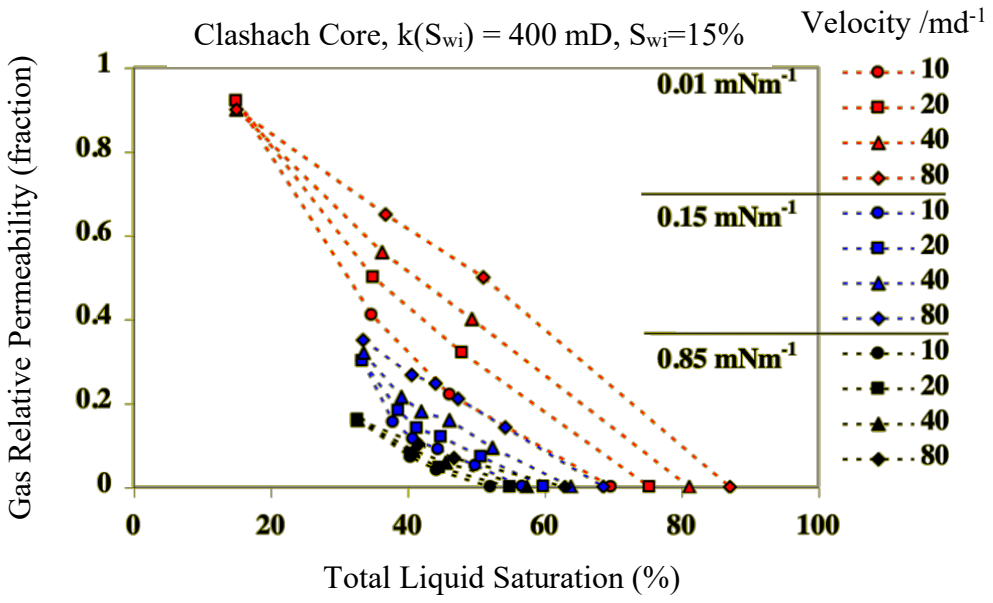

Figure 2.6—Variation of gas relative permeability with velocity and IFT–positive coupling effect (Institute of Petroleum Engineering 2018)

That is, the low IFT of the gas-condensate system combined with medium to high velocity (where viscous forces are dominant) dictates a flow regime that is different from conventional gas-oil systems. It produces a gas relative permeability that is higher than the value at lower velocities (positive coupling), and at even higher velocities, the inertial effect, caused by the fluid acceleration and deceleration as it is flowing through pore throats and pore bodies (Jamiolahmady et al. 2010) results in a lower gas relative permeability. Henderson et al. (2000) have shown the competition between positive coupling and negative inertia at different condensate saturations and velocities (**Figure 2.7**).

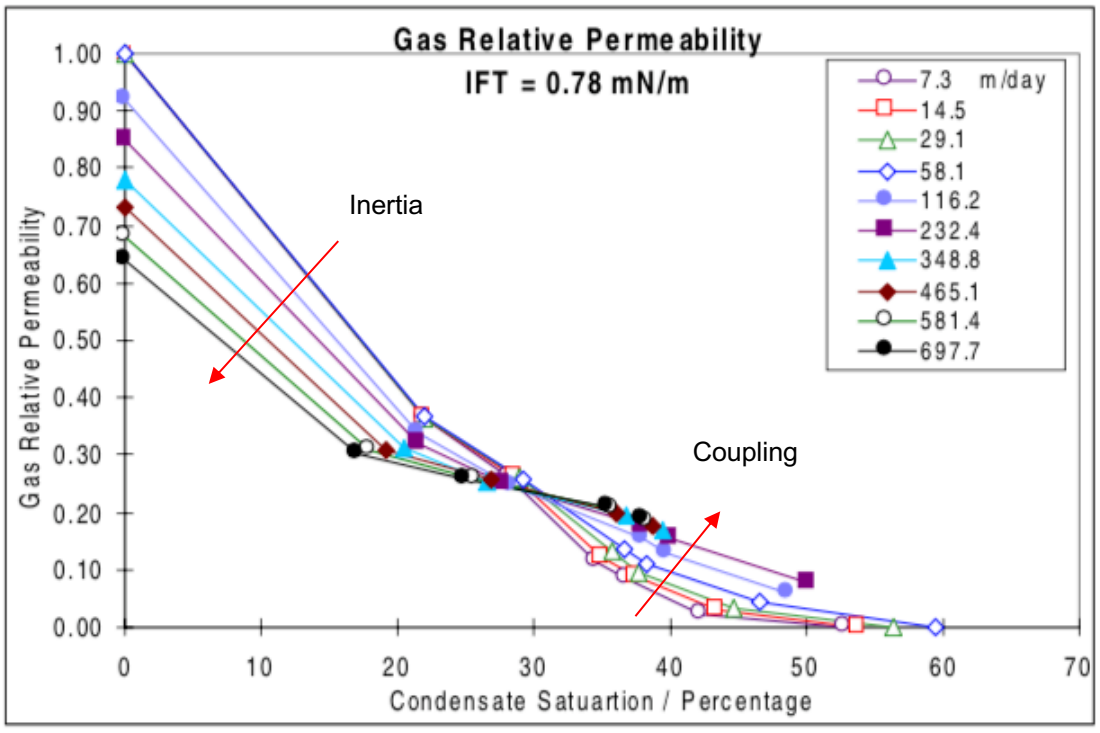

Figure 2.7—Variation of gas relative permeability with velocity, inertial and coupling effects at low IFT (Henderson et al. 2000).

The dependency of gas-condensate relative permeability on velocity and pressure due to coupling and inertia adds further complexity to any interpretation of pressure or flow rate data (Henderson et al. 1997; Jamiolahmady et al. 2000). In general, positive coupling effect is more pronounced at low to moderate velocities, especially at higher condensate

saturation, and the negative inertial effect is more dominant at moderate to high velocities, especially at lower condensate saturation. However, the positive coupling has been shown to be in strong competition with the negative inertia at very high velocities (Henderson et al. 2001), and the combination of the two high velocity effects is usually positive, reducing the impact of condensate bank. Typically, laboratory core-flood experiments are needed to measure core exponents for the inertial and capillary number effects on relative permeability. Several studies have tried to come up with a correlation based on rock samples (Henderson et al. 2000; Bang et al. 2006; Jamiolahmady et al. 2009); however, velocity effects in gas condensate systems is a complex function of core type, fluid properties and flow rate. There is no straightforward formula for identifying the flow regime or estimation of the dominance of inertia or coupling effect.

Published work has proved that accounting for such velocity effects in field simulations are appropriate and results in a good correlation with historical data (Carvajal et al. 2007). Li et al. (2009) has shown, in a carbonate gas-condensate reservoir in China, that if positive coupling effect is ignored in analysing gas condensate data the well deliverability decreases to 50% of its initial value considering the producing operation. Whereas when they accounted for the positive coupling, the well deliverability is significantly improved. However, to obtain relative permeability data, which are affected by coupling and inertia, demanding experiments are needed to be conducted on core samples in the lab that are both time-consuming and expensive (Mott et al. 2000; Jamiolahmady et al. 2009).

Considering that it is more realistic for a gas-condensate analysis to consider inertia and coupling, in this thesis, the work will rely on dynamic pressure data from well test, which inherently capture these velocity effects. Additionally, and more importantly, a method is proposed to analytically approximate the relative permeability data which accounts for both inertia and coupling, as will be shown in Chapter 5.

2.2.5 Well Testing Analysis in Gas-Condensate Reservoirs

Although productivity decline is one of the first indicators of condensate banking around the well, well testing analysis is often used as a tool to determine its presence (Fan et al. 2005). Liquid distribution around the well can be determined by analysing pressure buildup data. Briones et al. (2002) have shown that well test analysis is one of the most practical and reliable tools to detect the existence of the condensate bank. By analysing more than 30 well test data from the Santa Barbara field, the biggest Venezuelan gas-condensate field, it was shown that using well testing in analysing gas-condensate reservoirs helped in workover decisions, such as enhancing well production by hydraulic fracturing.

Transient pressure data in gas-condensate reservoirs are typically analysed using conventional single-phase flow theory. The single-phase approach relies on linearised radial flow equation for a real gas. Al-Hussainy et al. (1966) proposed this approach by introducing the real gas pseudo-pressure as:

$$p_p(p) = 2\int_{p_b}^{p_i} \frac{p}{\mu(p)\, z(p)} dp \qquad (2.4)$$

where the viscosity, μ, and compressibility factor, z, must be known in order to be able to evaluate the integral for a specific value of pressure, p. That is, the gas properties should be available as a function of pressure.

In this technique, the use of single-phase pseudo-pressure gives a derivative shape similar to a radial composite system highlighting the contrast in the gas mobility caused by the presence of the condensate (**Figure 2.8**). When using the single-phase pseudo-pressure, the assumption of zero-condensate mobility may not be appropriate.

In the single-phase approach, condensate banking is shown by a lower flow-capacity (kh) or mobility in the pressure derivative plot, compared to the single-phase gas region further away from the wellbore. This results in two plateaus in the pressure derivative plot (Figure 2.8). The permeability of each region

can be determined from the pressure derivative on a log-log plot of pseudo-pressure and shut-in time. When the test is long enough, and permeability of the single-phase region is determined, that permeability represents the reservoir absolute permeability. If only region-1 of the pressure derivative plateau is evident, it will not be possible to calculate the flow capacity of the reservoir and longer test time is required to see the outer single-phase region; this difficulty is more pronounced if other issues such as wellbore storage masks parts of the reservoir response.

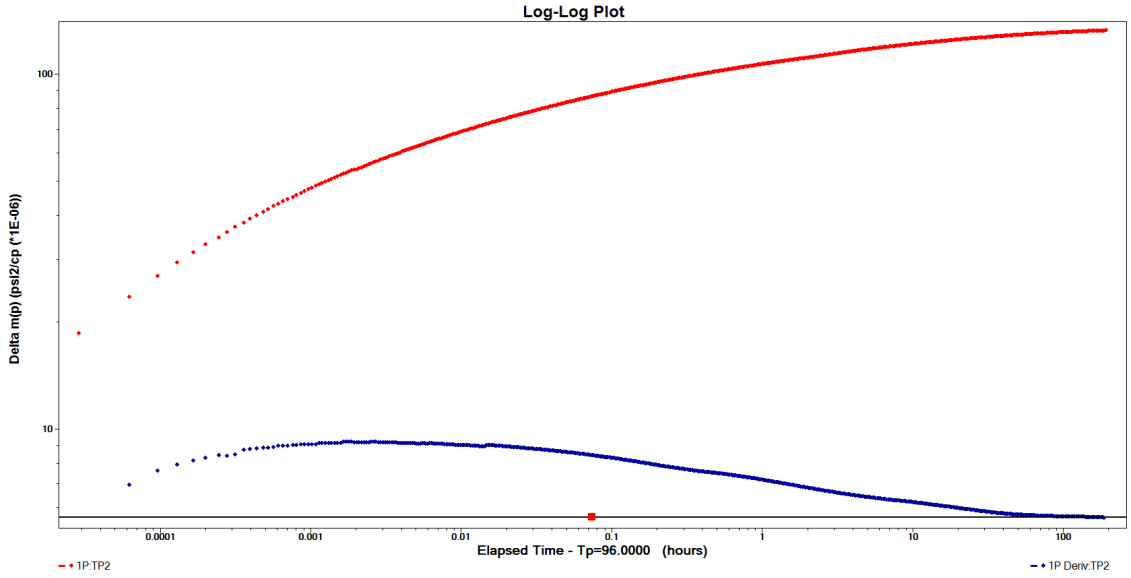

Figure 2.8—Pressure derivative of well test data for a gas-condensate reservoir showing condensate region at the early time followed by a single-phase gas region.

Due to the presence of condensate phase, the use of two-phase pseudo-pressure has been suggested to remove the condensate bank effect, but its application has not gained popularity because its calculation requires relative permeability data, which are usually not available. The treatment of two-phase steady-state radial flow was first considered by Muskat (1938) who introduced the concept of two-phase pseudo-pressure. The concept was later considered by Fussell (1973) and Jones and Raghavan (1988) who later proposed the following two-phase pseudo-pressure to the pressure transient analysis of a buildup test in gas-condensate reservoir (Jones et al. 1989):

$$p_p(p) = 2\int_{p_b}^{p_i}\left(\frac{k_{ro}}{\mu_o z_o} + \frac{k_{rg}}{\mu_g z_g}\right)pdp = 2\frac{RT}{M.W.}\int_{p_b}^{p_i}\left(\rho_o\frac{k_{ro}}{\mu_o} + \rho_g\frac{k_{rg}}{\mu_g}\right)dp \qquad (2.5)$$

Here, both gas and condensate mobilities are included in the function of pseudo-pressure.

When two-phase pseudo-pressure is used, a single plateau for both regions should be obtained in the log-log pressure derivative diagnostic plot (**Figure 2.9**). This plateau is corrected for the condensate bank effect, thereby obtaining permeability in the condensate bank region that is much closer to the actual single-phase absolute permeability. Using two-phase pseudo-pressure is important when the test period is not long enough to capture the single-phase gas outer region, region-2, or when the formation is tight in which a very long time for region-2 plateau is required. Two-phase pseudo-pressure gives more accurate reservoir properties than the single-phase pseudo-pressure method. Many in the literature have reported the benefit of the two-phase pseudo-pressure by evaluating the approach numerically with simulation data using base relative permeability curves (Saleh & Stewart 1992; Hernandez-G. et al. 1993; Raghavan & Jones 1996; Raghavan et al. 1999; Gringarten et al. 2006; Al Ismail & Horne 2010).

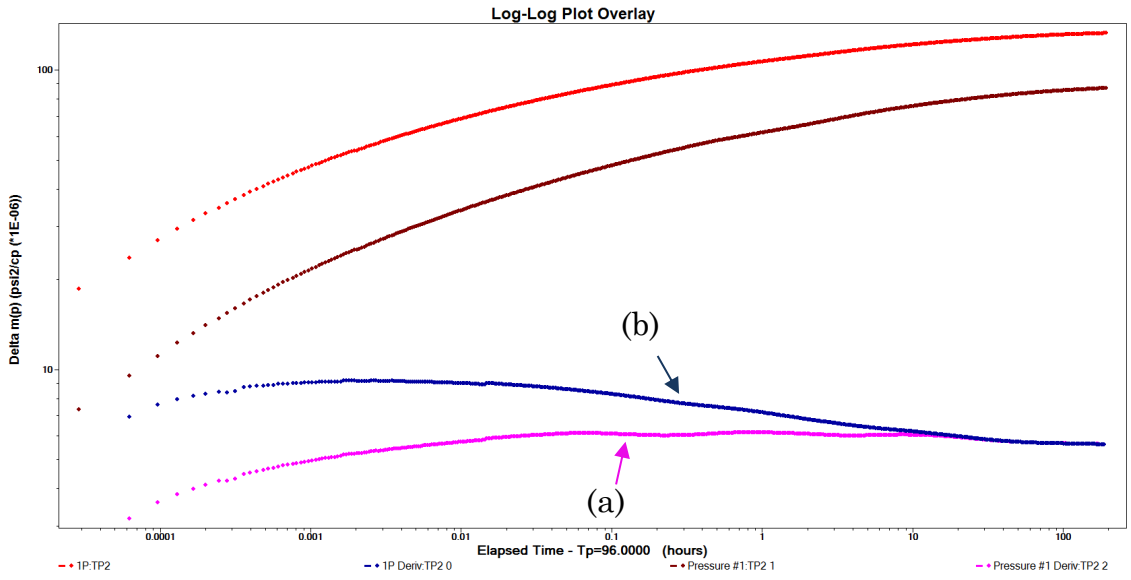

Figure 2.9—Pressure derivative of well test data for a gas-condensate reservoir showing the effect of using (a) two-phase pseudo-pressure (in pink colour for

pseudo-pressure derivative and brown for Δp_p) instead of (b) single-phase pseudo-pressure (in blue colour for pseudo-pressure derivative and red for Δp_p).

However, calculation of the two-phase pseudo-pressure is only viable if there are representative relative permeability data, which are usually not available. In practice, even though two-phase pseudo-pressure is shown to be useful, due to the lack of relative permeability data, it is more common to use a composite model with single-phase pseudo-pressure (Thompson et al. 1993; Hernandez-G. et al. 1993; Marhaendrajana et al. 1999). The two-phase pseudo-pressure is generally evaluated based on the steady-state assumption (O'Dell & Miller 1967) where the reservoir model is composed of a far region, $P > P_{dew}$, and a near wellbore region, $P < P_{dew}$, and both fluids flowing. An approach which is also followed by other investigators (Fussell 1973; Chopra & Carter 1986; Jones & Raghavan 1988). However, relative permeability data is still required, and if it is available, it is a function of saturation only. Therefore, a relationship between reservoir pressure and saturation is needed to calculate the two-phase pseudo-pressure. A number of methods have been proposed in the literature for predicting pressure-saturation relationship (Fetkovich et al. 1986; Becker et al. 2016). Another method proposed by Johnson & Jamiolahmady (in press) where the gas to total (gas plus condensate) flow rate (GTR)–a concept introduced by Jamiolahmady et al. (2007), and component weight fractions are related to pressure and producing pressure-saturation found to give comparable predictions to those produced by similar methods mentioned above. The relationship between pressure and saturation can be computed using (Jones & Raghavan 1988):

$$\frac{k_{ro}}{k_{rg}} = \frac{L\rho_g\mu_o}{V\rho_o\mu_g} \tag{2.6}$$

where L and V are the molar fraction of liquid and vapour, respectively. The left-hand side of the equation is a function of saturation (base relative permeability data), and the right-hand side is a function of pressure and can be approximated using the constant composition expansion (CCE) experiment.

Equation 2.6 is useful as it relates fluid PVT properties at a given temperature and pressure under two-phase steady-state flow conditions to the relative permeability ratio. First, $\frac{k_{ro}}{k_{rg}}$ is calculated as a function of pressure using Equation 2.3 at different pressure points. Then, if k_{ro} and k_{rg} are available as a function of saturation, S_o, a tabulation of $\frac{k_{ro}}{k_{rg}}(S_o)$ is generated. Thus, a relationship between k_{ro}, k_{rg} and pressure can be obtained. In other words, it establishes pressure-saturation relationship from PVT data and relative permeability data as a function of saturation.

Many authors have shown good results by employing two-phase steady-state based methods in the modelling of gas-condensate well deliverability (Fussell 1973; Jones & Raghavan 1988; Fevang & Whitson 1996; Jamiolahmady et al. 2007; Behmanesh et al. 2013; Mahdiyar & Jamiolahmady 2014; Johnson & Jamiolahmady 2015; Johnson & Jamiolahmady 2016; Taghizadeh Sarvestani et al. 2016).

In all the above, it is concluded that two-phase pseudo-pressure is superior to using single-phase pseudo-pressure. However, handling base relative permeability data is tricky, and the variety of approaches make it a complex solution for practical engineering. In addition to the fact that relative permeability data needs to be either available via demanding lab experiment or history matched which is not very helpful. Availability of base relative permeability data from core analysis in the lab is costly and complex for gas-condensate reservoirs. In addition, the relative permeability as a function of saturation does not account for velocity effects, which will be highlighted later in Chapter 5. On the other hand, using single-phase pseudo-pressure (Al-Hussainy et al. 1966) assumes immobile condensate, and the condensate region around the wellbore will distort the results.

2.3 Conclusion

Proper evaluation of reservoirs performance is essential as it impacts the economic prospect of field development. This task is particularly challenging for gas-condensate reservoirs due to the presence and flow of condensate. The complexity is further enhanced due to dependency of relative permeability to pressure and velocity due to coupling (an increase in gas relative permeability with an increase in velocity or a decrease in IFT) and inertia (a decrease in gas relative permeability with an increase in velocity). Assessment of the condensate banking, relative permeability data and the well productivity alterations will influence decision making concerning well workover (e.g. fracturing the reservoir, acid stimulation, or production control), production forecast, and overall field management. A successful evaluation will lead to better reservoir characterisation and performance prediction. The literature has shown that unsuccessful evaluation of gas-condensate reservoirs data can lead to substantial underestimation or overestimation of the condensate banking around the wellbore and thus, an overestimation or underestimation of potential performance (Fevang & Whitson 1996; Smits et al. 2001; Briones et al. 2002; Huerta Quinones et al. 2012).

Having additional tools to help evaluate gas-condensate reservoirs is therefore extremely helpful. One of the main issues is the availability of meaningful relative permeability data. The analytical approach proposed in this thesis for calculation of relative permeability as a function of pressure and velocity can aid in better understanding and analysing well data in such reservoirs, and improved management of the field. Other method to obtain a relative permeability that accounts for coupling and inertia is a lab-based experiments that are costly and cumbersome. The proposed method for relative permeability calculation from well test data is considered to be a very practical and attractive approach, as it will be shown in that such data can be used for pressure and production data analysis.

.

Chapter 3

Data Summary and Simulation Models

3.1 Introduction

The purpose of this chapter is to explain the basics of the reservoir model and the data sets used in this thesis. A base model is defined and described in this chapter, any deviation from this set-up will be discussed as needed in the other chapters. In particular, the intention is to have this chapter as a reference for subsequent chapters, in terms of fluid, rock or reservoir properties.

For all the case scenarios presented in this thesis, synthetic data sets were generated using the numerical simulator ECLIPSE 100 for oil and ECLIPSE 300 for dry gas and gas-condensate systems. Well bottom-hole pressure data versus time were simulated for the drawdown and buildup periods. The oil and dry gas scenarios were considered only for the verification of the pressure versus radius calculation method while the rest of the study focuses on the two-phase gas-condensate systems. In all cases, and when it comes to two-phase gas-condensate scenarios, the reservoir pressure is initially set above the dew point, however, once the drawdown period starts, the pressure around the well quickly drops below the dew point, and condensate develops around the wellbore.

3.2 Reservoir Model Description

The study throughout this thesis relies on synthetic well test data in order to verify the solutions and validate the presented analytical methods. The reservoir model used in the numerical simulator comprises of a single-well in a homogeneous single-layer with one grid in the angular and z-direction and 40 to 100 grid-blocks in the radial direction depending on the scenario. The model was set to have no aquifer support and have an outer radius varying from 1200 to 15000 feet depending on the rock permeability and scenario to ensure that no boundary effect is felt in the simulated well tests.

For most of the cases, a logarithmic block-size distribution was chosen so that near the wellbore the cells are very small and increases away from the wellbore by a factor of 1.1–1.3 to minimise fluctuation in the wellbore pressure (Mazloom et al. 2005). Table 3.1 shows reservoir model variations that changed to fit the requirement of the particular exercise as will be described in the following chapters. A schematic of the base model is shown in **Figure 3.1**.

Model Size Variations	**Model 1**	**Model 2**	**Model 3**	**Model 4**
Number of Gird-blocks	40	50	100	100
Reservoir Radius, r_e (ft)	5000	15000	1200	6000
Grid Distribution	Logarithmic	Last 10 fixed	Logarithmic	Logarithmic
Reservoir Thickness (ft)	100	200	200	70
Wellbore Radius (ft)	0.58	0.58	0.58	0.58

Table 3.1—Variations in reservoir model size.

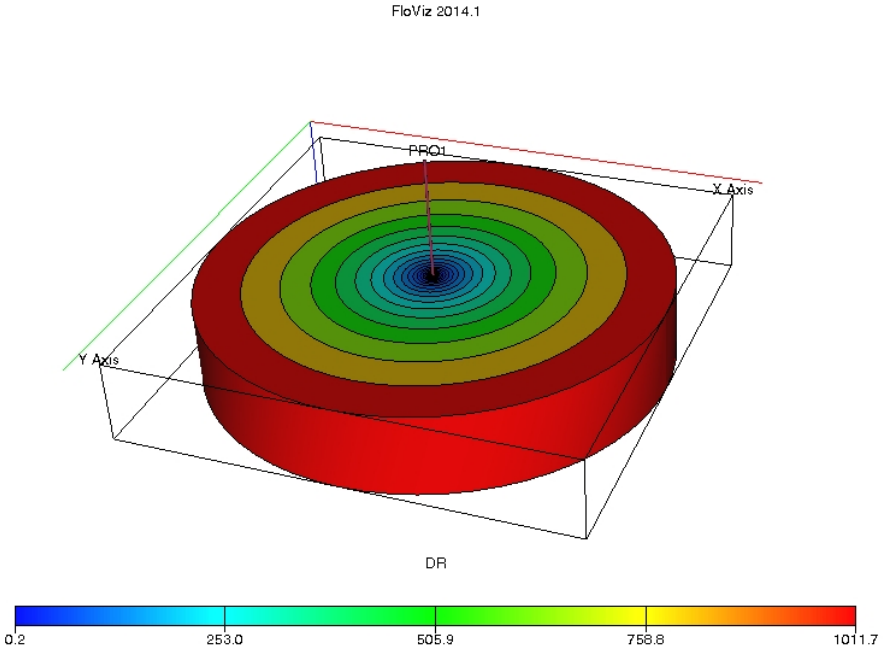

Figure 3.1—A schematic example of the reservoir model used in the numerical simulation.

In most cases, the model assumes no wellbore storage (e.g. as if the shut-in valve is set at downhole) to eliminate early masking of the well test data. Wellbore storage was only introduced to few cases to showcase its effect on the results, which will be discussed in section 5.6.1. In general, for the single-rate tests, the well was set to produce at a constant rate for 4 days, followed by a shut-in for 8 days, which is enough to capture the pressure response from the two-phase region to the single-phase region. Shorter and more realistic test duration were examined later in multi-rate tests (Chapter 6).

The choice for a radial system gives the ability to export grid properties versus radial distance, which is needed to verify the analytical computations in Chapter 4 and 5. There was no need to add further complexity in the system, as the aim was to verify the applicability of the suggested methods in a simple, homogenous system. Further complexities were examined in Chapter 5 for well geometry (horizontal wells, in section 5.6.2) and wellbore dynamics (wellbore storage, in section 5.6.1). However, there are endless possible formation

heterogeneities, and it was not within the scope of this work to test all of them; as a result, more suggestions were made in section 8.2 as future work.

3.3 Rock Data Set

Five different core samples were considered in this study. These core samples were chosen for their varying rock properties to cover a spectrum of reservoir quality from low to high permeability and to have a variety of relative permeability behaviour. The data was readily available for use within the HWU-GCR group, which eliminated the need to seek similar for new data set from other sources. These five core samples are RC1, RC10, TC11, RC6, and RC8 with permeability values of 0.18, 10, 11.1, 23.4, and 120 mD, respectively. RC1 and TC11 simulations included only two phases (oil and gas) with no connate water–although this might not be realistic, it would give a better understanding of water saturation effect, if any. However, both RC6 and RC8 have initial water saturation of 14.5% and 8.6%, respectively, which is a more realistic representation of reservoir rocks. For the dry gas scenario, the RC1 rock properties and rich gas condensate fluid, above its dew point pressure, were used. While for the single-phase oil system scenario, the RC10 rock with the permeability of 10 mD and a porosity of 0.25 was used. RC cores are sandstone reservoir cores and TC is carbonate outcrop. **Table 3.2** summarises the basic properties for all the five rocks.

Property	**RC10**	**TC11**	**RC1**	**RC6**	**RC8**
Porosity (%)	25	23.3	17.3	15.8	12.3
Phases	Oil	Oil/Gas	Oil/Gas	Oil/Gas	Oil/Gas
Permeability (mD)	10	11.1	0.18	23.4	120
Initial water saturation (%)	0	0	0	14.5	8.6
Rock type	Sandstone	Carbonate	Sandstone	Sandstone	Sandstone
Rock compressibility (psi-1)	4.0 ×10-6	3.0 ×10-6	4.49 ×10-6	4.49 ×10-6	4.49 ×10-6

Table 3.2—Rock properties used for the single-phase and two-phase gas-condensate systems.

Besides varying permeability, each core sample has different rock porosity, connate water saturation, base relative permeabilities curves, and core exponents—measured in the lab by the HWU-GCR team. Core exponents are required to adjust base relative permeability as it is a function of velocity and interfacial tension (IFT), which is discussed further in sections 2.2.4 and 3.5. This dependency is expressed in the ECLIPSE numerical simulator, but the level of impact is expressed by the core exponents. Details of the lab-obtained base relative permeability data are shown in **Figure 3.2** and in Table 3.3, Table 3.4, Table 3.5 and Table 3.6 for RC1, TC11, RC6 and RC8, respectively. These data were experimentally measured by the gas-condensate recovery research team at Heriot-Watt University and are used in the simulator as an input.

S_g	K_{rg}	K_{ro}
0.65	0	0.30
0.71	0.1101	0.1539
0.80	0.1753	0.0609
0.86	0.2368	0.0243
0.91	0.2825	0.0095
1	1	0

Table 3.3—RC1 gas and oil base relative permeabilities.

S_g	K_{rg}	K_{ro}
0.152	0	0.2474
0.31	0.0744	0.104
0.39	0.1927	0.067
0.452	0.3309	0.034
0.583	0.5945	0.02
0.707	0.7379	0.0123
1	1	0

Table 3.4—TC11 gas and oil base relative permeabilities.

S_g	K_{rg}	K_{ro}
0.455	0	0.241681
0.588	0.008899	0.020019
0.607	0.01285	0.014454
0.608	0.018233	0.010201
0.614	0.02731	0.00768
0.628	0.034439	0.005697
0.68	0.060251	0.003258
0.705	0.080833	0.002175
0.855	1	0

Table 3.5—RC6 gas and oil base relative permeabilities.

S_g	K_{rg}	K_{ro}
0.414	0	0.205718
0.512	0.0079	0.0177
0.539	0.0157	0.0088
0.621	0.0301	0.005
0.66	0.0614	0.0033
0.718	0.0873	0.0023
0.914	1	0

Table 3.6—RC8 gas and oil base relative permeabilities.

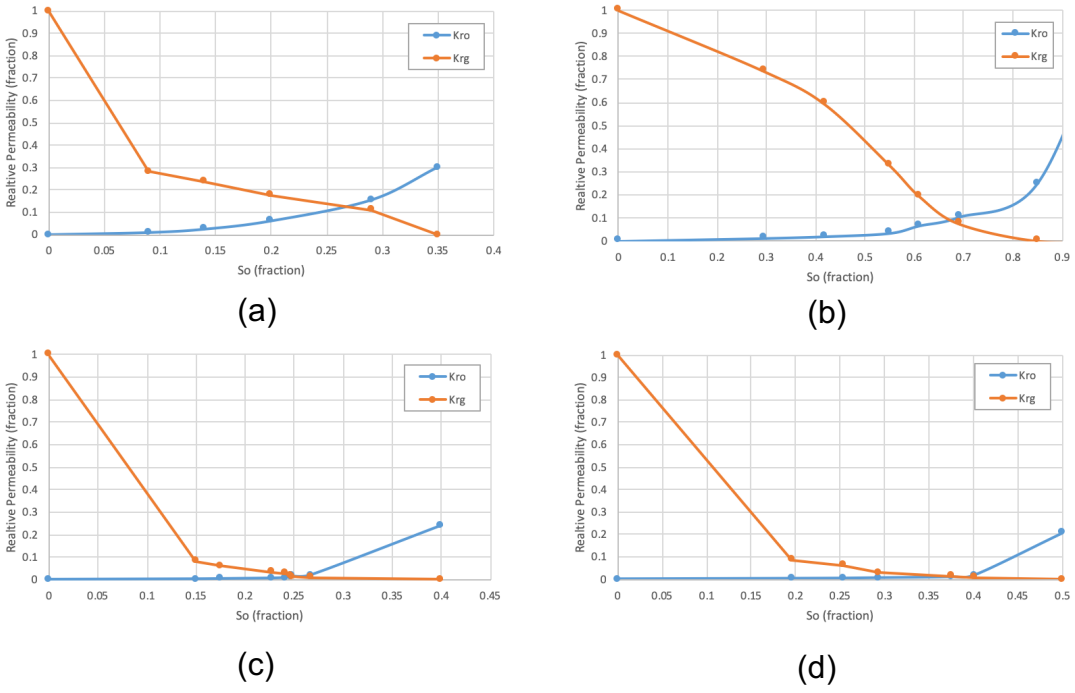

Figure 3.2—Plots of gas and oil base relative permeabilities for (a) RC1, (b) TC11, (c) RC6, and (d) RC8.

3.4 Fluid Properties

The spectrum of fluid used in this study varies. For the two-phase gas condensate fluids, a binary fluid composed of methane (C1) and n-decane (C10) with different condensate richness have been used–i.e. lean, moderate, and rich. On the other hand, for the single-phase scenarios, dry-gas and black oil were used. Table 3.7 shows a summary of the variation in compositions, apparent molecular weight (AMW), dew point pressure of each of the gas condensate fluid type and maximum liquid dropout (MLDO)–illustrated in **Figure 3.3**.

Component	Lean	Moderate	Rich
C1 (%)	95	91.5	88.5
C10 (%)	5	8.5	11.5
AMW	21.9	26.1	29.6
Dew point pressure (psia)	4259.8	5043	5288.5
MLDO (%)	6	15.6	27

Table 3.7—Fluid properties for gas condensate fluid under study.

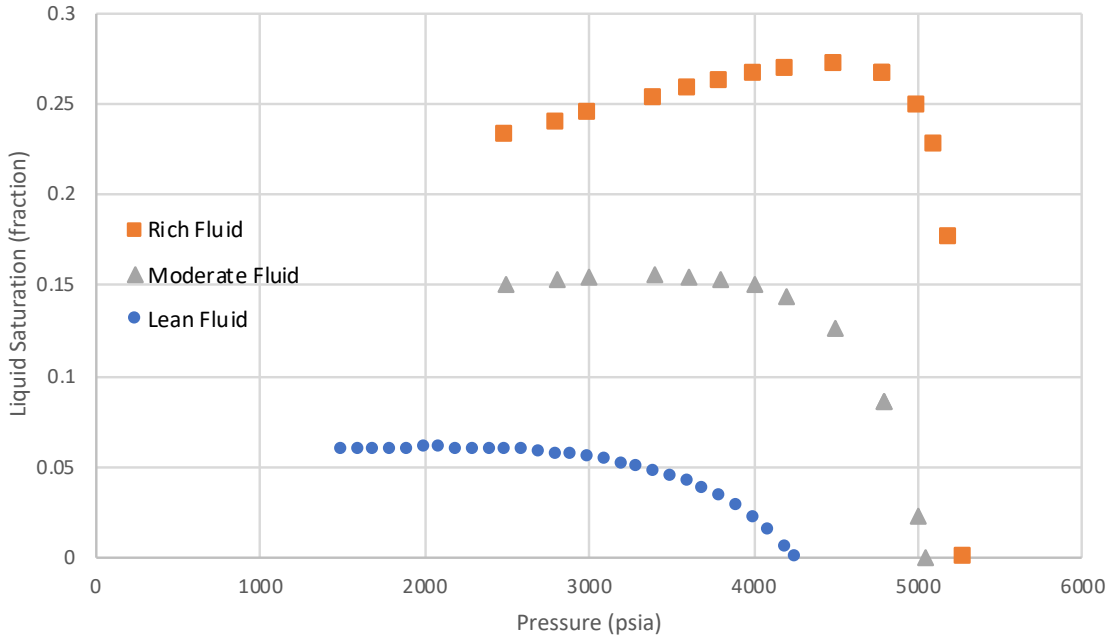

Figure 3.3—Liquid saturation curves for the three different fluids.

Constant composition expansion (CCE) and constant volume depletion (CVD) PVT tests are used to describe a gas condensate fluid and determine parameters such as density, volume and composition of liquid and gas phases for gas condensate fluid (Raghavan & Jones 1996; Whitson et al. 2000). In the CCE test, the fluid in the cell is expanded while the fluid composition remains constant and the volume occupied by each phase is noted at each expansion step. On the other hand, in the CVD test, the cell volume is kept constant, and excess gas is removed at each step at constant pressure and the properties at each stage and volume are measured (Danesh 1998). Due to gas removal in the CVD tests, the potential for further condensate dropping out of the gas is less than in the CCE tests (Dandekar 2013); hence CCE test predicts higher condensate saturation. Xu and Lee (1999) showed that fluid PVT properties (such as viscosity and density) in both lab CCE and CVD processes are good approximations of the actual reservoir properties.

The PVT properties of the fluids in this study were obtained by simulating laboratory experiment using the commercial software PVTi. The simulator uses the modified Peng-Robinson Equation of State (EOS). The CCE test, which would better represent the near wellbore gas-condensate flow behaviour, was used to output the density, viscosity and z-factor versus pressure. For the oil system, the fluid is set to be dead oil with a viscosity of 0.456 cp, and density of 53 lb/ft3.

3.5 Velocity-Dependent Model

The low interfacial tension (IFT) of gas-condensate systems dictates a flow regime that is different from conventional gas-oil systems. The dependency of gas-condensate relative permeability on velocity and pressure due to coupling (an increase in gas relative permeability with an increase in velocity or a decrease in IFT) and inertia (a decrease in gas relative permeability with an increase in velocity) adds further complexity to any interpretation of pressure or rate data (Henderson et al. 1997; Jamiolahmady et al. 2000).

Throughout this study, for the gas-condensate system, when velocity effects (inertia, coupling or both) need to be implemented in the data, it can be activated using the velocity-dependant relative permeability keyword in ECLIPSE 300, "VELDEP", and a model developed by the gas-condensate recovery research team at Heriot-Watt University (Henderson et al. 2000)—where empirical correlations were developed based on the relative permeability behaviour to the variation in fluid saturation, velocity and IFT. The model description below is from Henderson et al. (2000) where the capillary number is computed using the following formulation:

$$N_c = \frac{v_g \, \mu_g}{\sigma_{gc}} \tag{3.1}$$

where v_g is the gas velocity, μ_g is the gas viscosity and σ_{gc} is the IFT between gas and condensate. N_{cni} is the capillary number ratio of the base capillary number (N_{cbi}) to the capillary number of the required curve (N_{ci}). N_{cni} is defined as:

$$N_{cni} = \frac{N_{cbi}}{N_{ci}} \tag{3.2}$$

Base relative permeabilities are then adjusted by positive coupling effect using the following relationship:

$$k_{ri}(N_c) = (N_{cni})^{1/n_i} \, k_{rbi} + \left(1 - (N_{cni})^{1/n_i}\right) k_{rmi} \tag{3.3}$$

where k_{rbi} is the base relative permeability curve measured at the lowest capillary number (lowest velocity at the highest IFT), and k_{rmi} the miscible permeability curve (i is the phase, gas or condensate), expressed as:

$$k_{rmi} = \frac{(S_i - X_i S_{irb})}{(1 - X_i S_{irb})} \tag{3.4}$$

where X_i is a function from the relationship between capillary number ratio and residual phase ratio between base curve and the sought curve:

$$X_i = 1 - e^{(-mN_{cni})} \tag{3.5}$$

and exponent n_i is given as:

$$n_i = n_1 S_i^{*n_{2i}} \tag{3.6}$$

where S_i^* is the normalised phase saturation, given as:

$$S_i^* = \frac{S_i}{1-S_{wc}} \tag{3.7}$$

and m, n_1 and n_2 are obtained experimentally.

VELDEP keyword uses the base conventional relative permeability data (those not affected by coupling and inertia) to generate relative permeability at various velocity and pressure values for any grid block at any time.

There are four key triggers in the VELDEP keyword:

- "0 0 0 0": will not introduce inertia and coupling to the system, which means that the base relative permeability data provided will not change due to velocity effects.
- "0 0 0 2": activates inertia model only for gas.
- "1 1 0 0": activates coupling model only for gas and oil.
- "1 1 0 2": activates both coupling and inertia. This mode is the most important in terms of realism and is what will be used for most of the cases in this study when both effects are considered. Both effects would be competing with each other; in most cases considered here the coupling has the dominant overall effect of improving the gas relative permeability.

It is important to note the significance of velocity effects on the gas relative permeability, as previously shown in Figure 2.6 and Figure 2.7. To demonstrate the effect of coupling and inertia on a rich gas-condensate fluid productivity, four runs were made for each key trigger in the VELDEP keyword. That is, the first run was made with no inertia and no coupling, the second with only

inertia, the third with only coupling, and the fourth with both inertia and coupling. **Figure 3.4** shows the pressure drawdown for all the four scenarios.

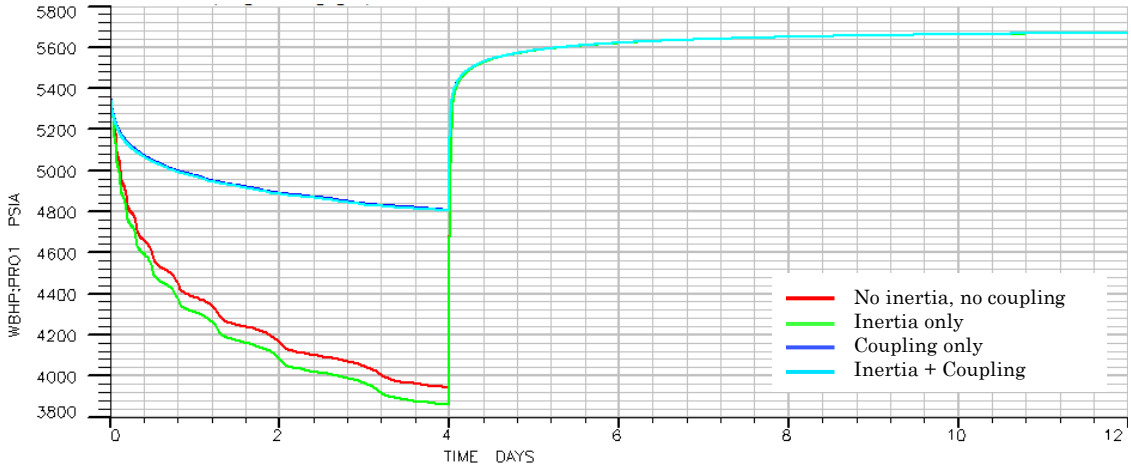

Figure 3.4—Changes in pressure drawdown, as shown in well bottom-hole pressure (WBHP), due to velocity effects.

Productivity index, $J = \frac{q}{\Delta p}$, can calculated to translate drawdown to well productivity. It can be observed that with only inertia introduced, there was a drop in the performance compared to the scenario where both inertia and coupling are deactivated. On the other hand, when coupling was activated, it showed great improvement in the productivity of the well dominating the inertia effect.

Chapter 4

Pressure Versus Distance Profile for Well Testing Buildup Data

4.1 Introduction

The work in this chapter expands on that of calculating the pressure versus radius profile from pressure transient data using the probe radius concept as first introduced by Osorio et al. (2005) for gas-condensate systems. In this chapter, the focus is to validate its applicability and define its limitations. To do this, first, it was tested for single-phase scenarios, before moving to more complex gas-condensate systems. In other words, the concept of calculating pressure versus radius profile from well test pressure versus time data was first applied to a single-phase oil system. Then a single-phase compressible gas system that requires single-phase pseudo-pressure was considered.

Once the results of the single-phase systems are positive, the method was then extended to the two-phase gas-condensate system, where both gas and condensate coexist and flowing. Initially, cases were studied with different fluid richness where velocity effects (inertia and coupling) were inactive all proving that the application of calculating pressure versus radius profile from buildup data for gas-condensate reservoirs is reliable. However, later, the focus was on cases where both inertia and coupling were active, to represent a realistic gas condensate fluid behaviour.

The resulting pressure versus radius profiles can be used to estimate condensate bank extent, which is a critical information to assess how deep the condensation buildup is around the well. Besides, Chapter 5 will discuss the ability to use the pressure versus radius profiles to estimate velocity-dependent relative permeability data as a function of pressure in the vicinity of the well within the reservoir.

First, a description of the probe radius concept and the pressure profile calculation method are discussed, followed by a highlight on the benefits of having pressure versus radius data. Then the results of the single-phase and the two-phase systems exercises are presented followed by sensitivity analysis on fluid richness, model gridding and rock quality.

4.2 Definition of the Probe Radius

Probe radius is the radius at which the flowing pressure in the reservoir at the time before shut-in is equal to the current well pressure measured with time at the wellbore during well test operation after shut-in. Peaceman (1978) through two independent mathematical derivations (using Bessel series and the Ei function), showed that the probe radius and the shut-in time are related by the following equation (converted to oilfield units):

$$\frac{k\Delta t_e}{\emptyset \mu c_t r_m^2} = 1689 \qquad (4.1)$$

In Equation 4.1, $\emptyset$ is the porosity, k is the absolute permeability, μ is the viscosity, c_t is the total compressibility, r_m is the probe radius, and Δt_e is the equivalent shut-in time, as suggested by Agarwal (1980):

$$\Delta t_e = \frac{t_p \, \Delta t}{t_p + \Delta t} \qquad (4.2)$$

In Equation 4.2, Δt is the time elapsed from the start of the transient test (buildup), and t_p is the effective producing time at a constant rate (drawdown).

The concept suggests that a given pressure change, Δp, which is measured at a shut-in time, Δt, during a buildup would have occurred in the reservoir at a distance, r_m, away from the well at the end of the preceding drawdown (**Figure 4.1**). In other words, Equation 4.1 converts bottomhole pressures from a buildup test into the reservoir pressure versus radius within the reservoir at the end of the drawdown period using the recorded shut-in buildup pressure versus time data.

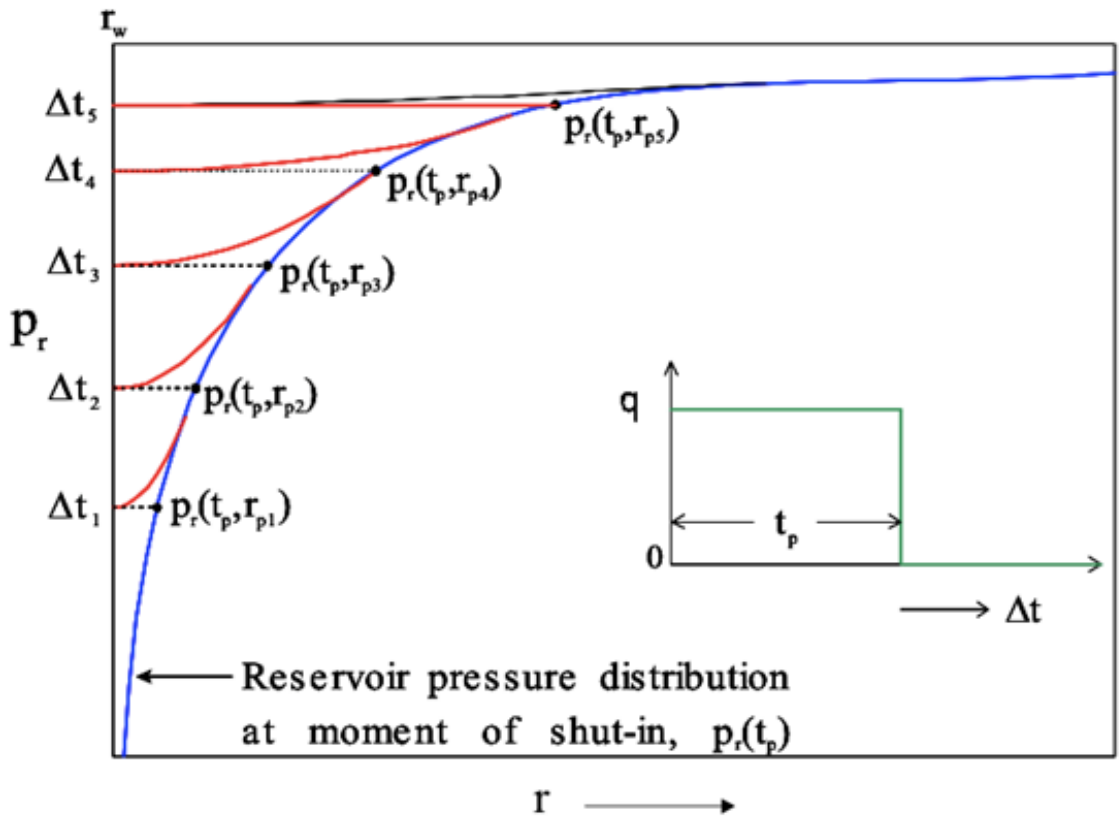

Figure 4.1—Illustration of probe radius concept (Osorio et al. 2005).

This was not considered to be a practical tool from well test analysis point of view given the fact that absolute permeability must be available. However, the way Equation 4.1 is going to be used is by solving for reservoir mobility.

In this thesis, to test the capability of calculating pressure versus radius, a numerical simulator is used where well test data (pressure drawdown and buildup) is used as an output, which is assumed to be equivalent to measured well test data; thus, through the numerical simulator's output, pressure versus

radius is also available to be compared with the calculated pressure profile for validation.

4.3 Calculating Pressure Versus Radius Profile

The first step in calculating the pressure versus radius profile requires both permeability, k, and viscosity, μ. Hence, mobility is defined as:

$$\lambda = \frac{k}{\mu} \tag{4.3}$$

Thus, Equation 4.1 can be re-arranged to give:

$$r_m = 0.02434 \sqrt{\frac{\lambda \, \Delta t_e}{\phi c_t}} \tag{4.4}$$

For the case where the oil system is used for validation purposes, mobility can be defined as:

$$\lambda = \frac{70.62 \, q_o \, B}{h \, \Delta p'} \tag{4.5}$$

where q_o is the flow rate of oil, B is the formation volume factor for oil, h is the formation thickness, and $\Delta p'$ is the derivative of pressure, Δp, with respect to the log of time.

Mobility for gas is obtained from the constant rate solution of the diffusivity equation including pseudo-pressure derivative, as described by Lee and Wattenbarger (1996):

$$\lambda_g = \frac{k}{\mu_g} = \frac{711 \, q_g \, T}{\mu_g \, h \, p_p(p')} \tag{4.6}$$

where q_g is the gas flow rate, T is the temperature, μ_g is the gas viscosity, h is formation thickness, and $p_p(p')$ is the time log derivative of pseudo-pressure, $p_p(p)$ as introduced by Al-Hussainy et al. (1966), expressed by:

$$p_p(p) = 2 \int_{p_b}^{p_i} \frac{p}{\mu(p) \, z(p)} dp \tag{4.7}$$

Theoretically, λ_g would reflect any changes with distance, as $p_p(p')$ changes. Any change in mobility from the condensate region to the single-phase gas region is accounted for in the values of the pseudo-pressure derivative, $p_p(p')$.

For gas-condensate systems, two-phase mobility term includes two-phase pseudo-pressure derivative, which require relative permeability data to compute. Such relative permeability data as a function of pressure are not available, therefore, in the proposed procedure, initially, single-phase pseudo-pressure data are used. Two-phase pseudo-pressure can replace these data once relative permeability data are available.

For all the gas and gas-condensate cases discussed in this thesis, the procedure of calculating pressure profile starts as following: first, the well bottom-hole pressure data from the numerical simulation is obtained (**Figure 4.2**).

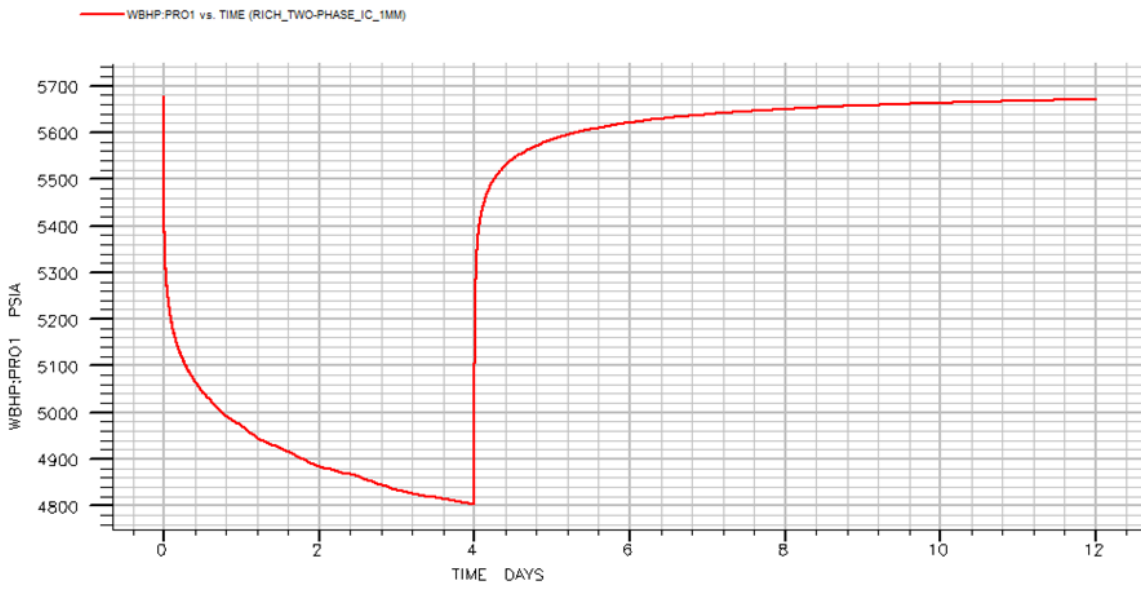

Figure 4.2—Example of well bottom-hole pressure (WBHP) versus time for a two-phase gas-condensate case numerically generated using a simulation software.

Single-phase pseudo-pressure $p_p(p)$ is then calculated by Equation 4.7. Using well test analysis software, such as PanSystem, with the calculated single-phase pseudo-pressure table, the buildup data are analysed to obtain the pseudo-pressure derivative with respect to time. These pseudo-pressure derivative data

with respect to time are then used in Equation 4.6 to obtain gas mobility values for each point in time. Since all parameters are only a function of pressure, the gas mobility, at each shut-in time, is easily calculated. Once the gas mobility values are calculated, Equation 4.4 is used to calculate radius values for each pressure point. Given the pressure values at each time at which a radius has been calculated, the pressure versus radial distance can be constructed (**Figure 4.3**).

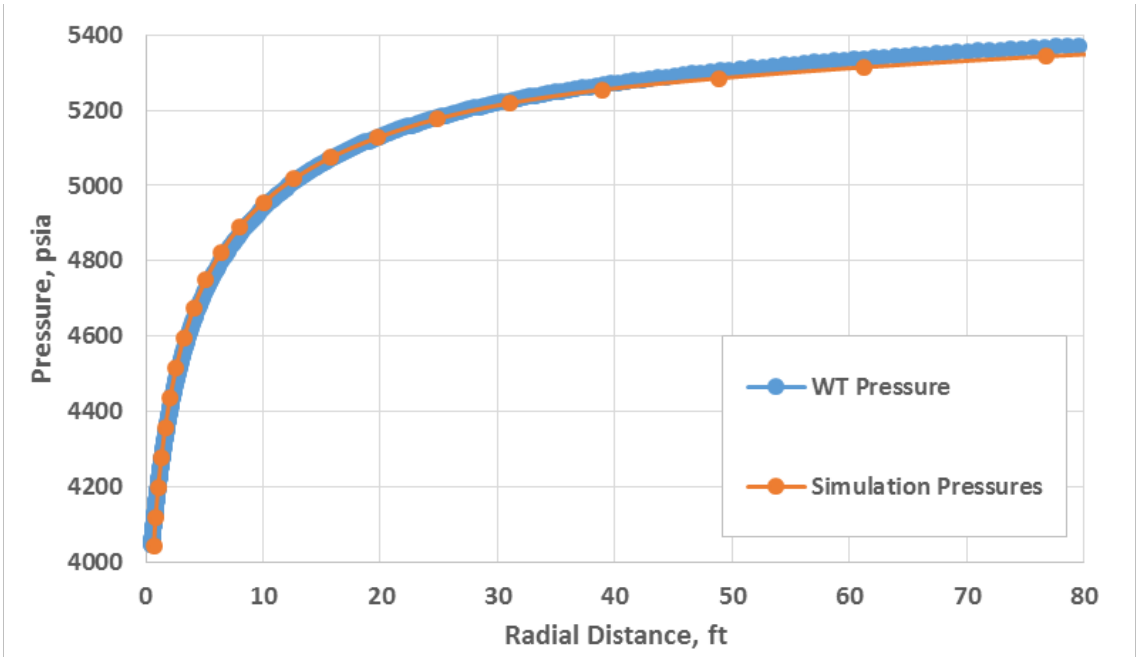

Figure 4.3—Example of pressure versus distance profile calculated from well test buildup data and compared with the numerical simulation output.

For the oil system case, Equation 4.5 is used instead of Equation 4.6 to calculate mobility, and pressure is used instead of pseudo-pressure.

In a systematic manner and to verify the reliability of data generated at the first stage, in this work, the analytically calculated pressure versus radius profile is compared with the pressure profile obtained from the numerical simulations that are available in this study (Figure 4.3). The data are verified by obtaining a good match with the output from the numerical simulator, before utilising the results in the next stage where relative permeabilities are calculated (Chapter 5).

4.4 Benefits of Pressure Versus Radius Profile in a Two-Phase Reservoir

Here, two main benefits of the pressure versus radius profile are discussed. The first, as shown later in section 4.6.3, is that it can be used to determine the extent of the condensate bank around the well. The second benefit, which will be discussed in Chapter 5, is that it can be used to generate pressure derivative with respect to distance to be used to calculate gas-condensate relative permeability data analytically.

In this thesis, the ultimate goal of this technique, besides obtaining the pressure versus radius profile, is to use it to calculate the relative permeability as a function of pressure for two-phase gas condensate systems. One of the advantages of knowing the relative permeability data as a function of pressure is that it allows us to calculate the two-phase pseudo-pressure, which is needed for any two-phase-based analysis technique, to accurately describe the two-phase flow. The difficulty of working with the two-phase pseudo-pressure is that it needs relative permeability data, which are not available.

4.5 Single-Phase Systems

Initially, the concept of calculating pressure versus radius profile was applied to a single-phase gas system. Upon finding some deviations between the analytically calculated profile and that from the numerical simulation, it was necessary to test the method on a single-phase oil system, for validation purposes as the original equations have been developed for slightly compressible liquid systems.

In both cases, the applicability of calculating pressure versus radius profile using buildup data was verified by producing reliable results that match the reservoir simulation output.

4.5.1 Pressure Profile—Oil System

For the single-phase oil system, a case was set-up where reservoir Model 1 (Table 3.1) was used with reservoir thickness of 50 ft and using the RC10 rock data (Table 3.2) and a black oil fluid system. Equation 4.4 was used to construct the pressure versus radius profile. **Figure 4.4** shows a comparison of the pressure versus radius profile, obtained from the numerical simulation with that calculated analytically from the well test data. Figure 4.4 shows that for a single-phase oil system, there is a perfect match between the two pressure profiles. Thus, it proves that the concept is reliable, and the approach and constructed model is validated. Next, the concept is tested for a single-phase gas system.

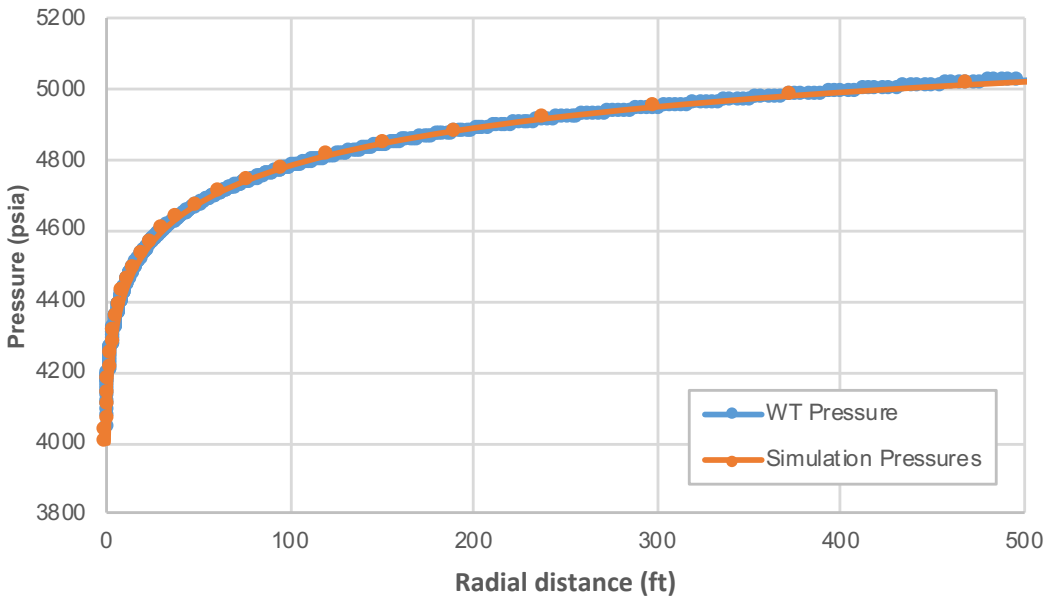

Figure 4.4—Comparison of pressure versus radius profile calculated based on probe radius with the corresponding profile output from the numerical simulation for the single-phase dead oil case.

4.5.2 Pressure Profile—Dry Gas System

For the single-phase dry gas system, a case was set up using the same reservoir model, Model 1 (Table 3.1), with RC1 rock data (Table 3.2) and a moderate richness gas condensate fluid (Table 3.7), but the pressure was always kept

above the dew point, to maintain the single-phase conditions. Pressure versus radius profile was then calculated using the described method. **Figure 4.5** compares the calculated pressure versus radius profiles with that from the numerical simulation. In this scenario, instead of pressure, pseudo-pressure was used.

As it is noted there is a good agreement between the two; however, after about 60 feet, there is a deviation in the pressure profile compared to the simulation pressure. To eliminate any scenario-based errors, the same procedure was followed for another case with slightly different rock properties. This time, the porosity was changed to 34.6% instead of 17.3%, (**Figure 4.6**) which resulted in the same trend of the mismatch at a distance further away from the well.

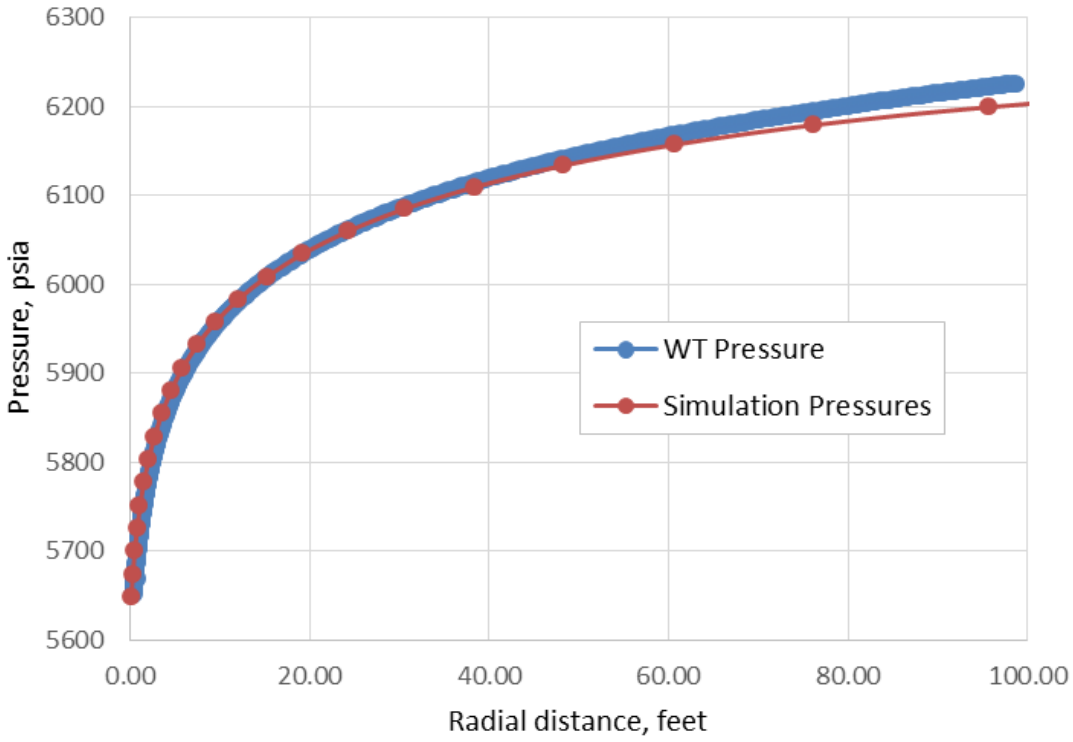

Figure 4.5—Comparison of pressure versus radius profile calculated based on probe radius with the corresponding profile output from the numerical simulation for the single-phase gas case.

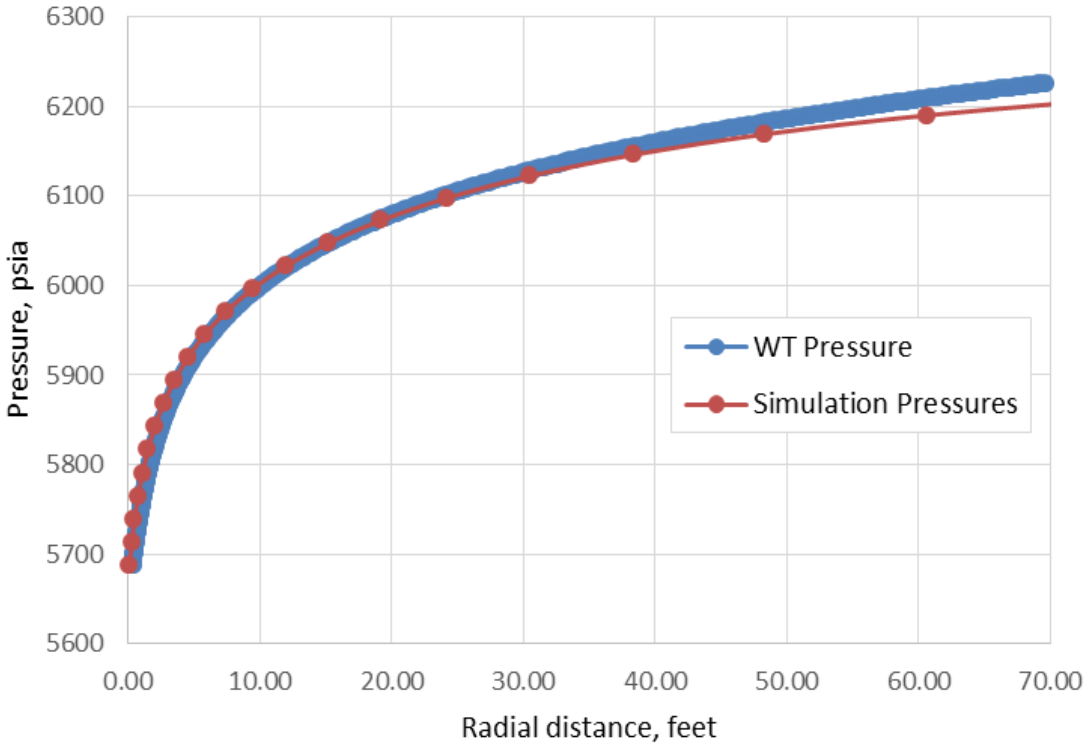

Figure 4.6—Comparison of pressure versus radius profile calculated based on probe radius with the corresponding profile output from the numerical simulation for the single-phase gas case with porosity of 0.346.

4.5.3 Model Grid Size Sensitivity

Before proceeding further, it has been established that the deviation in the pressure versus radius profile calculated from well test data compared to the simulated pressure profile, for the single-phase gas systems, is most likely to be the result of the pseudo-pressure approximation. However, to eliminate the possibility that the reservoir model gridding system might have influenced the deviation, a specific alteration to the grids was implemented and tested against the current model. Instead of having the grids increasing logarithmically away from the wellbore, ending up with large cells away from the well compared to the cells nearer the well, the grids were set to have a small uniform size of 20 ft each across the whole flow domain—except for the first 50 ft around the well where smaller grids were considered to have a better resolution of flow dynamics due to velocity effects around the wellbore (**Figure 4.7**).

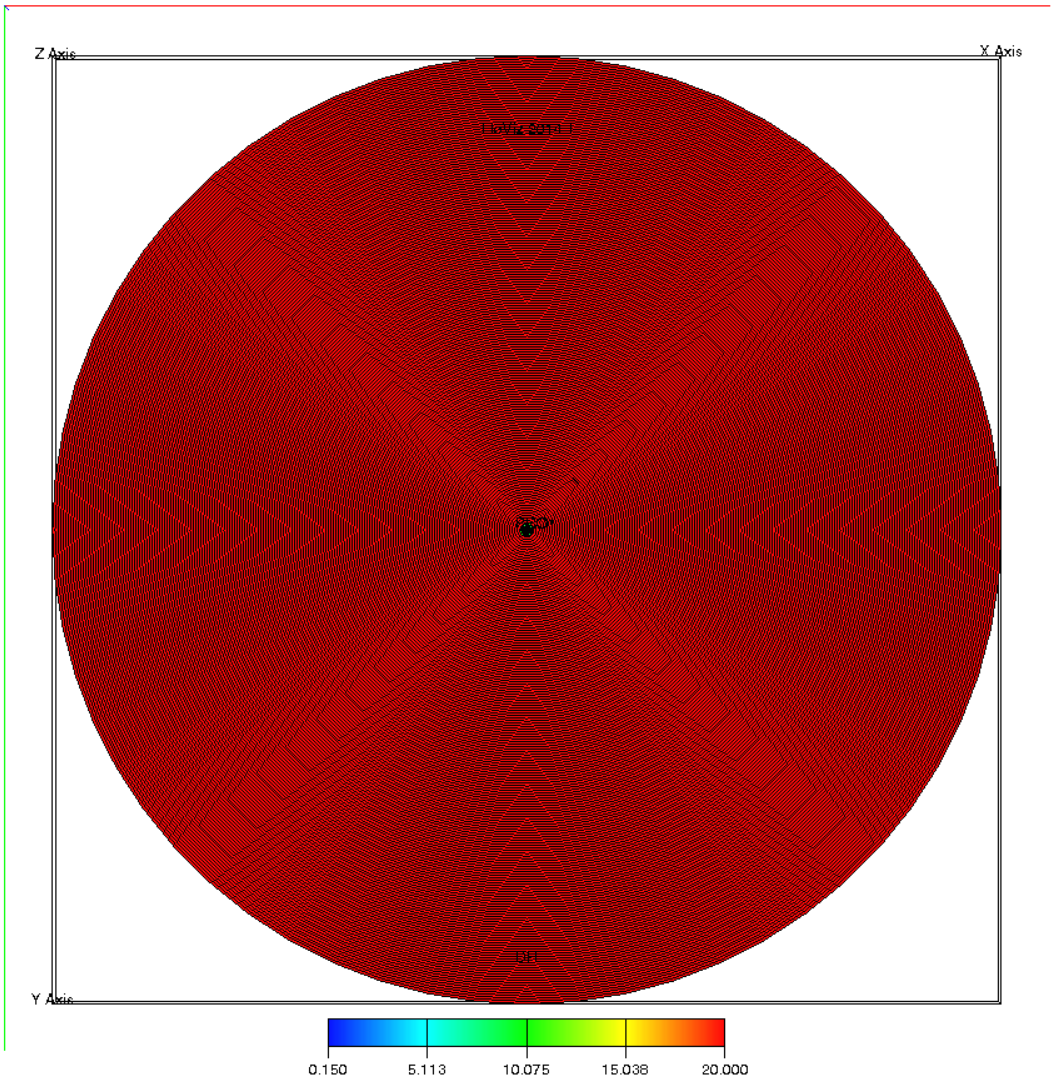

Figure 4.7—Snapshot of the reservoir model using uniformly small-sized grid-blocks.

This resulted in a significant increase in the number of grids for the reservoir with the same outer radius value. Hence, the number of grids is set to be 200 instead of 40 for Model 1.

The simulated bottom-hole pressure data of the new model was analysed for a rich gas condensate, and the pressure versus radius profile was obtained. The result (**Figure 4.8**) was showing the same deviation trend existed in original reservoir model of 40 logarithmically increasing grid-blocks (**Figure 4.9**). Figure 4.10 shows an overlay comparison between the two different pressure

profiles obtained using different gridding models. Therefore, this eliminated the possibility that such a deviation in the pressure versus radius profile could be due to the grid-size distribution. The data fluctuation at about 40 ft were a reflection of data noise in the well test pressure versus time and can be ignored or removed by smoothing the original data set (as will be discussed later in section 5.4).

At this point, it is safe to assume that the deviation is due to the approximation of the pseudo-pressure function and not artificially generated due to the numerical grid system. It is to note that, it takes much longer to run the simulation model with 200 smaller grid-blocks, compared to that with 40 logarithmically increasing grid-blocks. As there was no improvement gained on the results, the logarithmically increasing grid-blocks distribution was considered for all the remaining study.

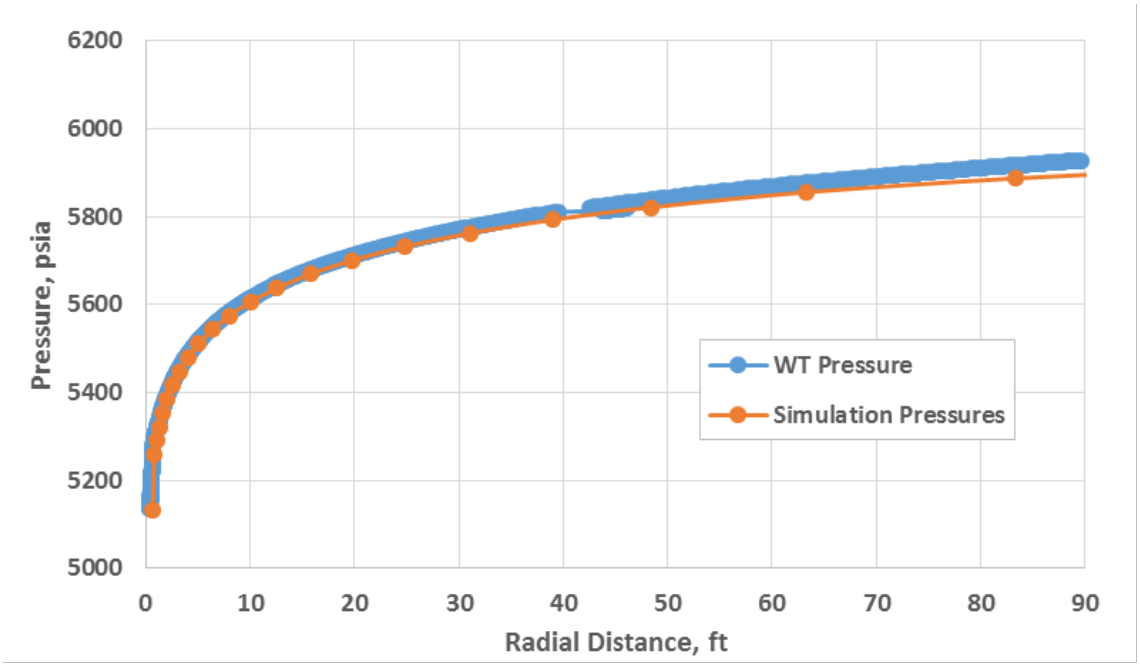

Figure 4.8—Pressure versus radius profile calculated by probe radius compared to the corresponding numerical simulation data, uniform size reservoir model of 200 grid-blocks.

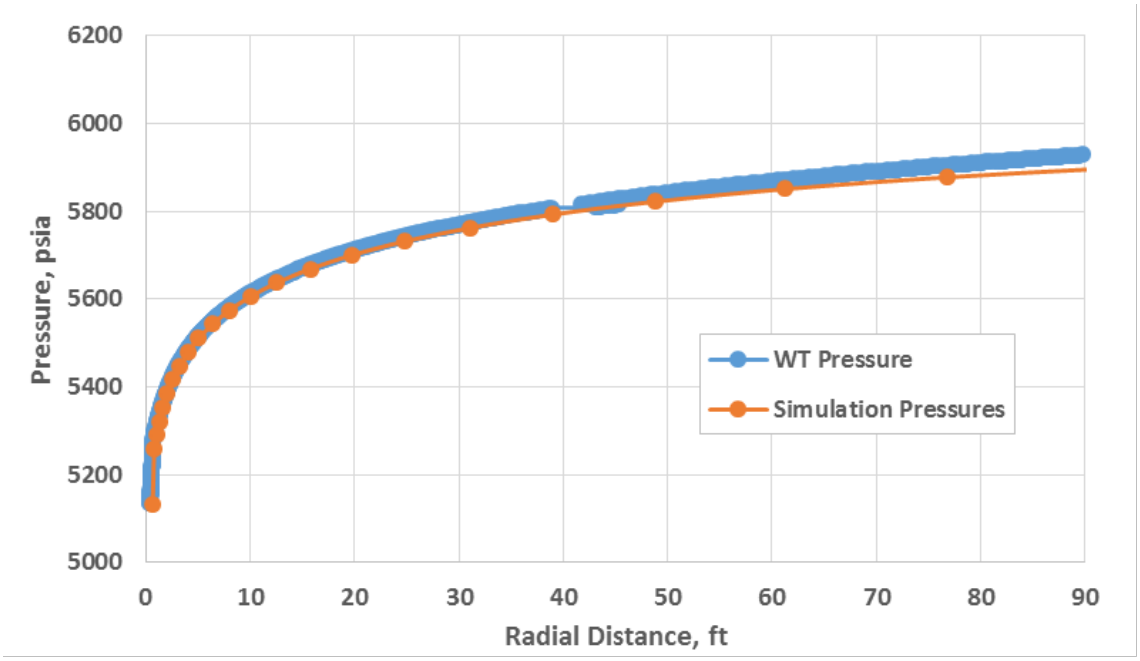

Figure 4.9—Pressure versus radius profile calculated by probe radius compared to the corresponding numerical simulation data, original reservoir model of 40 grid-blocks increasing logarithmically.

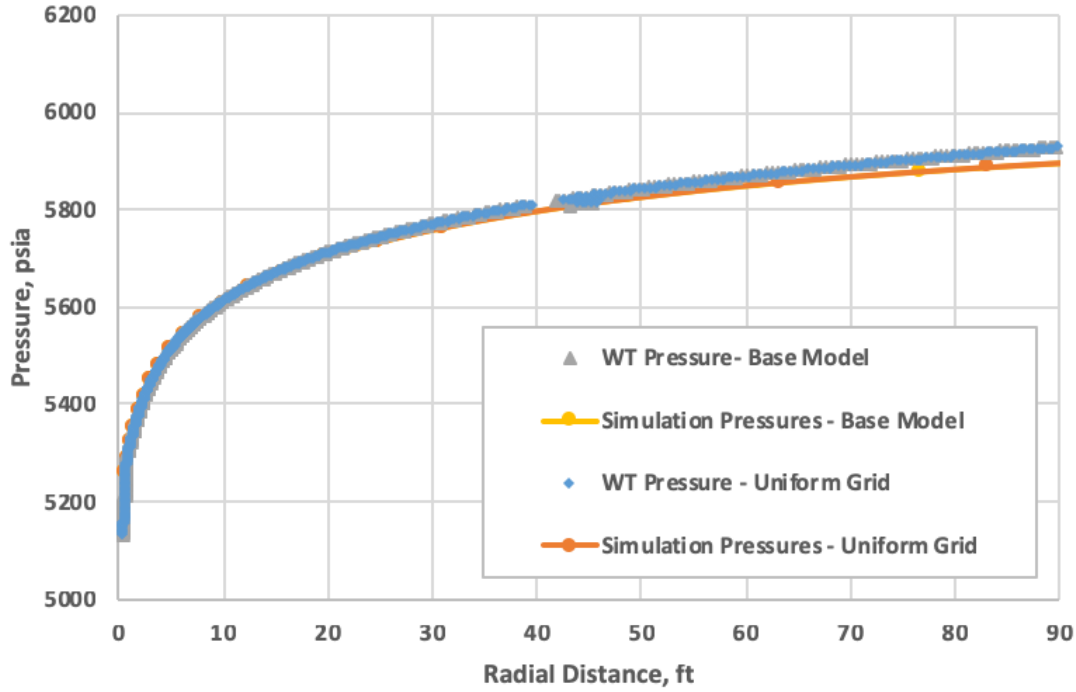

Figure 4.10—A comparison between pressure versus radial distance using two different gridding system.

4.5.4 Conclusion and Discussion

From the results above, it was concluded that the extension of the concept originally developed for a liquid with small and constant compressibility to a gas system works with a small caution, that the data further away from the wellbore will have a slight deviation in the pressure profile. This deviation is believed to be due to the pseudo-pressure approximation (Equation 4.7). That is, the diffusivity equation was derived from three principles: conservation of mass, equation of state for slightly compressible liquids, and Darcy's law. In order to propose a mathematical solution to the diffusivity equation it must assume that fluid viscosity, μ, and total compressibility, c_t, are constant. This derivation gives the known diffusivity equation form for liquids:

$$\frac{1}{r}\frac{\partial}{\partial r}\left(r\frac{\partial p}{\partial r}\right) = \frac{\phi\mu c_t}{0.000264\,k}\frac{\partial p}{\partial t} \tag{4.8}$$

To replace the slightly compressible liquid equation of state with that of gas would results in a more complex and non-linear equation. However, it can be partially linearised by using the pseudo-pressure function (Equation 4.7), that is repeated here:

$$p_p(p) = 2\int_{p_b}^{p_i}\frac{p}{\mu(p)\,z(p)}dp \tag{4.7}$$

which gives the following diffusivity equation for gas:

$$\frac{1}{r}\frac{\partial}{\partial r}\left(r\frac{\partial p_p}{\partial r}\right) = \frac{\phi\mu c_t}{0.000264\,k}\frac{\partial p_p}{\partial t} \tag{4.9}$$

This equation is then subjected to the corresponding boundary and initial conditions to obtain the corresponding semi-log equations describing the variation of pressure with time within the wellbore during the drawdown and buildup tests. It should be noted that for buildup the superposition for a linear system is also applied to give the Horner time function.

In summary, the application of liquid-based equations has been extended to gas systems, with large variations in their fluid properties (i.e. viscosity and

density) with pressure, using the pseudo-pressure concept, Equation 4.7. Therefore, it is suggested that this discrepancy between original derivation and the approximated solution is the source of the deviations between the gas pressure versus radius calculations and the numerical simulation data as they are perfectly matched for the liquid case, Figure 4.4.

It is worth noting that for this work's purpose, what is important is the area around the wellbore, where condensate is forming, and velocity effect is in action; hence this pressure versus radius profile technique can be applied given that the results are approached cautiously beyond the point of deviation.

4.6 Two-Phase System

In this section, the application of probe radius concept is extended to two-phase gas-condensate systems, with different fluid richness and with and without velocity effects. This part is the most important, as ultimately the goal is to utilise the generated pressure versus radius profile to calculate relative permeability data (Chapter 5), and two-phase pseudo-pressure. Successful results here mean that the method can be used in two-phase gas-condensate flow conditions.

The procedure followed is similar to that for the single-phase system. This time; however, the synthetic well bottom-hole pressure data are obtained from the numerical simulation of flow for two-phase gas-condensate conditions (e.g. the system pressure is allowed to drop below the dew point for the condensate to develop in the reservoir, mainly around the wellbore).

4.6.1 Fluid Richness Sensitivity

As a start, three cases with different fluid richness were set, to test the fluid richness sensitivity. The three levels of richness are lean, moderate, and rich (Table 3.7). All the three cases were based on the RC1 rock data (Table 3.2) with reservoir Model 1, and the velocity-dependant keyword (VELDEP) in the numerical simulator turned off (e.g. no inertia or coupling are considered)–as

the aim here is only to observe how the pressure profile calculation respond to different condensate richness.

The pressure versus radius profile was calculated using Equation 4.4 for each case and then compared with the corresponding pressure profile output from the numerical simulation data as shown in **Figure 4.11, Figure** 4.12 and **Figure** 4.13 for lean, moderate and rich, respectively.

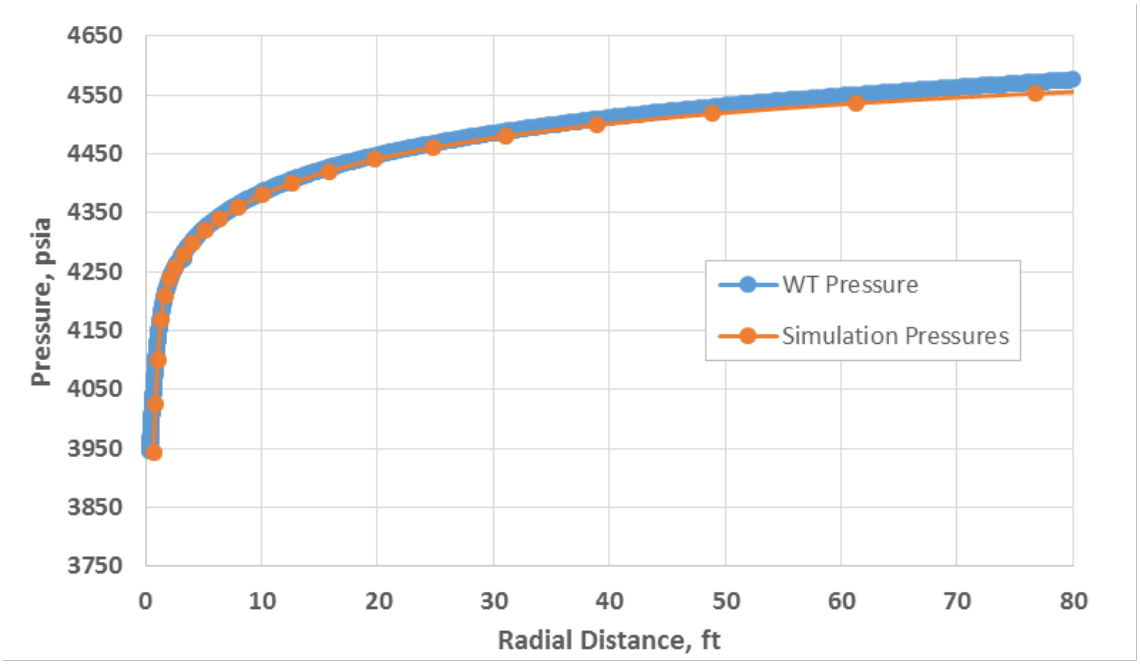

Figure 4.11—Pressure versus radius profile calculated by probe radius compared to the corresponding numerical simulation data, two-phase lean gas-condensate.

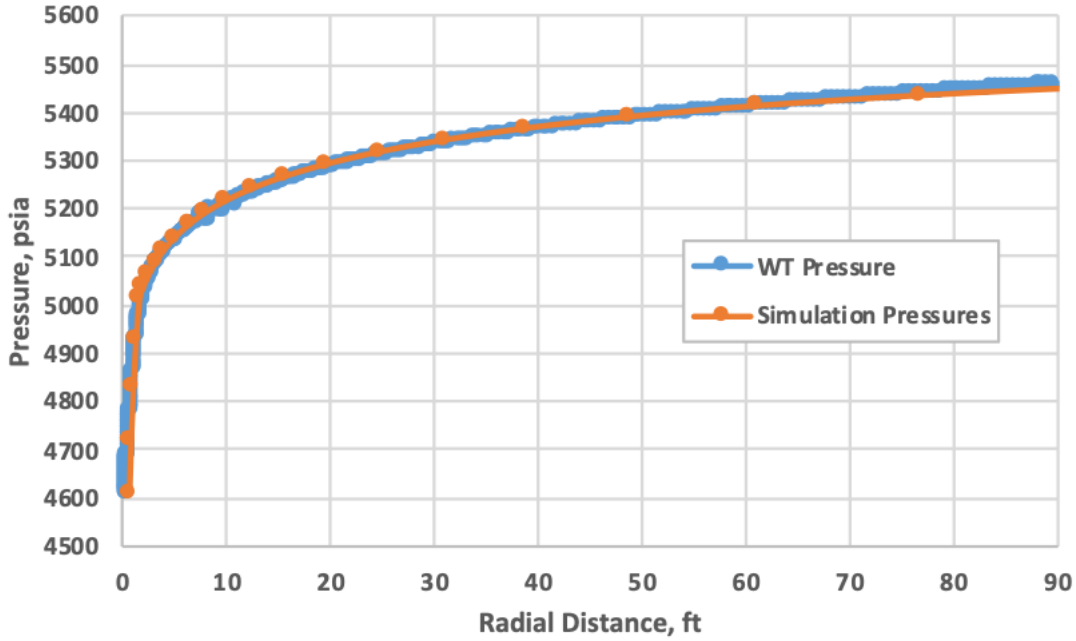

Figure 4.12—Pressure versus radius profile calculated by probe radius compared to the corresponding numerical simulation data, two-phase moderate gas-condensate.

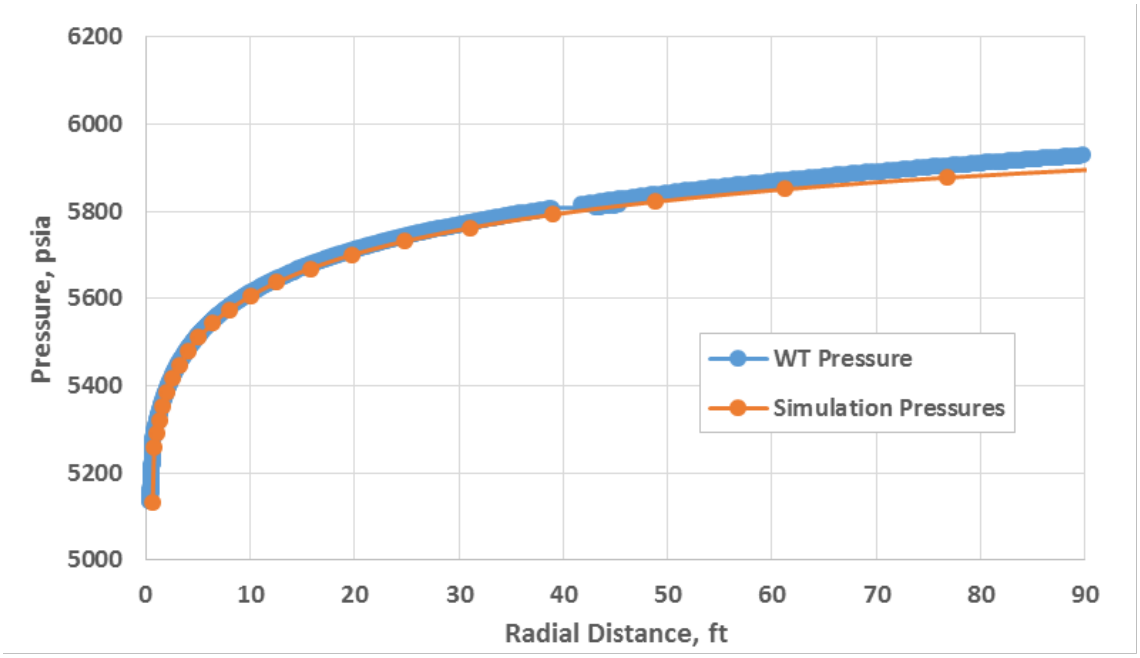

Figure 4.13—Pressure versus radius profile calculated by probe radius compared to the corresponding numerical simulation data, two-phase rich gas-condensate.

Figure 4.11, Figure 4.12 and Figure 4.13 show that the calculated pressure versus radius profiles obtained from well test data are closely matching the pressure profiles obtained from the numerical simulator for all the three different fluid richness which further confirms the applicability of the approach for two-phase gas-condensate systems when two-phase exist and flowing around the wellbore. That is, the pressure versus radius profiles obtained from well test data are reliable.

4.6.2 Rich Fluid with Different Rocks Models

Up to this point, it has been verified that the concept works on single-phase oil, single-phase gas, and two-phase gas-condensate at different fluid richness without velocity effects with. However, the ultimate goal is to apply the method on two-phase flow conditions where the velocity effect is significant, which is a more realistic scenario for gas-condensate reservoirs. As a result, the velocity-dependant keyword (VELDEP) was turned on for both coupling and inertia in the numerical simulator (as discussed in section 3.5). In this section, the scenario with maximum two-phase presence is considered–that is the cases presented below are based on rich gas-condensate system. As with lower condensate richness, the effect of two-phase and velocity effects will always be less.

Four cases of single constant-rate buildup tests are discussed in this section. During the production in all cases, the aim was for the pressure to go below dew-point enabling the condensate to form around the well. Table 4.1 summarises the four cases. In the first three cases, reservoir Model 1 (Table 3.1) was used with 40 grids in the radial direction, and an outer radius of 5000 ft, which is large enough to avoid well test data hitting the boundary. For Case 4, however, a larger reservoir, Model 2, was used as RC8 higher permeability requires bigger outer radius to ensure the boundary dominated flow is not attained. Initial reservoir pressures were varied for each case. The criteria for their selection was basically to have enough pressure drop,

depending on the used production rate value, to change the reservoir condition from single-phase gas to two-phase gas and condensate.

Case	Rock	Drawdown (days)	Buildup (days)	Gas Rate (MMscf/D)
Case 1	RC1	4	8	1
Case 2	RC1	4	16	1
Case 3	RC6	4	8	50
Case 4	RC8	4	8	170

Table 4.1—Characteristic of the considered single-rate cases.

The first case, Case 1, was simulated based on the RC1 rock properties (Table 3.2) using reservoir Model 1. The well test design was set to have four days of drawdown with a flowing gas rate of 1 MMscf/D followed by eight days of buildup (**Figure 4.14**) with an initial reservoir pressure of 5700 psia. **Figure 4.15** shows the calculated pressure versus radius profile for Case 1.

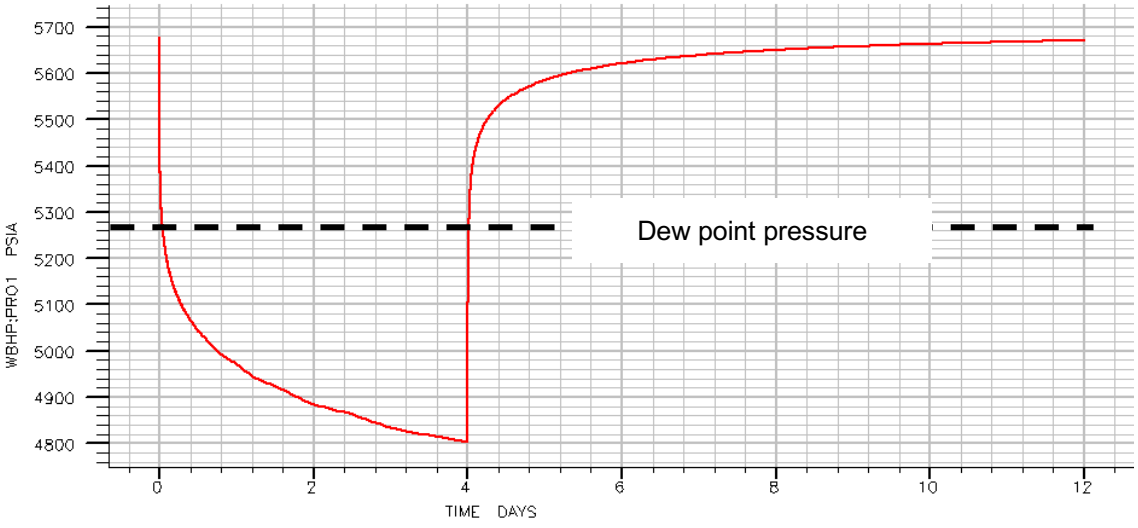

Figure 4.14—Well bottom-hole pressure (WBHP) versus time for Case 1.

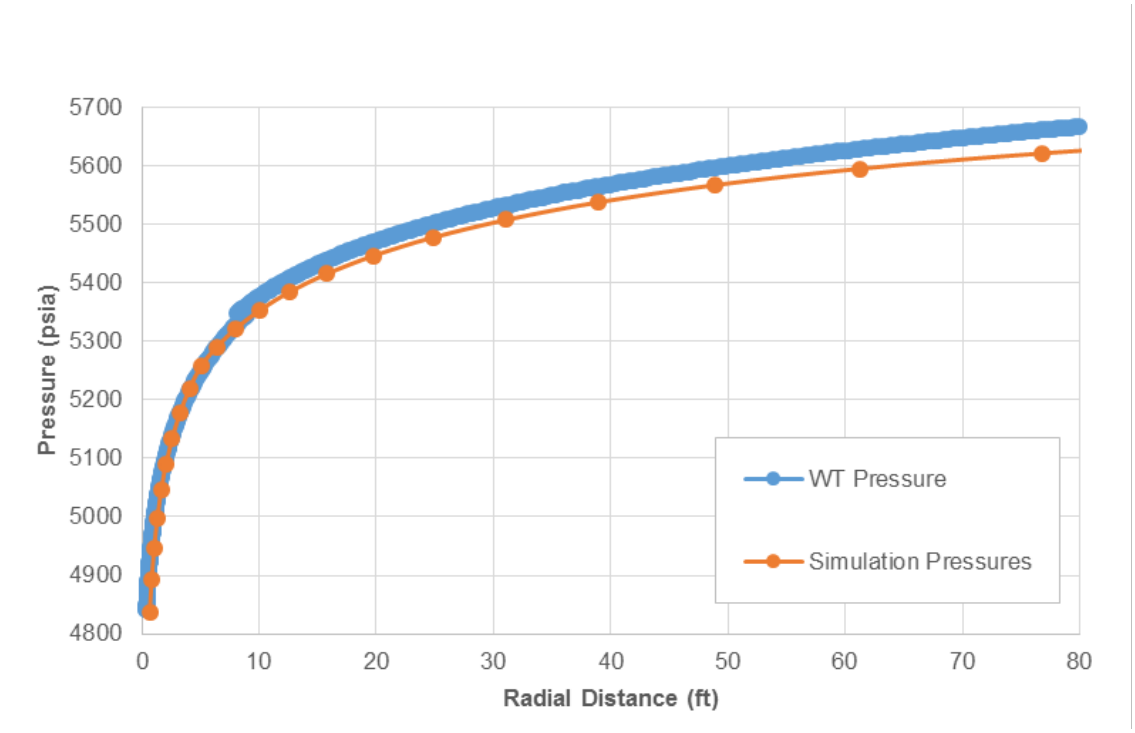

Figure 4.15—Pressure versus radius profile calculated by probe radius compared to the corresponding numerical simulation data for Case 1.

Case 2 is based on the same rock properties, RC1, with reservoir Model 1 but this time to encourage more condensate development around the well, the drawdown period was extended to 16 days instead of four days (**Figure 4.16**) with an initial reservoir pressure of 5500 psia. **Figure 4.17** shows the calculated pressure versus radius profile for Case 2.

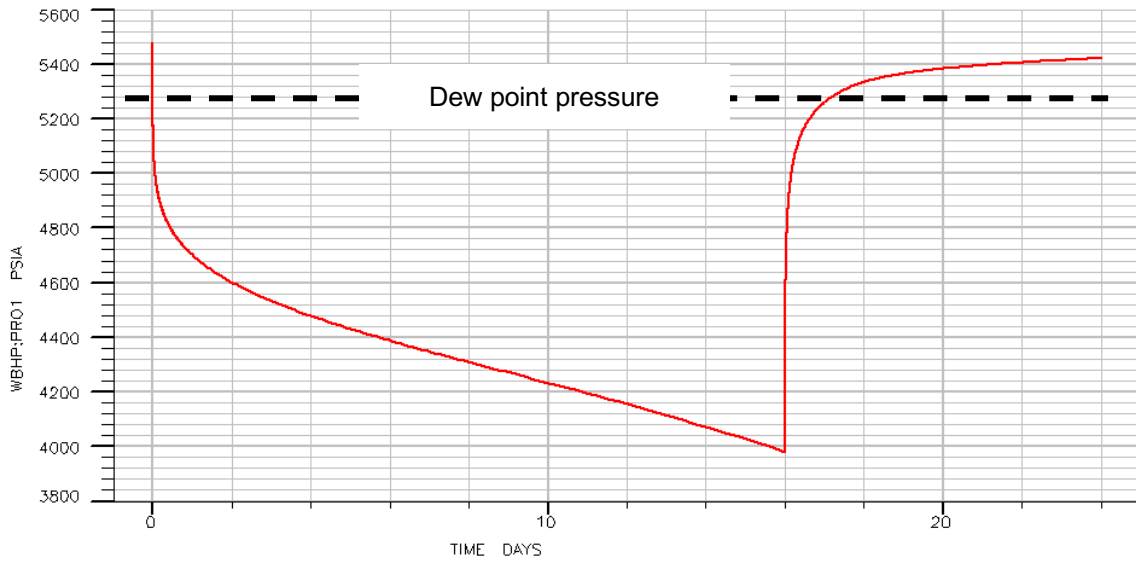

Figure 4.16—Well bottom-hole pressure (WBHP) versus time for longer production, Case 2.

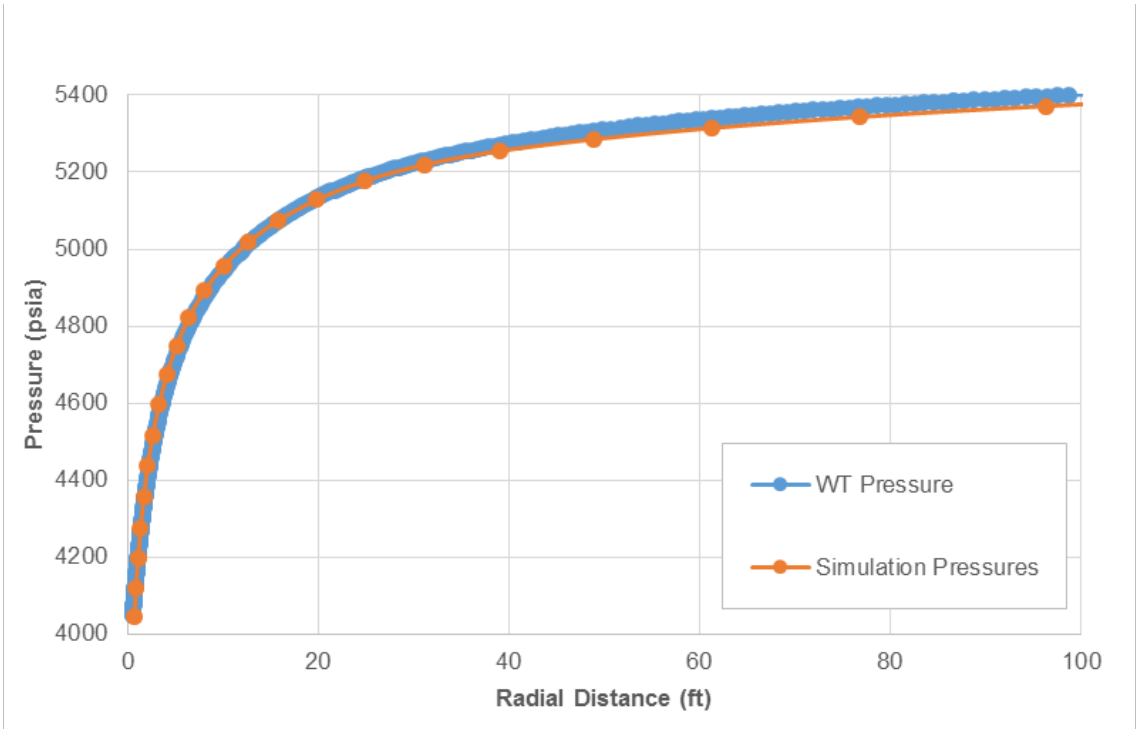

Figure 4.17—Pressure versus radius profile calculated by probe radius compared to the corresponding numerical simulation data for Case 2.

Case 3 is based on the RC6 rock properties and reservoir Model 1, with a drawdown period of four days followed by eight days buildup. This case was

analysed to test the concept on a higher permeability rock, i.e. 23.6 mD. It was set with an initial reservoir pressure of 5400 psia and a flowing gas rate of 50 MMscf/D (**Figure 4.18**). The calculated pressure versus radius profile for Case 3 is shown in **Figure 4.19**.

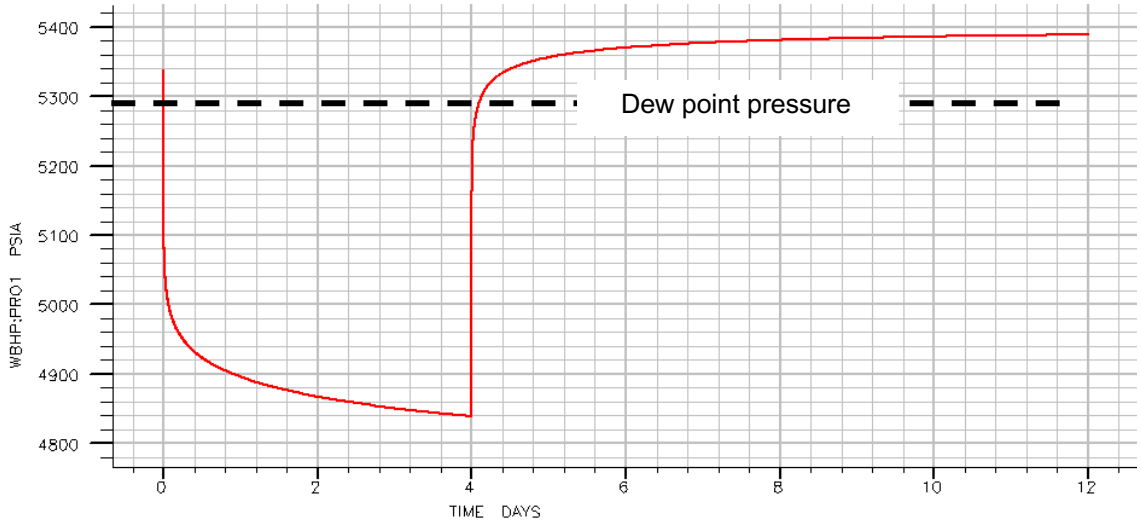

Figure 4.18—Well bottom-hole pressure (WBHP) versus time for Case 3.

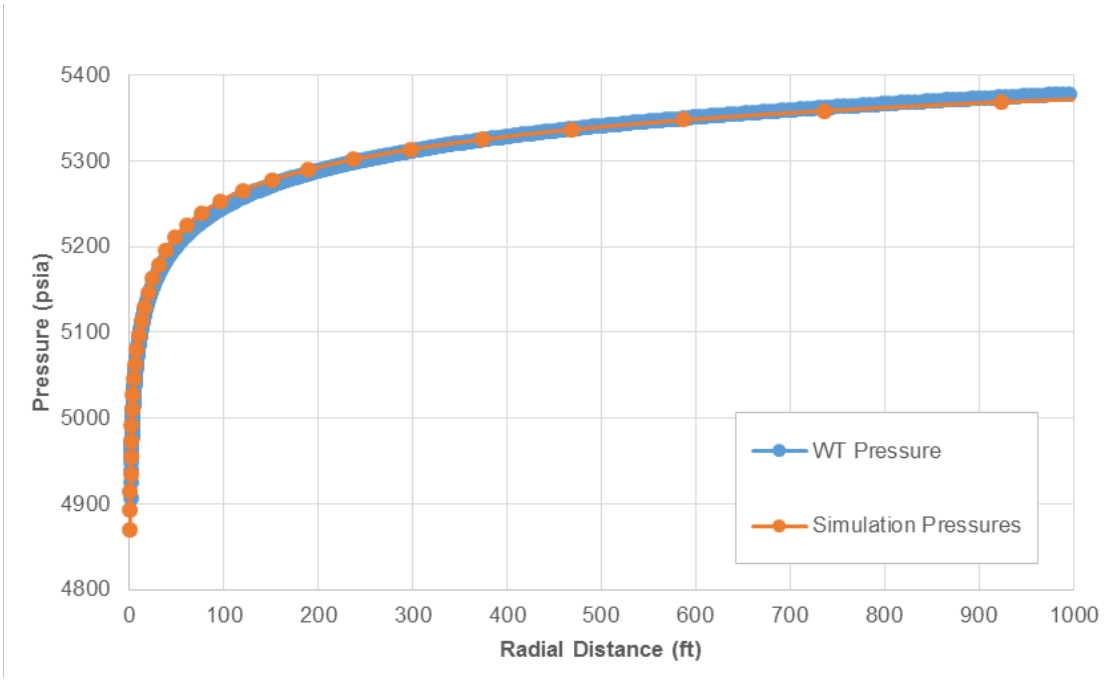

Figure 4.19—Pressure versus radius profile calculated by probe radius compared to the corresponding numerical simulation data for Case 3.

Case 4 is based on the RC8 rock properties, which was analysed to test the concept with even higher permeability rock, i.e. 120 mD, as production conditions and velocity effect should change accordingly. Drawdown was set to be four days followed by eight days buildup with an initial reservoir pressure of 5400 psia and a flowing gas rate of 170 MMscf/D (**Figure 4.20**). The calculated pressure versus radius profile for Case 4 is shown in **Figure 4.21**.

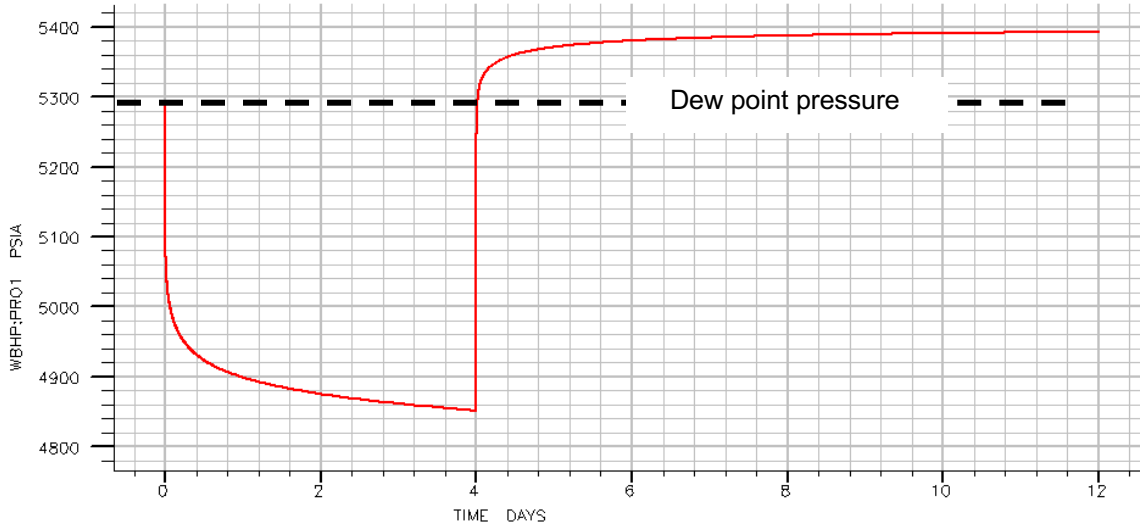

Figure 4.20—Well bottom-hole pressure (WBHP) versus time for Case 4.

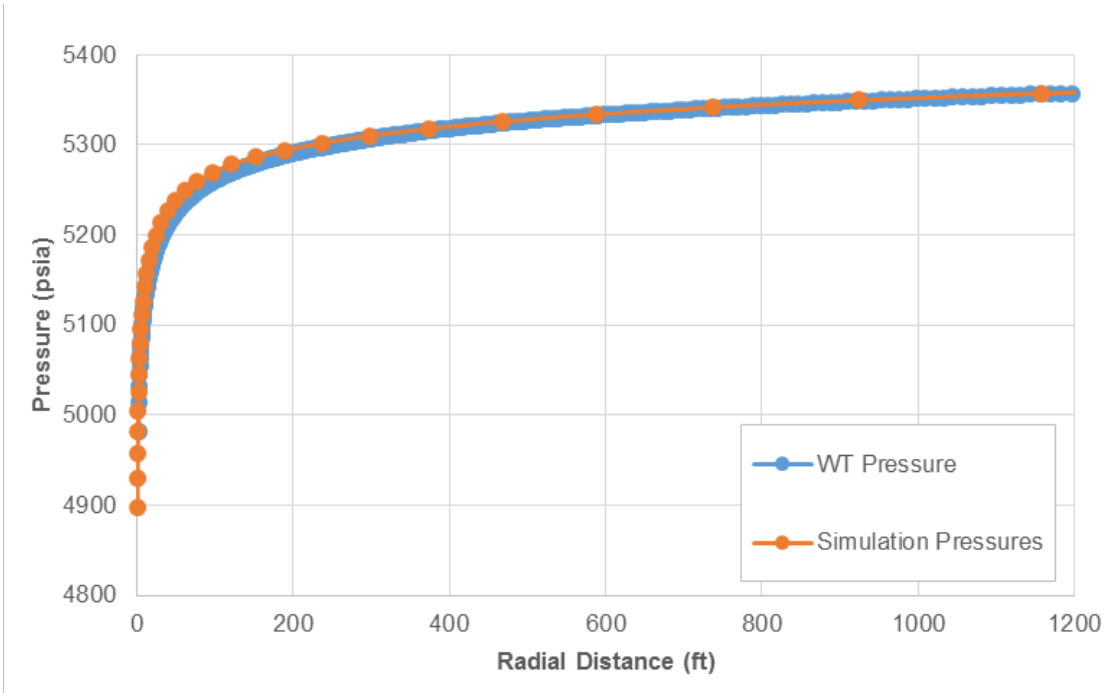

Figure 4.21—Pressure versus radius profile calculated by probe radius compared to the corresponding numerical simulation data for Case 4.

Overall, the calculated pressure versus radius profiles from well test data for gas-condensate system with velocity effects closely match the pressure profile from the numerical simulation. This suggests that the method is reliable for gas-condensate applications considered here.

4.6.3 Condensate Bank Extent from Pressure Versus Radius Profile

As mentioned earlier, one of the benefits of the pressure versus radius profile is the ability to determine the radial extent of the condensate bank around the wellbore. By having pressure versus radius profile, and knowing the dew point pressure, the radial extent of the condensate can be determined.

In the earlier cases, given the dew point of 5288.5 psia for the rich gas condensate, the extent of the condensate bank is estimated to be approximately 6, 43, 196 and 187 ft away from the wellbore for Cases 1, 2, 3 and 4, respectively. These values reasonably match the corresponding condensate bank radius values from the simulation output as shown in Table 4.2.

	Depth of the condensate bank (ft)	
	Estimated from pressure profile	**Numerical simulation radius when $k_{ro}>0$**
Case 1	6	6
Case 2	43	54
Case 3	196	183
Case 4	187	168

Table 4.2—Condensate extent in the reservoir, estimated from the pressure versus radius calculated from well test compared to the numerical simulation output.

4.7 Conclusion

This chapter examines the reliability of calculating pressure versus radius profile from pressure versus time buildup data from tests on wells in gas-condensate reservoirs. The calculation is based on the probe radius concept originally proposed for single-phase systems.

The concept of calculating pressure profile was first applied for the single-phase oil and single-phase gas systems. The results were then verified showing excellent agreement between the calculated pressure versus radius profile and those output from the corresponding numerical simulation. A slight deviation was noticeable far away from the wellbore in the case of single-phase gas systems, but there was no deviation along the whole distance tested in the case of single-phase oil systems. This deviation was attributed to the approximation in the pseudo-pressure concept accounting for the gas compressibility and viscosity variation with pressure. It should be noted that the difference between the well test-based pressure versus radius profile and that based on the numerical simulation data for the gas system is not significant. Furthermore, the thesis is focusing more closely on the area around the wellbore, where velocity effect plays a significant role, and there are no such deviations in the nearer to the well, i.e. the concept should work for that purpose. The applicability of the method was then tested for two-phase gas-condensate

systems with good agreement between the two pressure profiles for different fluid richness and with and without velocity effects. At this stage, the author is comfortable to say that the calculated pressure versus radius profile in two-phase gas-condensate systems gives consistent results under the conditions considered in this work.

- The method also shows that the condensate bank extent around the wellbore can be successfully determined from the pressure versus radius profile when the dew point pressure is known.

- It is to note that the primary goal of calculating pressure versus radius profile from well test data is to use it in relative permeability calculations for two-phase gas condensate systems, which is discussed in next chapter.

Chapter 5

Velocity-Dependent Two-Phase Relative Permeability from Well Test Data

5.1 Introduction

One of the main goals of this thesis is to improve the two-phase analysis of well test and production data in gas-condensate reservoirs. To attain this goal, it is essential to use the two-phase pseudo-pressure concepts to describe the flow behaviour around the wellbore accurately, where two-phase flow exists. However, the two-phase pseudo-pressure calculation needs relative permeability data as a function of pressure, which are not usually available. One of the benefits of calculating the reservoir pressure versus radius profile from well test data—as presented in Chapter 4, is that it can be used to obtain the relative permeability data, in the vicinity of the well as will be presented in this chapter.

The approach relies on a reasonable approximation of relative permeability data, calculated analytically, from the pressure gradient at any measured point using two-phase Darcy flow theory and the assumption of steady-state flow near the wellbore. The steady-state assumption applies for gas-condensate systems when the total composition of the single-phase fluid entering the two-phase region is close to that produced at the wellbore and is valid after an

initial period of rapid condensate buildup. Under such conditions, there is mass transfer between the two phases, but the overall composition remains constant as the condensate that drops out around the wellbore by the flowing gas is equal to that flowing out to the wellbore and produced. Additionally, it has been shown, for a single-phase fluid, that pressure behaviour under pseudo-steady-state and transient condition is close to that of steady-state behaviour near the wellbore which is the primary interest here (Stewart & Jamiolahmady 2016). In this thesis, the results show that the assumption of steady-state would work within the conditions considered in this work, as will be discussed in section 5.5.

Common relative permeabilities data are usually obtained from core measurements in the lab and reported based on saturation. However, when they are measured using the steady-state method they can be reported as a function of fractional flow. The work presented in this thesis is around pressure data, so it is convenient that saturation data are not needed, that is a relationship between pressure (and its gradient) and relative permeability is sufficient as captured by the proposed approach. In other words, in this method saturation data, which are not available, do not enter into the calculation as relative permeabilities data depend only on pressure and its gradient. Considering that in this method relative permeabilities data are not reported as a function of saturation would suggest that such data are of limited use for other applications. However, it has to be added that if velocity effects are important, the near-wellbore relative permeability data obtained here are the ones that most simulators would use as a function of pressure in their calculations. That is, most reservoir simulators use a formulation that calculate velocity dependent relative permeability with base relative permeability data, which are not velocity dependent, as one input. If near-wellbore velocity effects are important, the other input data are core-specific constants which determine the impact of velocity on relative permeability. These core specific constants are usually determined by history matching of production data or the corresponding velocity dependent relative permeability data measured in the

laboratory on the core samples under steady-state conditions. These measurements are demanding and costly, therefore, calculating relative permeability data from available well test data is practically very attractive.

5.2 Analytical Calculation of Velocity-Dependent Relative Permeability Method

This chapter relies on the results of the earlier chapter (Chapter 4). That is, in order to calculate relative permeability from well test data, the pressure versus radius profile is needed.

The method involves the calculation of the pressure derivative with respect to radial distance from the estimated pressure versus radius profile. These data are then used in the following equations (Equations 5.1 and 5.2) to estimate gas relative permeability (k_{rg}) and oil relative permeability (k_{ro}). These two equations derived in Appendix-A are based on Darcy's law and the steady-state assumption that should be valid for near wellbore area.

$$k_{rg} = \frac{1}{5.615} \frac{m_T \mu_g (1-x)}{\alpha_1 kh\, \rho_g r \left(\frac{\partial \mathrm{p}}{\partial r}\right)} \tag{5.1}$$

$$k_{ro} = \frac{1}{5.615} \frac{m_T \mu_o x}{\alpha_1 kh\, \rho_o r \left(\frac{\partial \mathrm{p}}{\partial r}\right)} \tag{5.2}$$

where m_T is the total gas plus condensate mass rate, x is the liquid mass fraction, kh is the flow capacity (permeability by thickness), ρ_o and ρ_g are the condensate and gas densities, μ_o and μ_g are the condensate and gas viscosities, r is the radius, α_1 is a unit conversion factor for oilfield unit system (0.007082), and $\left(\frac{\partial \mathrm{p}}{\partial r}\right)$ is the velocity dependent pressure gradient at radius r. The absolute permeability value in this equation can either be estimated from the single-phase gas region or obtained from other sources (e.g. logs, cores, previous well tests).

It should be noted that the relative permeability data calculated using this method would include velocity effects due to coupling and inertia. To verify the reliability of the calculated relative permeability data at this stage, they are compared with the corresponding values obtained from the numerical simulations as output.

The calculated relative permeability data initially was affected by numerical issues when calculating the differential component $\left(\frac{\partial p}{\partial r}\right)$ in Equations 5.1 and 5.2 which resulted in noise and fluctuations. As a result, an investigation on the source of the noise and a solution to overcome this issue is discussed in the next section.

5.3 Workflow Summary

In this section, a summary of the steps involved in the proposed methods is presented as a workflow. The aim is to make a connection on how the approach works from one concept to another. The workflow can be described in three stages (Figure 5.1). In addition, Appendix-B shows a tabulated sample of data calculations involved for stage one (pressure versus radius profile) and two (relative permeability as a function of pressure) below.

Stage one is where well test pressure derivative is used to calculate gas mobility and calculate pressure versus radius profile. This stage was described in detail in Chapter 4.

In stage two, the gradient of pressure versus radius is used to calculate gas and oil relative permeabilities at any measured point using the two-phase Darcy flow theory and the assumption of steady-state flow near the wellbore. This has been described in this chapter.

Finally, in stage three, with the available velocity-dependent relative permeability data as a function of pressure, the two-phase pseudo-pressure is

calculated and can be utilised for other reservoir description and management purposes (e.g. analysis of nearby wells, analysis of two-phase production data).

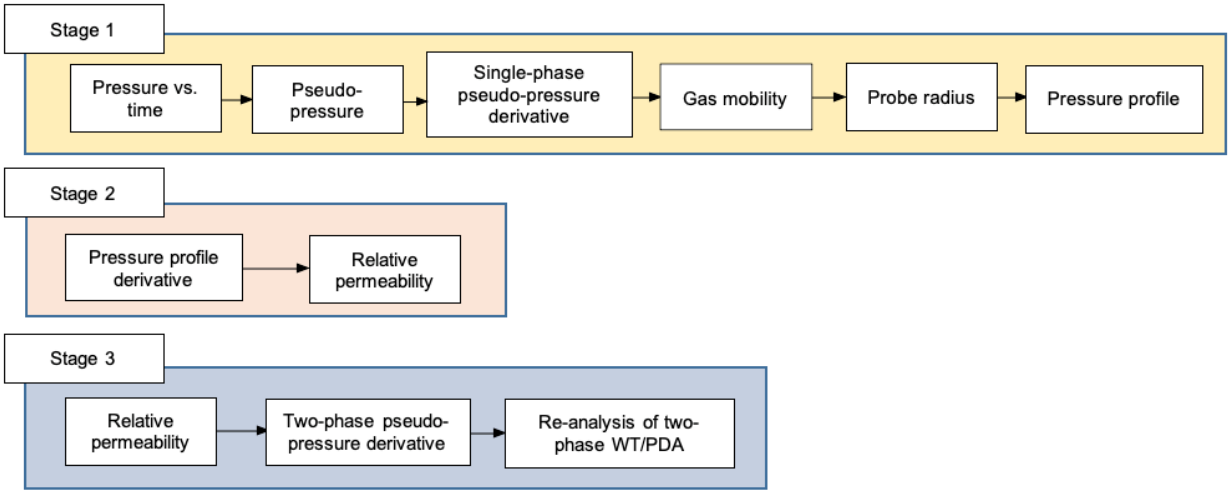

Figure 5.1—Workflow for the suggested methodology to calculate pressure profile and kr data, in addition to two-phase pseudo-pressure.

5.4 Numerical Dispersion in the Pressure Derivative

5.4.1 Introduction

Initially, the calculated relative permeability data were suffering from large oscillations (**Figure 5.2**) which were attributed to the derivative nature of the calculation. The source of the noise can be seen in a close-up look at the pressure versus radius profile (**Figure 5.3**) and is traced back to the pressure derivative data of the buildup tests.

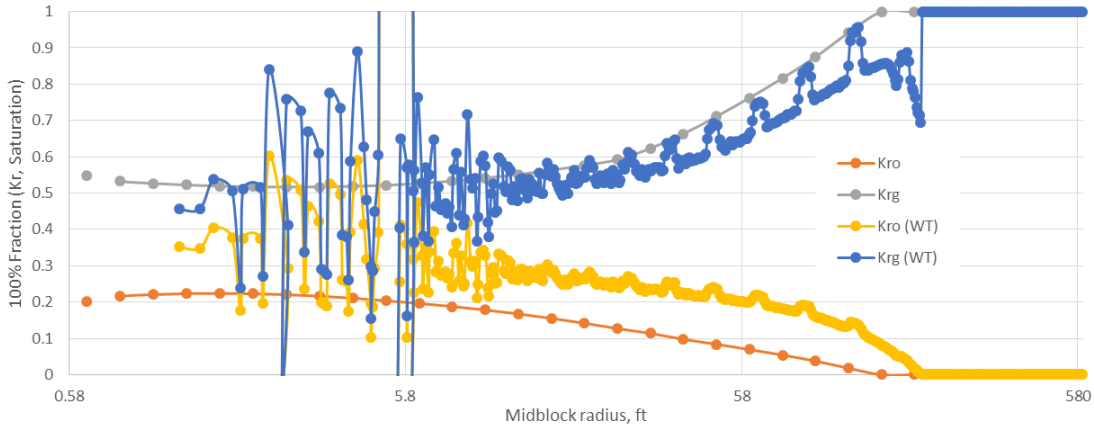

Figure 5.2—Relative permeability versus radius away from the wellbore calculated analytically showing large oscillation.

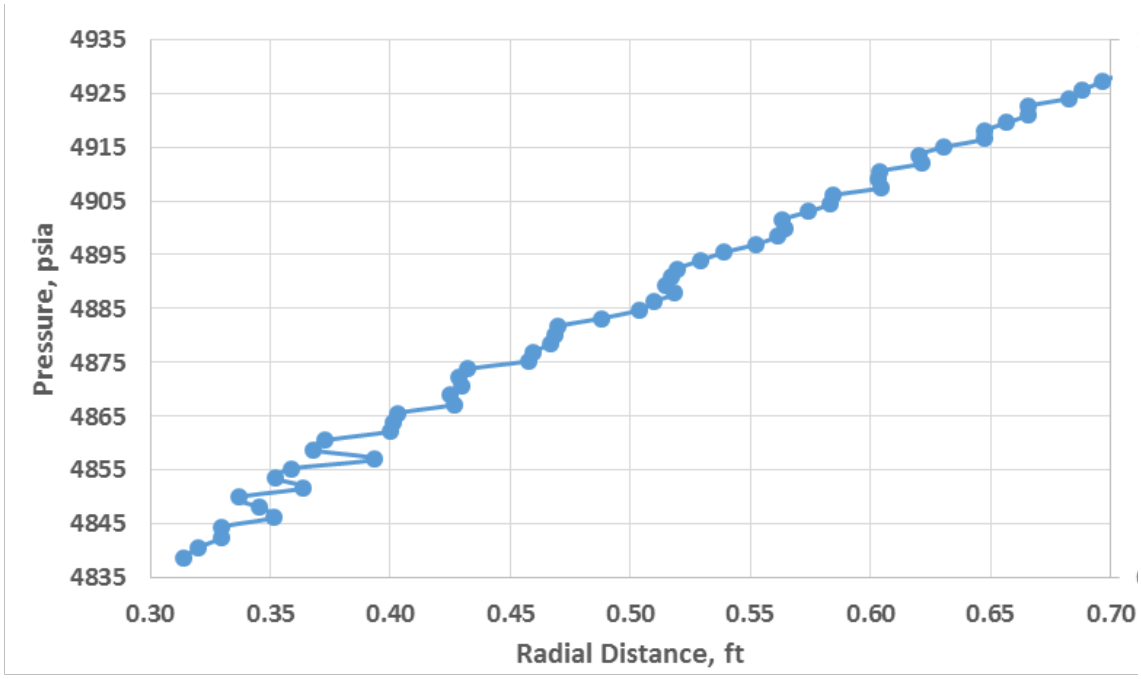

Figure 5.3—Close-up of the noise as seen in the calculated pressure versus radius profile.

Significant attempts were dedicated to understanding the exact nature and propose a practically attractive way to remove this behaviour. An extensive investigation including discussions with senior colleagues from the Heriot-Watt maths department concluded that such oscillations could be removed using various methods. Initially, the well-defined polynomial trendline functions and the spline function were considered to be fitted to the pressure data which

would ensure smooth derivative. However, this technique was found to be cumbersome as different fit functions were required for different cases. Therefore, other more practically attractive methods were sought to remove the oscillation to a satisfactory level, one of the methods considered was the smoothing tool that is available in most of the well test analysis software (e.g. Saphir, PanSystem). In PanSystem, which was used for this work, the smoothing tool is based on the 3-point average technique (Bourdet et al. 1989)– also known as moving average. This technique, when properly applied, reveals more clearly the underlying trends. However, one needs to be careful not to overdo it as it could distort the data beyond reality. As an alternative smoothing technique, the fit-function can still be used for the pressure derivative with respect to distance. It is shown here that using a fit-function would result in smoother relative permeability data, compared to using the built-in smoothing tool in the well test software. However, as mentioned earlier, a unique function would be required for each case, which is not practical.

The smoothing techniques can be used on either the pressure derivative data or on the pressure versus radius gradient depending on which data set to be used which will be discussed in more details in the following section. In the end, it was found that the oscillations could be sufficiently removed by smoothing the pressure derivative.

However, before presenting the results of applying different smoothing methods, the next section will explore where the noise is coming from and verify its potential causes.

5.4.2 Noise Troubleshooting

To investigate the source of the noise, first, single-phase oil data set was examined. **Figure 5.4** shows the pressure versus radius profile for the slightly compressible black-oil case, which should theoretically be more in-line with the method used to calculate the pressure profile. That is, the simulation pressure profile should match the one calculated from well test data and the calculated pressure versus radius derivative should be smooth. However, as noted in

Figure 5.4, there are some oscillations here too. Similar oscillations are observed for the two-phase case without the inertia or coupling effects (i.e. VELDEP keyword was turned off in the numerical simulator) as seen in **Figure 5.5**. These results confirm that at least some parts of the fluctuation in the data presented earlier is coming from the numerical simulation process using the ECLIPSE commercial reservoir simulator. In other words, the simplifying assumptions made, including two-phase flow nature of the data, which are not consistent with original derivation of the equations are not the only reason for such oscillations.

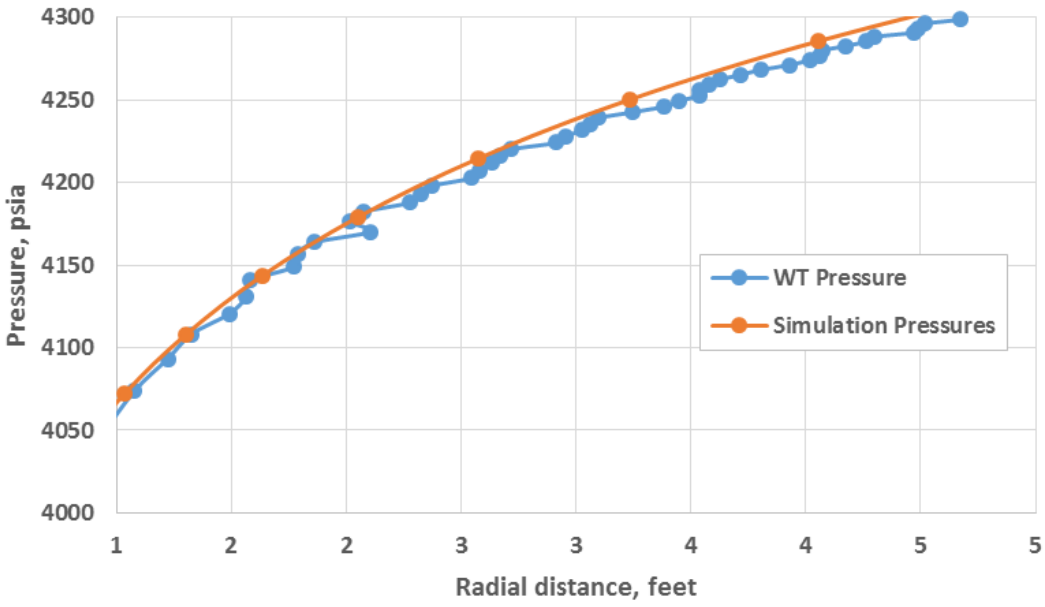

Figure 5.4—Close-up of pressure versus radius profile showing data oscillation in the single-phase oil system.

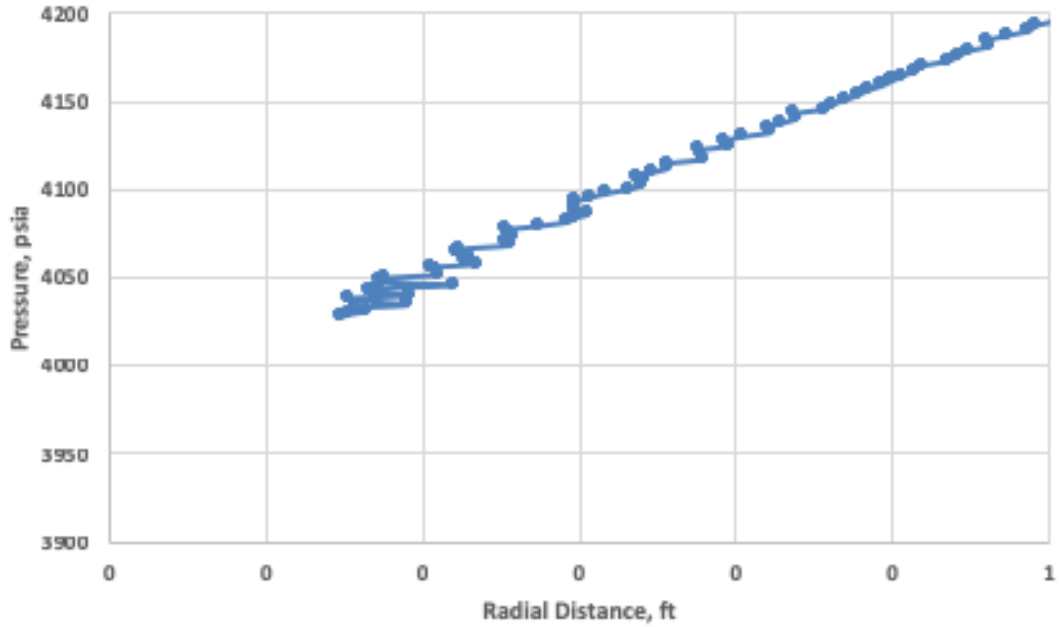

Figure 5.5—Close up of pressure versus radius profile showing data oscillation in the two-phase gas-condensate system (rich) with no velocity effects.

To remove any doubt over calculation-induced noise, the derivative calculation that was used in the analytical approach followed in this thesis was investigated by looking at the interpolation calculation step of the INDEX look-up function used in Excel. INDEX function was used to return an interpolated value from an array of data. The interpolation method was compared with a simple hand calculation and also with an interpolation code, and the results were the same. In other words, the look-up function in excel was not influencing the noise observed in the pressure profile.

At this stage, in order to better understand the source of the noise, Saphir was used to re-generate the pressure data for the same black-oil system. The use of Saphir here is to compare the effect of numerical calculation on the pressure data output from different software. As shown in **Figure 5.6** and **Figure 5.7**, the pressure versus shut-in time derivative obtained from Saphir is free from oscillation compared to that obtained from ECLIPSE. The data generated in Saphir are based on the numerical modelling capability of this software. It is

important to note that Saphir uses Voronoi gridding while ECLIPSE uses Cartesian gridding, which could explain part of the disagreement between these two sets of data.

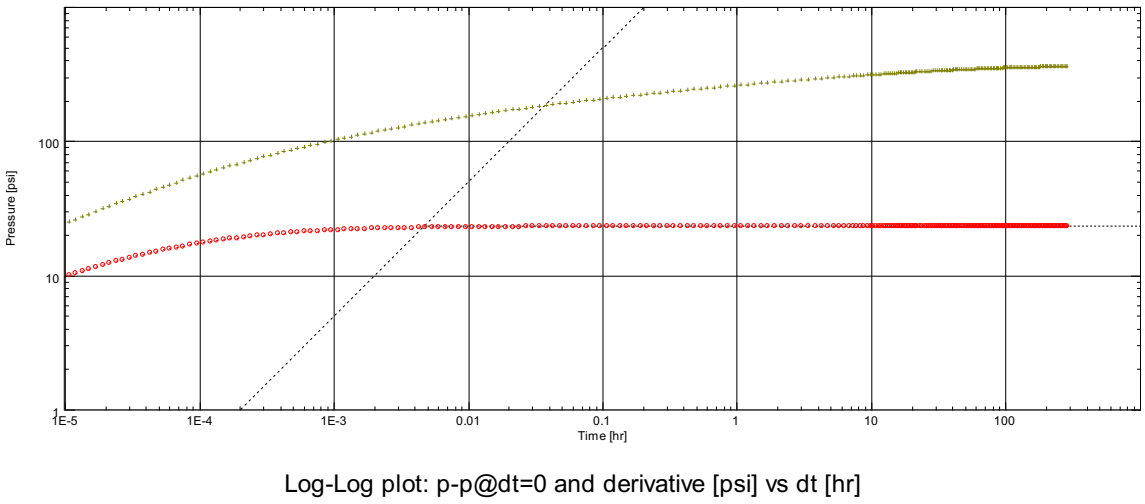

Figure 5.6—Pressure derivative for the data generated by Saphir for the buildup test in black-oil fluid system.

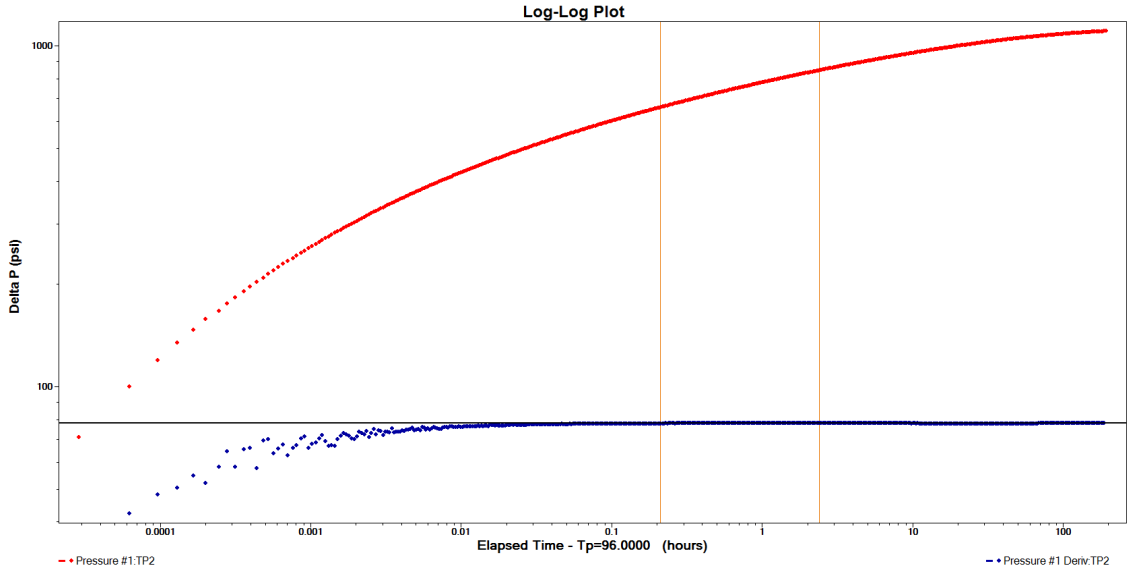

Figure 5.7—Pressure derivative for the data generated by ECLIPSE for the black-oil case, note the fluctuation at early time.

To further investigate the gridding sensitivity, the area around the wellbore in ECLIPSE's numerical model was adjusted to be as close as possible to the one

in Saphir, by introducing a theta value of 12. The results from ECLIPSE still show the same data oscillation (**Figure 5.8**). The sensitivity analysis for the number of grids and grid-block size in ECLIPSE numerical model was also carried out. Different grid numbers were used varying from 40, 100, 500 to 1000 grids. In addition, a uniform gird-block size was considered versus the used logarithmically increasing grid-blocks. All gridding techniques yielded the same results, with no significate influence on the outcome (**Figure 5.9**). Moreover, time-step discretisation was investigated, i.e. smaller and larger time steps were used. The overall outcome was not affected by the changes in time-steps either.

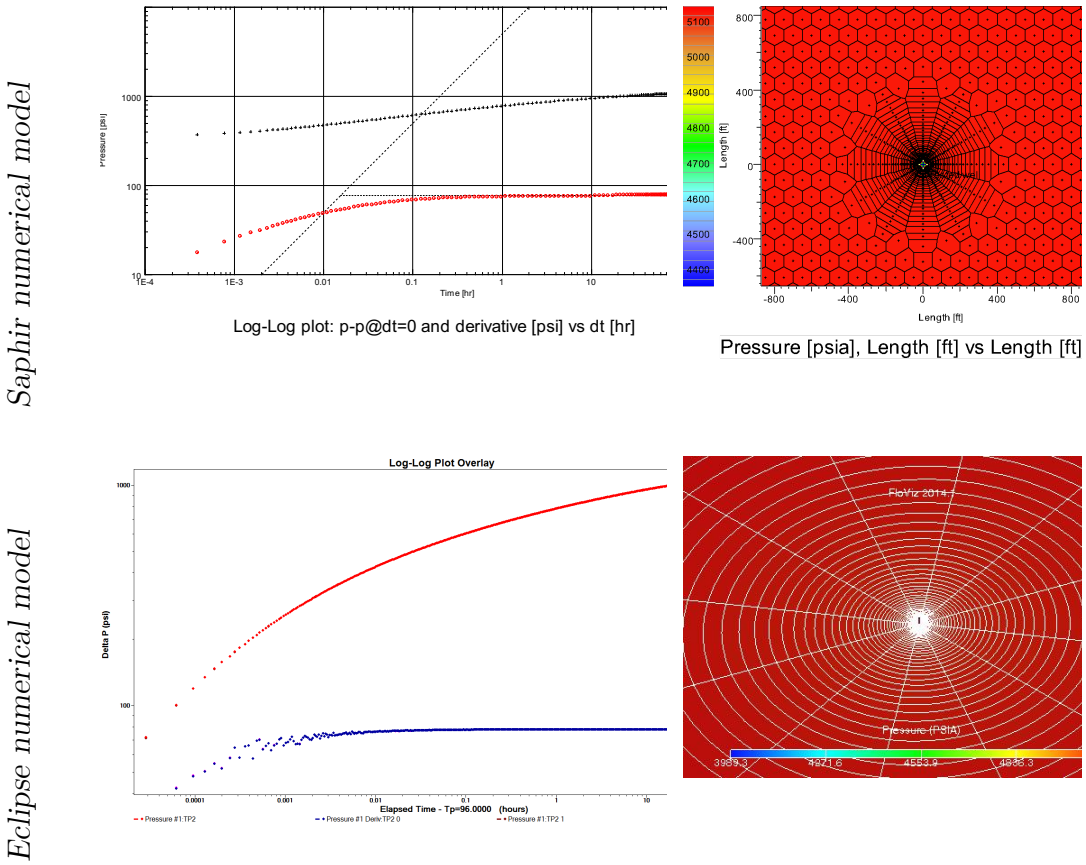

Figure 5.8—Comparison between Saphir numerical model versus ECLIPSE numerical model (with theta of 12 around the wellbore) with pressure derivate of the buildup showing oscillation in the ECLIPSE data.

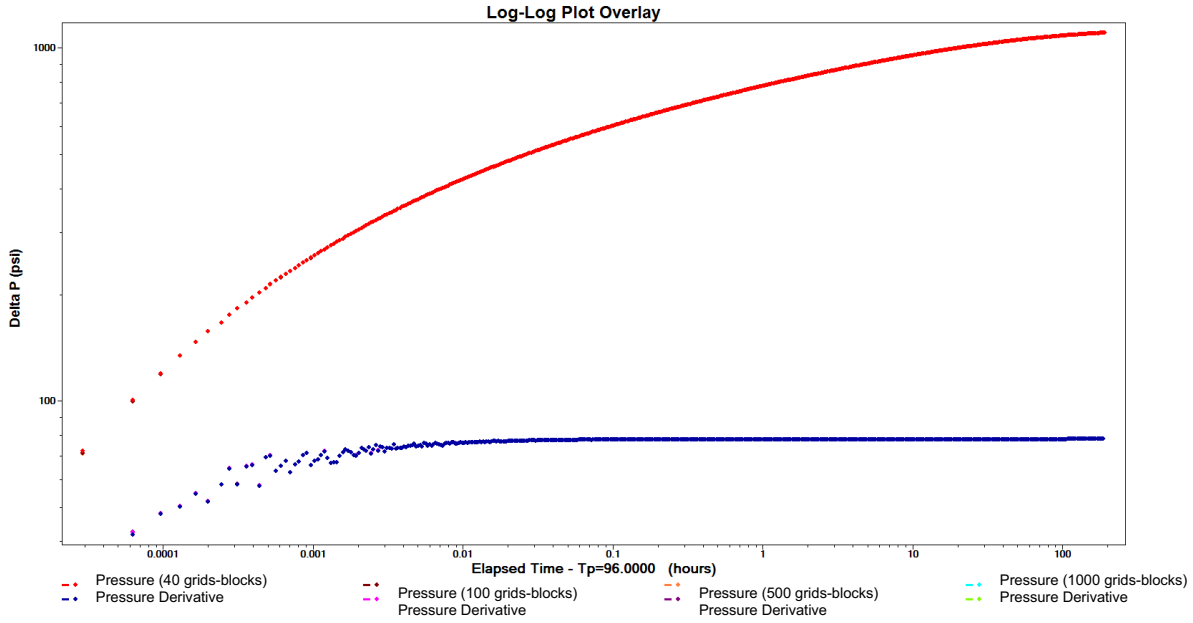

Figure 5.9—Different grid-block sizes yield similar pressure derivative (overlaying each other) and data oscillation is still observed.

The investigation above gives more weight to the claim that noise, at least for the single-phase black oil case, is coming from ECLIPSE's numerical simulation. It should be noted that Saphir does not have the capabilities to generate two-phase gas-condensate pressure data with inertia and coupling effects (e.g. like the VELDEP keyword in ECLIPSE). Therefore, it was not suitable to be used for the purpose of this study.

At this stage, it is more plausible that such noise is inherited in the numerically generated data and not from the analytical approach. However, it has to be added the presence of such noise is an integral part of real data. That is, it is also important to remember that in reality, there are other sources for noise, such as data filtration processes, gauge inaccuracies and malfunctions and tool sampling frequency, to name a few. That means that the discussion here on tools to reduce data oscillation is useful to consider, regardless of the specific source of the noise presented in this thesis.

5.4.3 Excel Fit-Functions

In order to reduce the data fluctuation, initially, trendline functions were used manually in Microsoft Excel to fit the data of the pressure versus radius, in order to remove any oscillation. While this resulted in much improved overall results, it was not ideal for every case, and in many cases, multiple functions were required for one data set. Furthermore, there was a discontinuity between multiple fits that translated into sudden jumps in the relative permeability data. Although the polynomial trendline function did improve the results concerning oscillation compared to the original calculation, however, it induced a wave-like effect related to the nature of the polynomial function (**Figure 5.10**). Thus, it was concluded that the polynomial fit function is not a preferred choice.

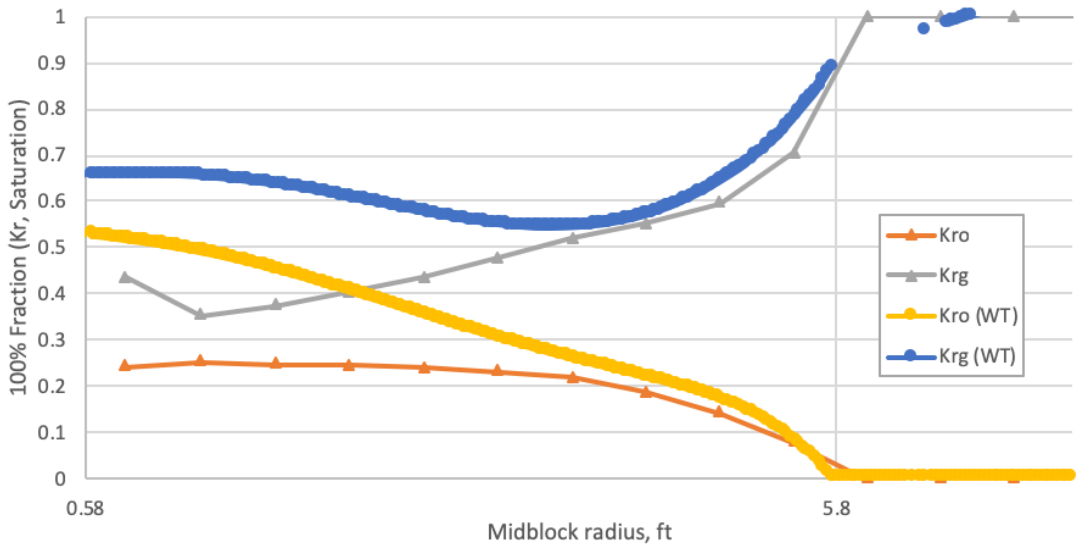

Figure 5.10—Calculated relative permeability showing the wave-like effect due to the use of polynomial trendline function to smoothen probe radius data.

5.4.4 Complex Fit-Functions

To overcome this, an advanced predictive modelling software, Eureqa (**Figure 5.11**), was used which utilises a combination of mathematical functions to generate one equation that describes the data set. For the results reported

here, this software has been used per case basis, and potentially, can be used to define one fit-function that fits all.

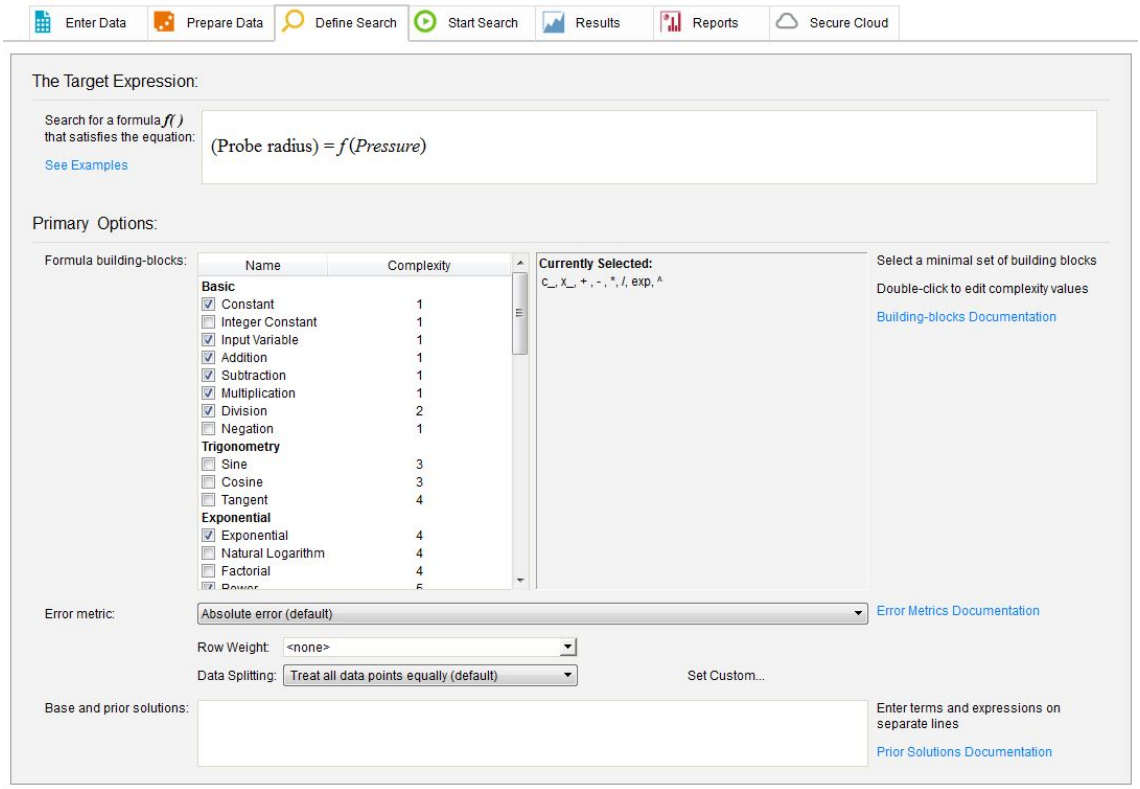

Figure 5.11—Predictive modelling software Eureqa that can use various mathematical function as individual building blocks for the target combined expression.

Given the anomaly seen from polynomial fit functions, the fitting requirement chosen for the software was set to adapt non-polynomial functions. Three cases initially used this approach.

For Case 1 the fit function obtained was:

$$Radius = 0.568 + 375.72^{(0.00123 \times p - 6.2)} \tag{5.3}$$

and for Case 2,

$$Radius = 1.174 \times e^{\left(\frac{-2463.8}{p - 5953.1}\right)} - 3.715 \tag{5.4}$$

while for Case 3,

$$Radius = 5.36E^{-4} \times e^{((1.87E^{-18} \times p^5) + (2.965E^{-37} \times p^{10}))} \quad (5.5)$$

where p is pressure. These functions would give a smoother pressure versus radius profiles (**Figure 5.12**) compared to Figure 5.3.

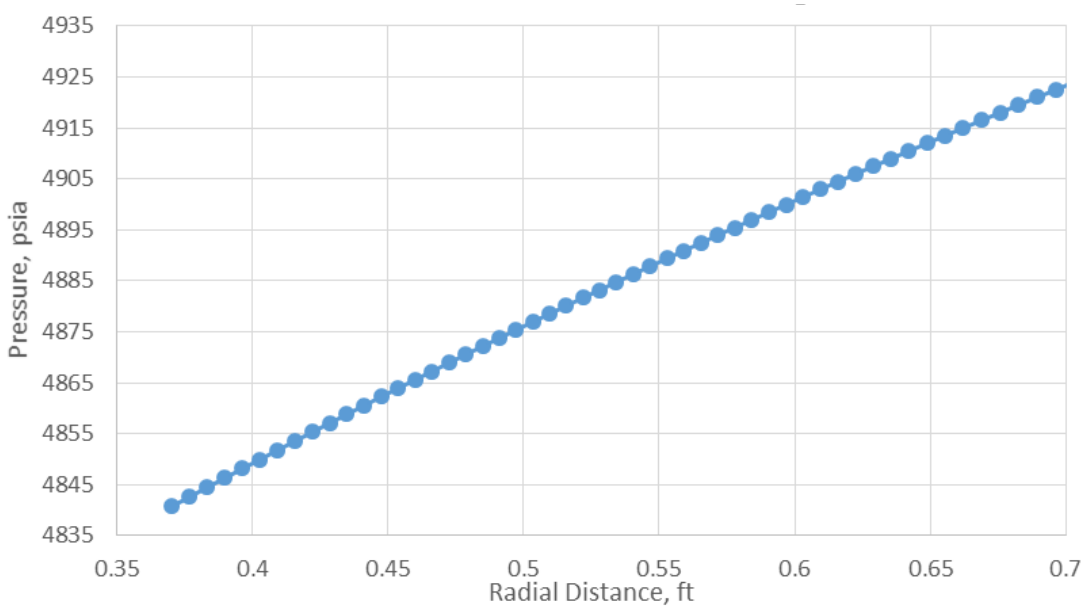

Figure 5.12—Close-up of the pressure versus radius after smoothing using a Eureqa fit-function.

Figure 5.13 shows a comparison between the originally calculated pressure versus radius profile, and the same pressure profile after smoothing using the fitted function. The noise is not very obvious when the pressure versus radius profile is examined as a whole; except for the two points of fluctuation (the first at about 8 feet and the second at about 38 ft) both of which are artefacts reflected from the pseudo-pressure versus time derivative as seen in (Figure 2.9) that were ignored. However, as a result of smoothing, the relative permeabilities data looks better overall (**Figure 5.14**).

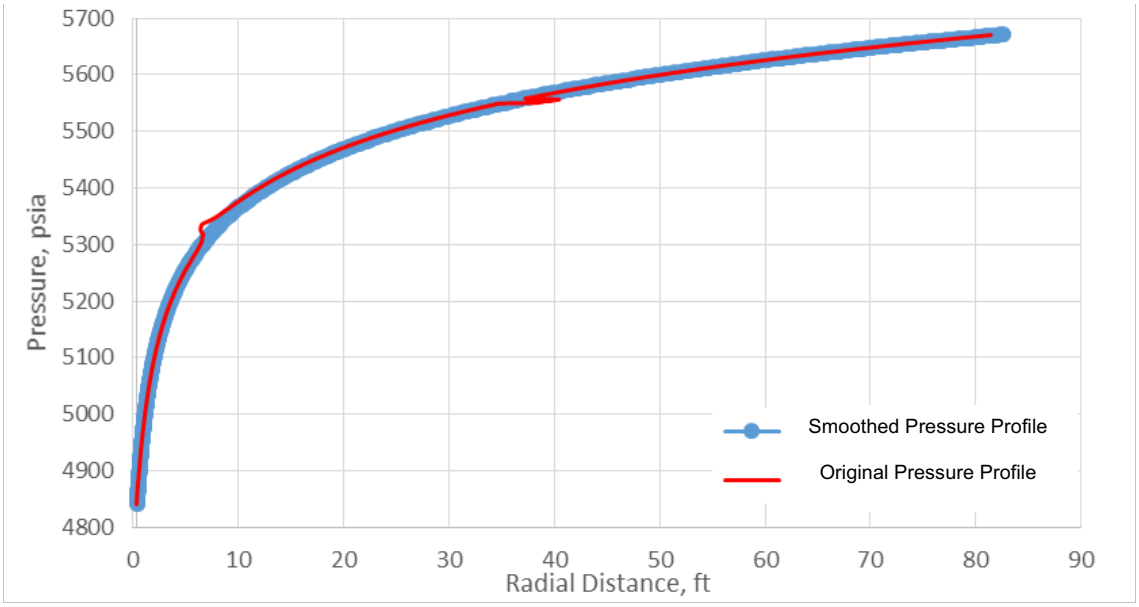

Figure 5.13—Pressure versus radius profile comparison between the original calculation and the smoothened data.

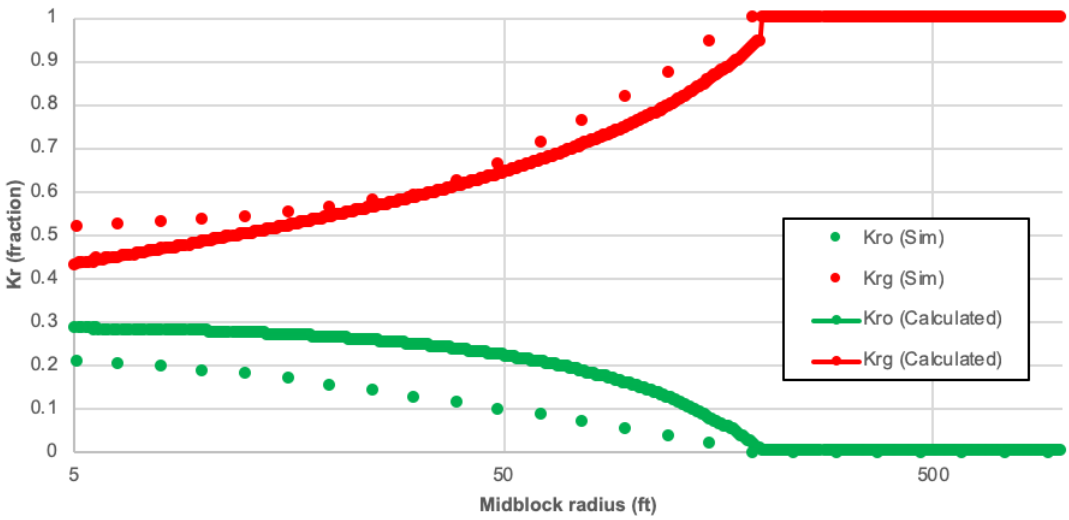

Figure 5.14—Calculated relative permeability after using a smoothened pressure versus radius profile.

The fitting functions obtained from Eureqa drastically enhanced the end-results of the relative permeability data with almost no oscillation compared to the earlier approach. Initially, the exponential relationship of radius versus pressure of the form $r = f(p)$ was used. The results showed that the fit-function

equations distinguishably varied for different datasets. In other words, such a relationship makes it difficult to find a common form for the fit-function that can be used for different cases, which suggests the approach is unattractive especially for practical purposes. To mitigate this issue, a logarithmic relationship of the form $p = f(r)$ was tried. The idea is that based on the form of the solution and background maths involved, it is easier to find a general form if pressure is expressed by a logarithmic relationship of the radius. Given this, the fit functions were redefined as follows:

For Case 1, instead of having the exponential equation (Equation 5.3), the following logarithmic fit-function is obtained instead:

$$Pressure = 4989.96 + 165.08 \times \ln(Radius) - 0.641 \times (Radius) \qquad (5.6)$$

Also, for Case 2,

$$Pressure = 4183.5 + 342.64 \times \ln(Radius) - 3.9 \times (Radius) \qquad (5.7)$$

Also, for Case 3,

$$Pressure = 4930.63 + 69.16 \times \ln(Radius) - 0.031 \times (Radius) \qquad (5.8)$$

In other words, it was possible to define the following common form for the fit-function using the logarithmic relationship between pressure and radius data:

$$Pressure = \mathrm{a} + (\mathrm{b} \times \ln(Radius)) - (c \times (Radius)) \qquad (5.9)$$

where a, b and c are constants that change on a case basis.

It is worth noting that these are not the only fit-functions that define the relationship between pressure and radius. That is, different fit-functions with varying complexity can be obtained; however, the aim was to find one that is simple, common and yet sufficient for the purpose of the analysis.

The calculated pressure and relative permeability data, using this new fit-function forms, based on the proposed logarithmic relationship agree well with the pressure and relative permeability data output from the simulator for the

cases considered; **Figure 5.15** shows one example. The level of agreement with the numerical simulation relative permeability data is reasonable but understandably somewhat more inferior compared to using a more unique exponential fit-functions (Figure 5.14). However, one fit function of the form described by Equation 5.9 that can describe the data in all the three cases is more practical.

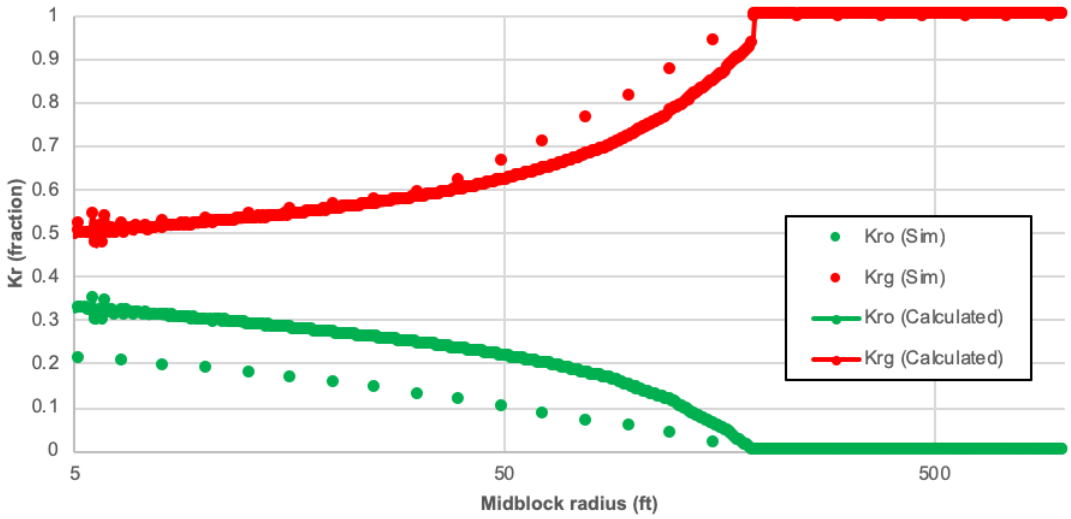

Figure 5.15—Calculated relative permeability using a logarithmic relationship of the form: $P = f(r_p)$ *compared to the numerical simulation output.*

This exercise has shown that it is possible to develop a common fit-function form making this approach more practically attractive; that is, the pressure versus radius profile for all the three cases can be fitted to Equation 5.9, with varying constants for each case (a, b, and c). However, it needs further investigation and validation to optimise and generalise the sought functional form. Another available and more practically attractive approach was investigated, which at this stage seems to be good enough for this work's purpose. The next section will discuss it in detail.

5.4.5 Smoothing Tools in Pressure Transient Analysis Software

Existing well testing software do not provide fit-functions tools like the ones presented earlier, which would make the concept of taking the dataset outside

of the software for just smoothing practically less attractive. Hence, another option that is available and practically more attractive was considered.

Both Pansystem and Saphir software (as the two most widely used package in the industry) have smoothing capabilities based on the 3-point central differentiation algorithm (Bourdet et al. 1989) that can heavily, but not entirely, reduce the noise. It is important to note that Saphir currently cannot handle two-phase gas-condensate system or to calculate two-phase pseudo-pressure data. For that purpose, Pansystem is relied on to analyse the pressure data presented in this thesis. The smoothing tool in Pansystem enables the user to directly smooth the pressure versus shut-in time derivative which integrates very well with the workflow in this study.

In order to evaluate its effectiveness, Case 3 is taken as an example with smoothing constant value of 2.0 applied to its pressure derivative. As shown in **Figure 5.16**, the resultant derivative, in comparison to the original data with the default smoothing constant value of 0.07, is smoother.

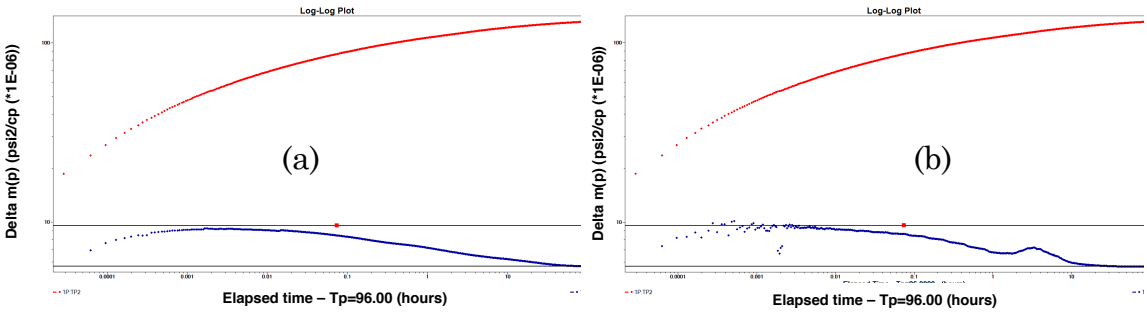

Figure 5.16—(a) Well test pressure derivative for Case 3 with a smoothing constant of 2.0 and (b) with the default smoothing of 0.07.

This in return has significantly reduced the oscillation seen in the calculated relative permeability data (**Figure 5.17**). It seems that the level of smoothness provided by the software is sufficient in this particular case.

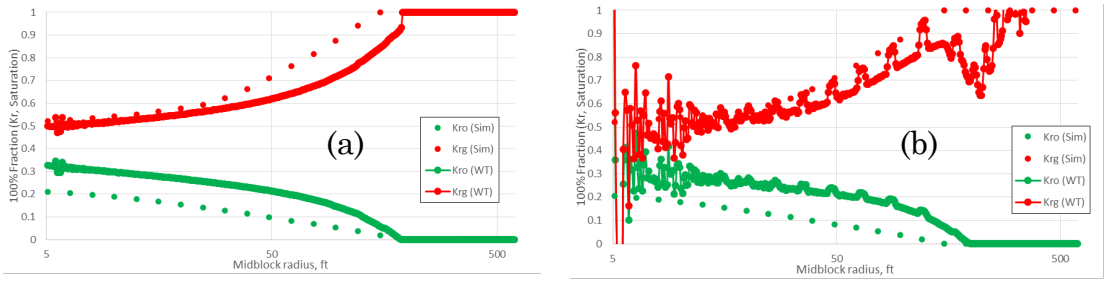

Figure 5.17—Relative permeability data calculated by analysing well test buildup versus the numerical simulation output (a) after applying the smoothing factor, and (b) without any smoothing factor applied to the pressure derivative.

It should be noted that users are advised not to use high values for smoothing constants in order not to distort the shape of the derivative. Thus, such tools might have some limitations regarding of how much the user should smoothen the data. These suggest that there would be added value in using the fit function described earlier not only because the fit function completely removes the oscillations but also because in some cases the smoothing option might not sufficiently remove such oscillations. However, the practical attractiveness of using smoothing tools available in well test software will make their application more desirable.

5.4.6 Fit Function Versus Built-in Smoothing Tools

Figure 5.18 shows a comparison between k_{rg} data from the numerical simulation and the analytically calculated k_{rg} data without any smoothing, with fit function and with PanSystem based smoothing techniques.

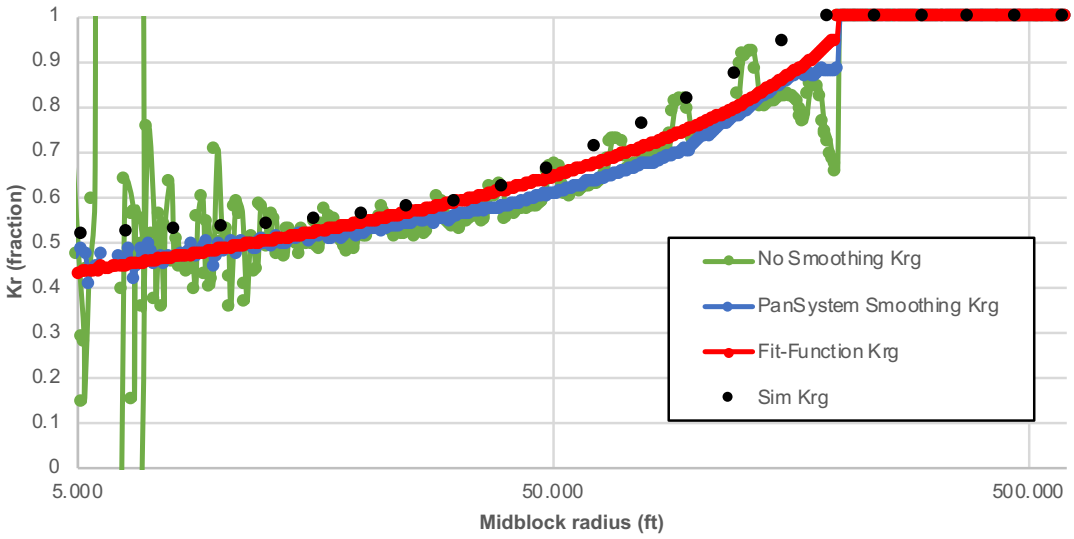

Figure 5.18—Comparison between simulation kr output data and those using different types of smoothing techniques and the one without smoothing.

These data highlight the need for smoothing which is best achieved using a fit function, although the PanSystem based smoothing technique also gives acceptable results. It should be noted that fit-function is applied to the pressure versus radius profiles, while PanSystem smoothing technique is applied to the pressure versus shut-in time derivative. Hence, hereafter in this thesis, the results of the relative permeability data are presented only after a smoothing technique is applied to the pressure versus radius derivative data. Both techniques were used in the next section; a unique fit-function was applied for two cases of the single constant-rate scenarios and the PanSystem built-in smoothing function was used for the other two cases of single-rate in addition to the multi-rate scenarios that will be presented in Chapter 6.

5.5 Results

In the discussion of results below, the analytically calculated relative permeabilities data are compared to the numerical simulation output to verify whether the suggested method produces reasonable results. The approximation of relative permeabilities are determined satisfactory based on the deviation

from the numerical simulation data, which in most cases does not exceed a maximum of ±0.1 for both k_{rg} and k_{ro}. Eventually, the results were further validated when two-phase production data analysis (as will be discussed in Chapter 7) produced accurate formation permeability estimation using the calculated relative permeabilities presented in this chapter.

5.5.1 Analytical Calculation of Relative Permeability

The same four cases that were discussed in 4.6.2 were used in this section. In all the cases, reservoir Model 1 was used, except for Case 4 with a higher permeability, where Model 2 was used with a bigger reservoir radius (Table 3.1). **Table 5.1** summarises the four cases with the indication of the smoothing technique used for each.

Case	Rock	Smoothing Technique
Case 1	RC1	Fit-function
Case 2	RC1	Fit-function
Case 3	RC6	PanSystem*
Case 4	RC8	PanSystem*

* *Based on the moving average method.*

Table 5.1—Smoothing technique used for the considered single-rate two-phase gas-condensate cases.

With the smoothened pressure versus radius profiles, Equations 5.1 and 5.2 were used to calculate the gas and oil relative permeability, respectively. The calculated relative permeability versus radius data for Case 1 is compared with relative permeability data output from the numerical simulation as shown in **Figure 5.19**. In this case, the relative permeability data does not match very well but the trends are similar, and the calculated relative permeability data indicate the formation of a condensate bank up to about 6 ft from the wellbore which agrees closely with the pressure profile and the simulation output data.

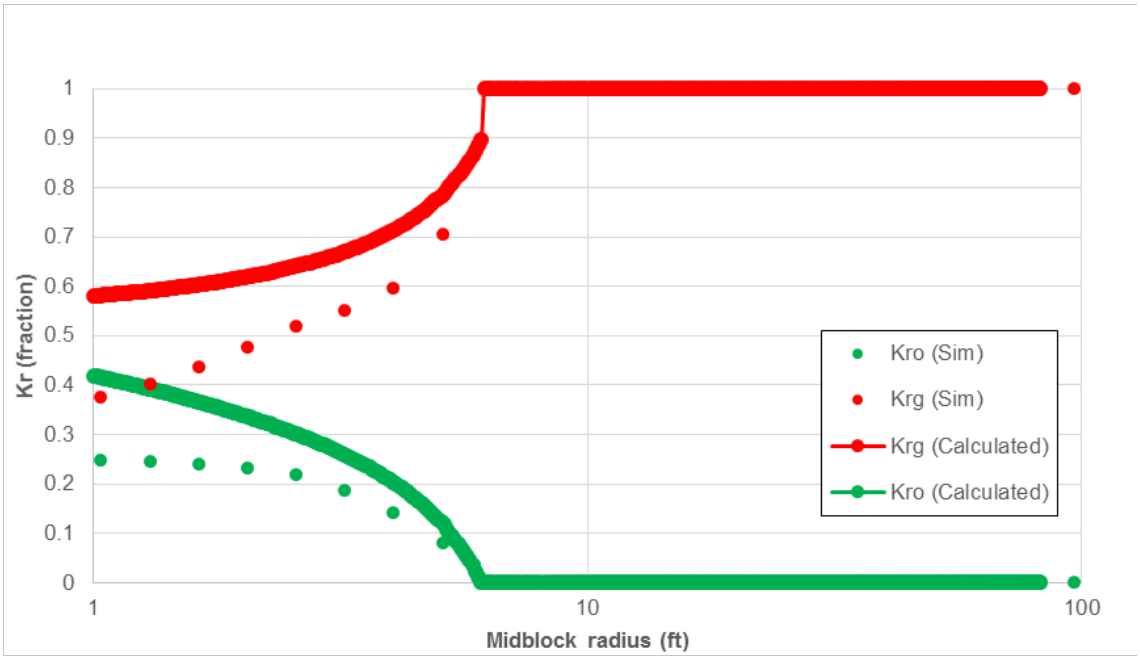

Figure 5.19—Analytically calculated relative permeability versus radius compared to relative permeability data output from the numerical simulation for Case 1.

For Cases 2, 3 and 4 (**Figure 5.20, Figure** 5.21 and **Figure** 5.22**,** respectively) the calculated k_{rg} data are very close to the k_{rg} data output from the numerical simulation. While k_{ro} is slightly off-match, it still follows a good trend. The results compared to Case 1 are considerably better. The extent of the condensate bank differs in each case. For Case 2 it covers approximately 43 ft around the well, while in Case 3 it goes up to 196 ft and for Case 4 it is approximately 187 ft, which, as for Case 1, all agree with the corresponding condensate bank radius values from the pressure versus radius profile and simulation output data. Table 5.2 shows a summary of the condensate bank radius values obtained from the relative permeability versus radius profile along with the ones estimated from the calculated pressure versus radius profile, and the ones estimated from the numerical simulation grid block, which might be slightly inaccurate when the grid block size is large.

Case	Depth of the condensate (ft)		
	Estimated from pressure profile	**Estimated from K_r profile**	**Numerical simulation radius when $k_{rg}>0$**
Case 1	6	6	6
Case 2	43	43	54
Case 3	196	196	183
Case 4	187	187	168

Table 5.2—Condensate extent in the reservoir, estimated from the pressure versus radius, calculated relative permeability versus radius and those output from the simulator.

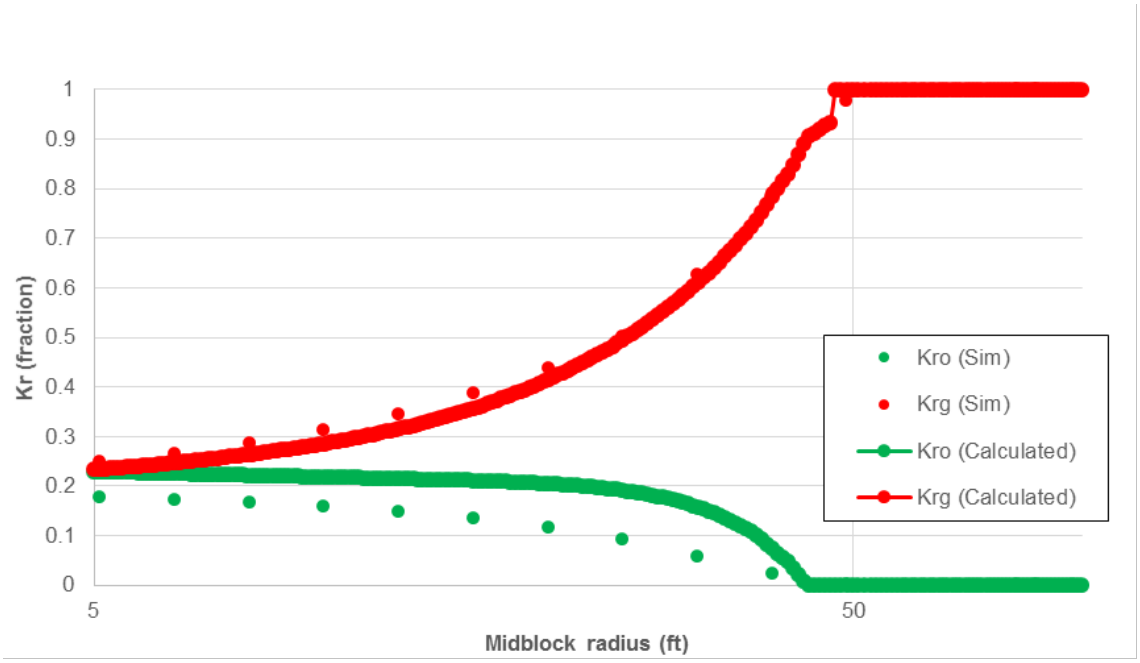

Figure 5.20—Analytically calculated relative permeability versus radius compared to relative permeability data output from the numerical simulation for Case 2.

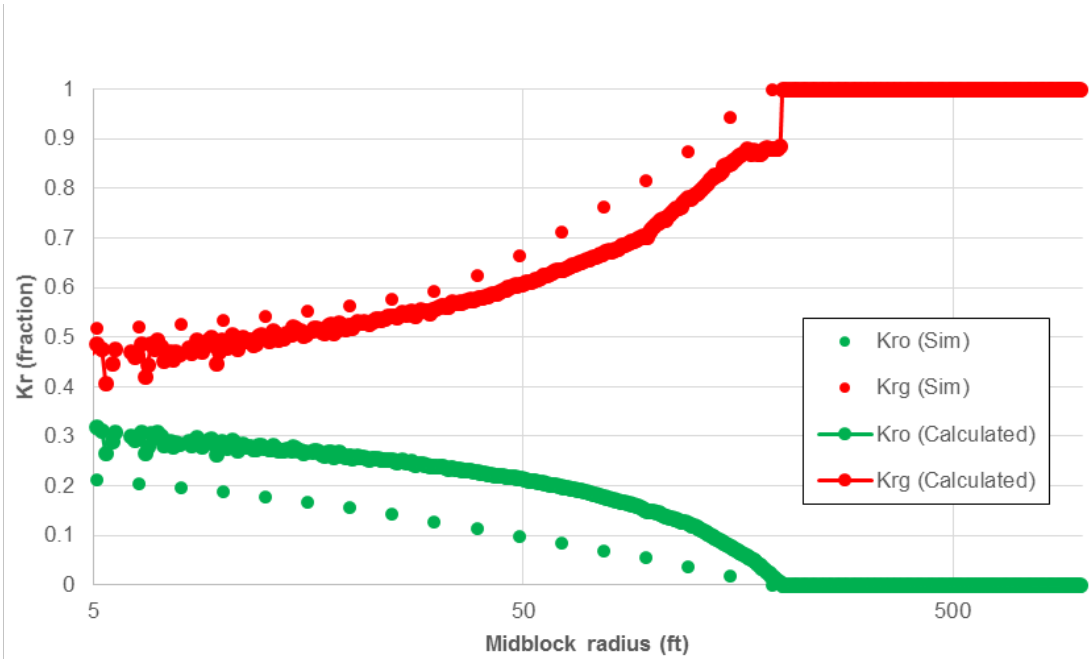

Figure 5.21—Analytically calculated relative permeability versus radius compared to relative permeability data output from the numerical simulation for Case 3.

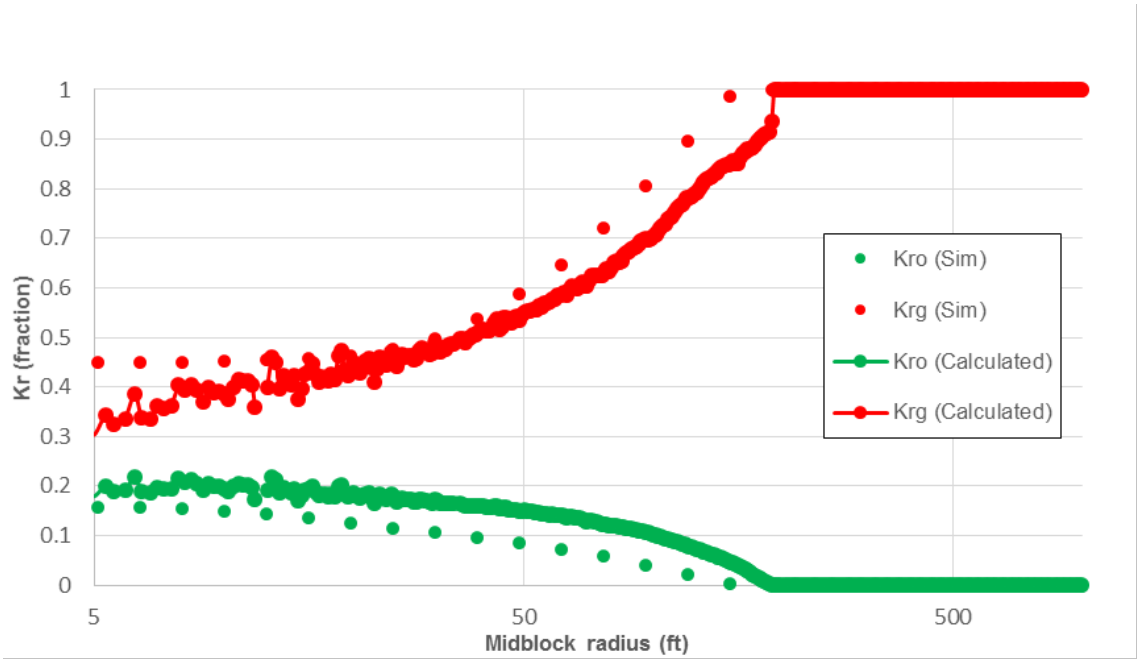

Figure 5.22—Analytically calculated relative permeability versus radius compared to relative permeability data output from the numerical simulation for Case 4.

It can be observed that when PanSystem's built-in smoothing tool is used, as in Case 3 and 4, it could result in some minor fluctuations compared to the fit-function smoothing technique but still the level of agreement is acceptable.

For the purposes of this work, the yielded relative permeability results, even for Case 1, are sufficient to carry on the two-phase approach. As it will be shown, the calculated relative permeability data above are used in two-phase production analysis technique (Chapter 7) and produced good results in terms of production decline type-curve match and formation permeability estimation. Furthermore, the obtained relative permeability data can be used for other reservoir engineering calculations. It is important to keep in mind that the exercises described here have been performed for a rich fluid system with the most considerable extent of two-phase contribution (as an extreme case), i.e. the method should work for leaner fluids.

5.5.2 Two-Phase Pseudo-Pressure

The relative permeability data analytically calculated here are a function of pressure and not saturation. This is unlike what is presented in the literature, where lab-based relative permeability used to analyse two-phase problem is a function of saturation. As mentioned earlier in section 2.2.5, in order to use the relative permeability as a function of saturation, a correlation between relative permeability and pressure is established by utilising the steady-state relationship (Equation 5.10) as presented in Jones and Raghavan (1988) work, which is based on O'Dell and Miller (1967) two-phase steady-state theory.

$$\frac{k_{ro}}{k_{rg}} = \frac{L\rho_g\mu_o}{V\rho_o\mu_g} \tag{5.10}$$

However, for pseudo pressure calculation, saturation data are not required. That is, the relative permeability required for the two-phase pseudo-pressure computation is a function of pressure. Hence, once relative permeability data are computed from well test data as a function of pressure, the two-phase pseudo-pressure can be calculated based on the Jones and Raghavan (1988) definition of the pseudo-pressure:

$$p_p(p) = 2\int_{p_b}^{p_i}\left(\frac{k_{ro}}{\mu_o z_o} + \frac{k_{rg}}{\mu_g z_g}\right) p dp = 2\frac{RT}{M.W.}\int_{p_b}^{p_i}\left(\rho_o \frac{k_{ro}}{\mu_o} + \rho_g \frac{k_{rg}}{\mu_g}\right) dp \qquad (5.11)$$

which in turn could be used to improve data analysis using two-phase concepts, as will be shown in Chapter 7 with production data analysis.

5.6 Challenges and Limitations

In this section, the applicability of the proposed method of calculating pressure versus radius profile and relative permeability is examined when certain challenges are present in the well test data. First, in 5.5.1, one of the most common phenomena, wellbore storage, is discussed and a case is analysed to showcase the implications of having such a distortion of data. In the second part, 5.5.2 below, the applicability of the method on horizontal wells are discussed, and the limitation is explained concerning the nature of the flow equation combined with data availability and complex flow geometry that are present in horizontal wells.

5.6.1 Wellbore Storage

In practice, well test data quality may face challenges that can distort the data, as discussed in section 5.4.2, or ones that can mask the formation response data as in the case of wellbore storage (WBS). WBS occurs when the valve is not in front of sandface and the total outflow is a summation of formation outflow and flow due to compressibility of the fluid from the sandface to the valve position. It should be noted that the objective is to analyse the reservoir response and not what happens within the wellbore. WBS is one of the main data disturbances that could occur in well test data analysis. It appears in the pressure derivative in the early time data as a unit slope, representing pure WBS, followed by a hump that represents a transition zone where both wellbore and reservoir flow are present. This signature can mask the true reservoir early-time data and sometimes a portion or all of the following middle-time data which could make analysing the well test pressure data challenging.

To test how the proposed method works in such conditions, a wellbore volume was introduced in one case to simulate the WBS effect. In this simulation, the reservoir had the same rock and fluid properties as those used for Case 3 (RC6 rock). Initially, a case was constructed that WBS does not significantly affect the well test data analysis. For this case, the wellbore volume was calculated to be around 2857 ft^3 based on the wellbore storage coefficient of 0.2. **Figure 5.23** shows the pressure derivative with the WBS effect. Note that when the WBS effect dissipates–roughly around 1 hour, the condensate bank region (region-1) can be observed followed by the single-phase, dry gas, region (region-2) after roughly 10 hours.

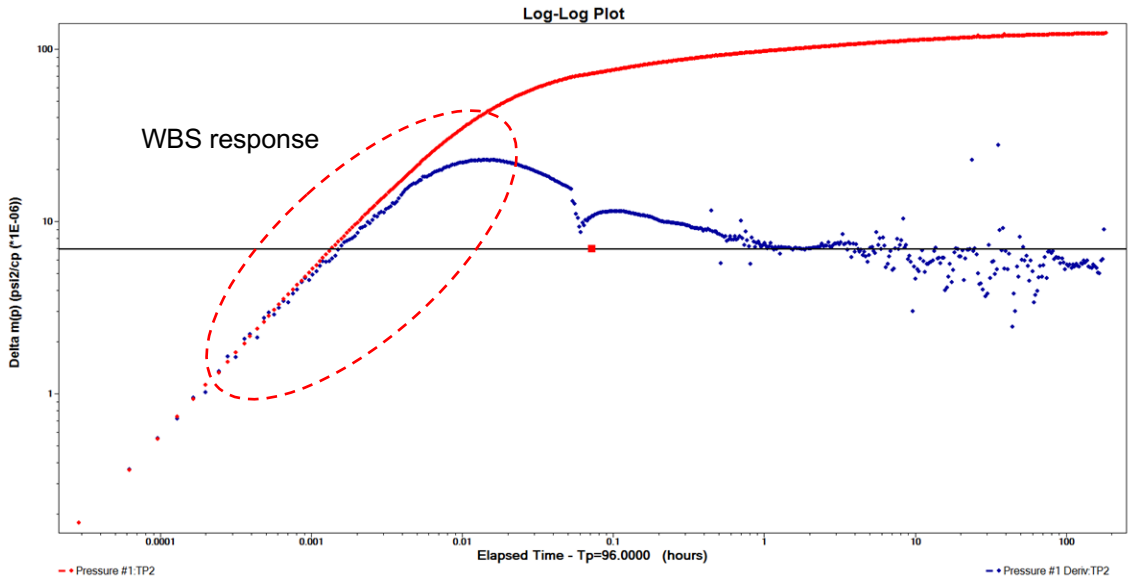

Figure 5.23—Pressure derivative with the WBS effect scenario for Case 3.

Following this, to evaluate the effectiveness of the procedure, the test parameters were changed. It should be noted that unless both regions are apparent on the pressure derivative (as seen in Figure 5.23), the data analysis can be uncertain or misleading. Here two scenarios were considered; in the first scenario, it is assumed the two-phase region is partially masked and the plateau observed corresponds to the two-phase region with not long enough test duration to see the single-phase region signature. In the second scenario, it is assumed that the WBS completely masks the condensate bank region and the observed plateau is related to the single-phase region (**Figure 5.24**). In other

words, in the latter case, only one single pressure derivative plateau is visible, assuming, as in reality, it was unknown if this single plateau was related to two-phase gas and condensate (i.e. condensate bank effect) or single-phase dry gas.

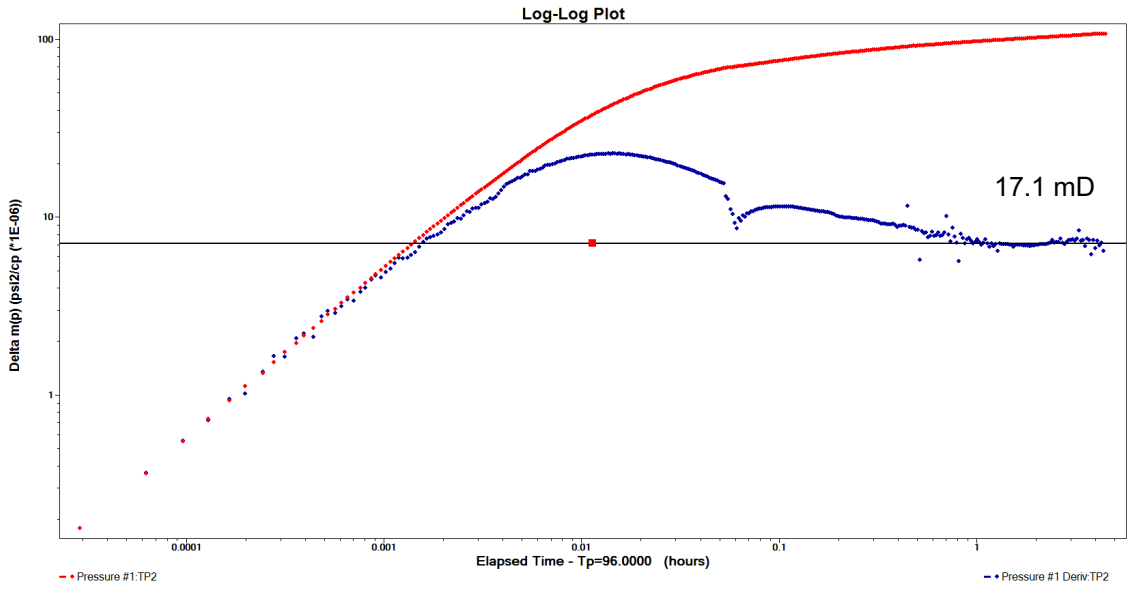

Figure 5.24—Pressure derivative for the shorter version of Case 3 WBS scenario.

The main aim is to show that the suggested procedure would give a reasonable result for the first scenario, where the pressure derivative plateau corresponds to the condensate bank. The second scenario is addressed later in another exercise.

Figure 5.24 shows the shorter test duration for Case 3 with the WBS effect. In this scenario, the WBS effect is apparent followed by a single plateau in the pressure derivative. The permeability obtained from this pressure derivative plateau, without using any correction that could be obtained following the suggested procedure, is equal to around 17.1 mD (27.5% less than input permeability of 23.6 mD). Before the data to be analysed using the proposed method, a smoothing technique was applied to the pressure derivative, with a smoothing constant of 1.8 (**Figure 5.25**).

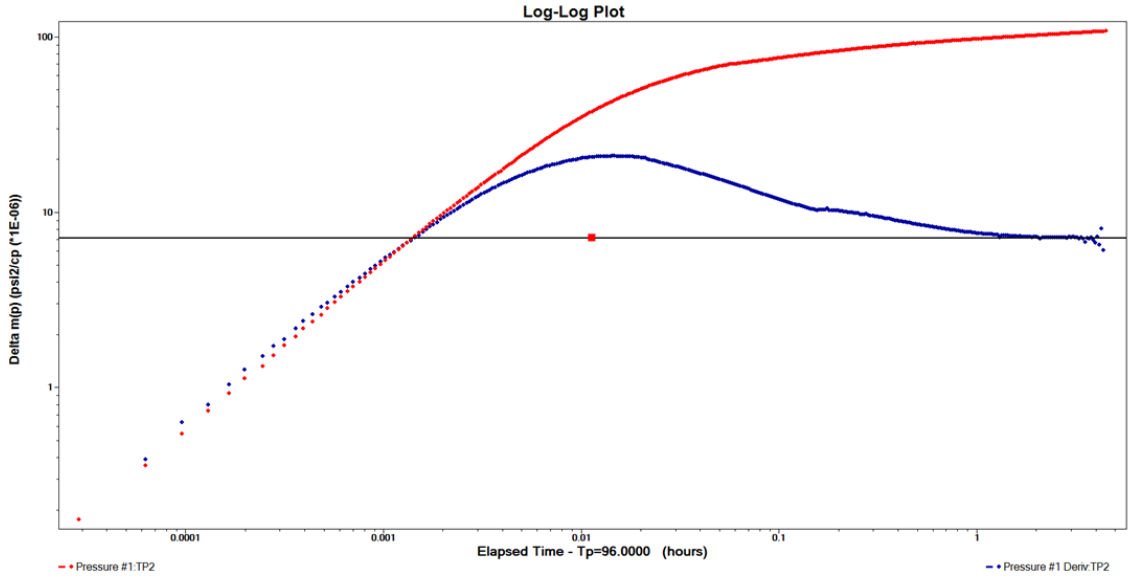

Figure 5.25—Pressure derivative for the shorter test duration of Case 3 WBS scenario, with smoothing constant value of 1.8 applied in PanSystem.

Using these pressure derivative data, the pressure versus radius profile and in return, the corresponding relative permeability data were calculated, as shown in **Figure 5.26** and **Figure 5.27** respectively. In this part of the calculation, the data points coming from pure WBS were ignored in the pressure derivative data and its pressure versus radius gradient. As they only reflect the wellbore fluid expansion response which will not give consistent and representative results. As can be seen in Figure 5.27 the noise has not been completely eliminated using the smoothing technique in Pansystem. However, as will be shown next, the applied smoothing constant and resultant relative permeability data are good enough to improve the well test pressure derivative. That is, these relative permeability data were then used to calculate the two-phase pseudo-pressures and re-analyse the well test data.

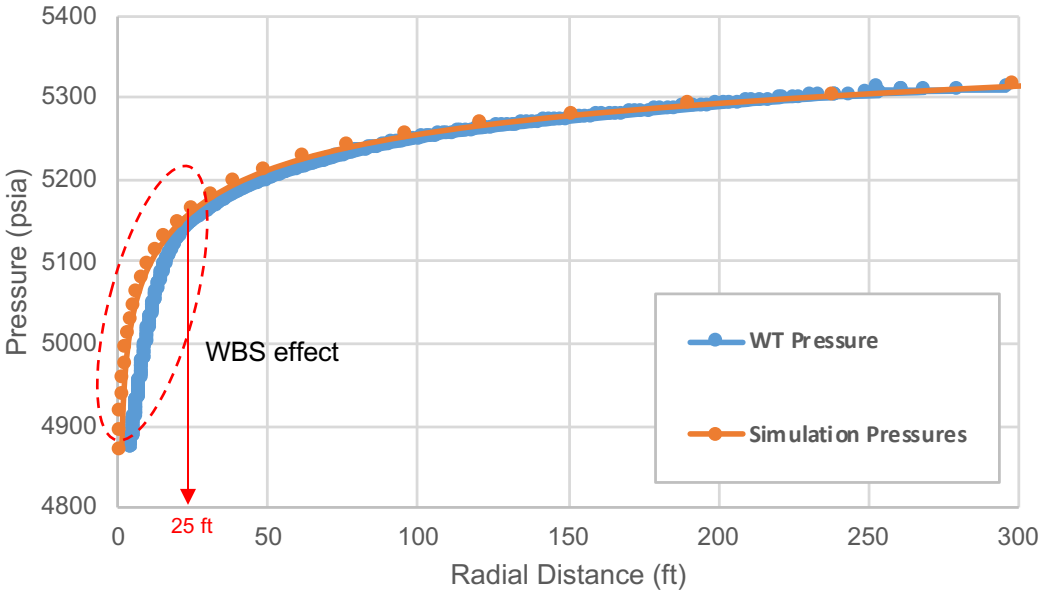

Figure 5.26—Pressure versus radius profile calculated from well test data for Case 3 with WBS.

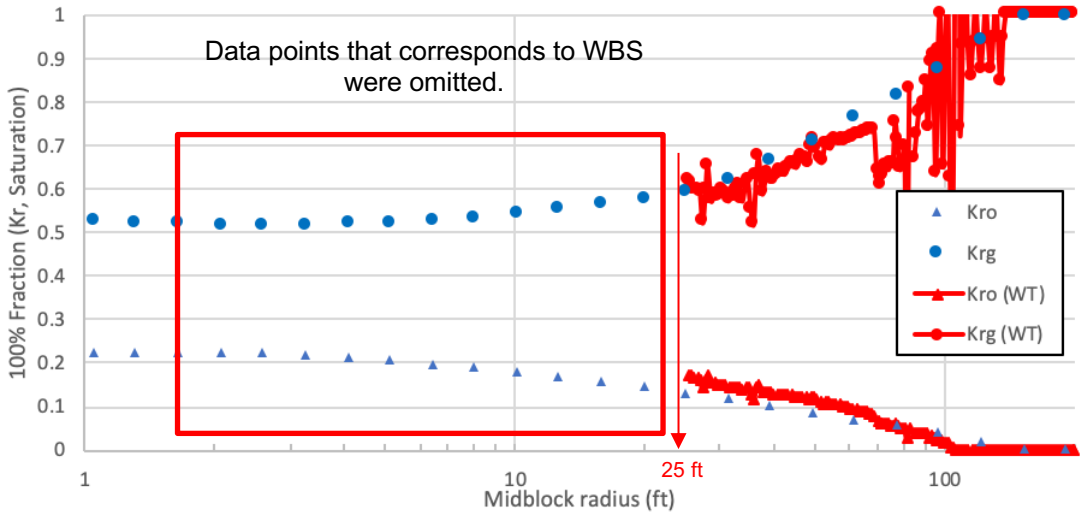

Figure 5.27—Calculated kr data for Case 3 with WBS. The very early data attributing to pure WBS was omitted.

As noted in **Figure 5.28**, the pressure derivative, after correction, gives a value of 21.2 mD for permeability that is closer to the absolute permeability value,

23.4 mD, compared to the previous value of 17.1 mD obtained with a simple single-phase based well test analysis shown in Figure 5.25. It is clear from **Figure 5.29** (which is an overlay of the data of Figure 5.25 and Figure 5.28) that the derivative plateau has been lowered (corrected) and the permeability value obtained has improved.

Figure 5.30 shows a comparison between the new improved pressure derivative and the pressure derivative for the more extended test duration data set, where both region-1 and region-2 exist. Here, it can be clearly observed that the corrected condensate bank region (region-1) in this case with WBS gave a permeability value similar to that obtained from the single-phase gas region (region-2) for the case without WBS.

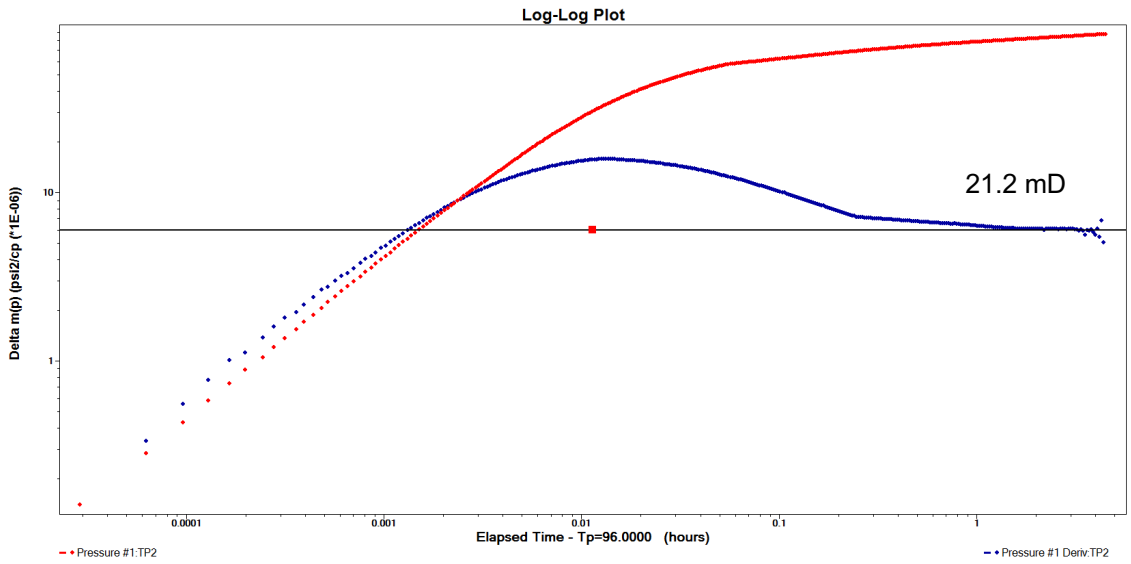

Figure 5.28—Pressure derivative for the shorter version of Case 3 WBS scenario, after using the calculated two-phase pseudo-pressure which has corrected the condensate bank plateau to give permeability of 21.2 mD.

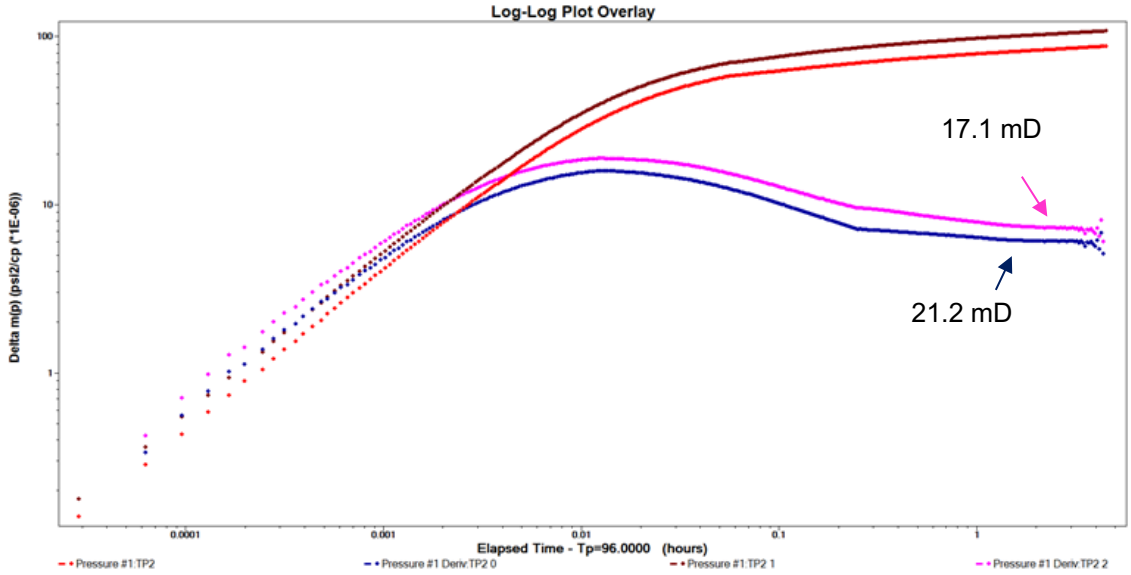

Figure 5.29—Comparison between single-phase pseudo-pressure derivative (in pink for the derivative and brown for Δp_p), and two-phase pseudo-pressure derivative (in blue for the derivative and red for Δp_p).

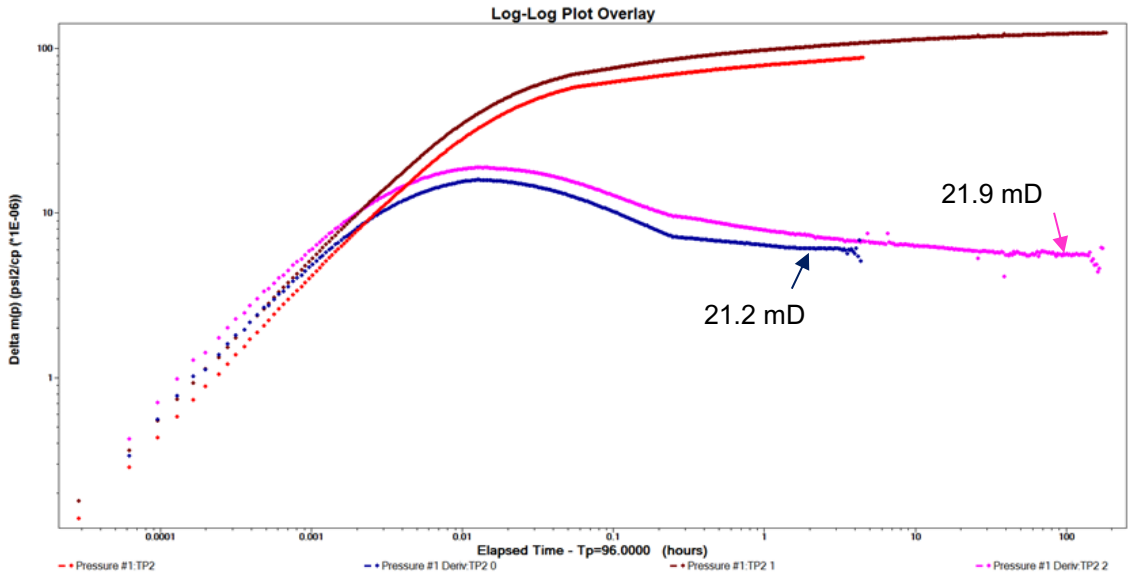

Figure 5.30—Comparison between the new improved pressure derivative for the short WT using the two-phase pseudo-pressure data (in blue for the derivative and red for Δp_p) and the original pressure derivative for the whole data set, where both region 1 and region 2 exist (in pink for the derivative and brown for Δp_p).

To address the second scenario, the case was set-up where the single-phase plateau was also present. The idea was to make sure that the procedure only improves the condensate bank region, and not the single-phase region. In other words, when the two-phase pseudo-pressure that is calculated based on the relative permeability data are used to re-analyse the well test data, only the condensate bank plateau change to give a value close to absolute permeability, while the second plateau remains the same (**Figure 5.31**). This indicates that a second plateau is still representing the single-phase region which gives the absolute reservoir permeability. In addition, it will ensure that when only the single-phase region is observed, due to WBS masking condensate bank, the obtained permeability would not be overestimated. This also confirms that the suggested method works for cases where only a single-phase region plateau is present.

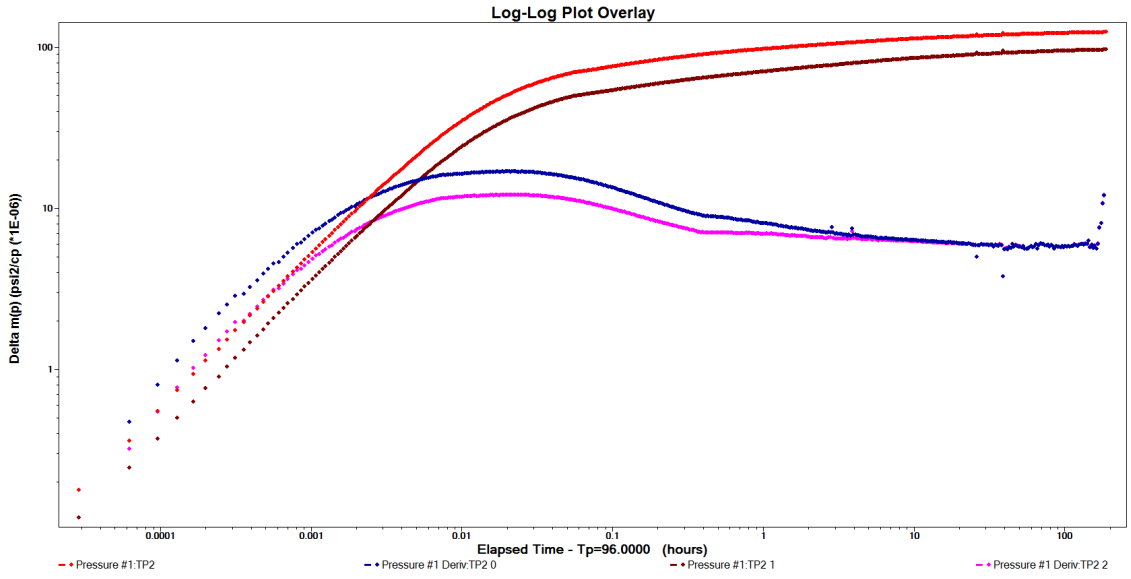

Figure 5.31—Comparison between the new improved pressure derivative using the two-phase pseudo-pressure data on a more extended test scenario for Case 3 (in pink for the derivative and brown for Δp_p), and the original pressure derivative for the whole data set (in blue for the derivative and red for Δp_p). Notice that only the condensate bank region was corrected.

The findings of these exercises confirm that in the case where WBS effect masks portion of the well test data, the approach could prove very beneficial by providing the absolute reservoir permeability from any of the two regions– region-1, or region-2.

These exercises showcase the challenges posed by the quality of the well test data. That is, if WBS is more severe, even less useful data points can be used to compute the pressure versus radius profile and relative permeability analytically from well test data. In general, avoiding WBS related issues is recommended by using downhole shut-in valves and gauges, instead of a surface shut-in system.

5.6.2 Limitation in Horizontal Wells Application

Horizontal wells have gained popularity in the past 30 years. There are many types of reservoirs where the benefits of horizontal drilling outweigh the benefits of a vertical well (e.g. reservoirs with thin reservoir layers, or with high vertical permeability, or vertical fractures, and reservoirs where water coning or gas cap can be an issue). However, horizontal wells are also costly, technically more challenging to operate, and require more sophisticated completion to maximise its benefits.

Due to the geometry characteristic of a horizontal well, various flow regimes occur in the pressure transient data (**Figure 5.32**) making it much more complicated to interpret. Solution models for horizontal well are available to diagnose and analyse the well test data.

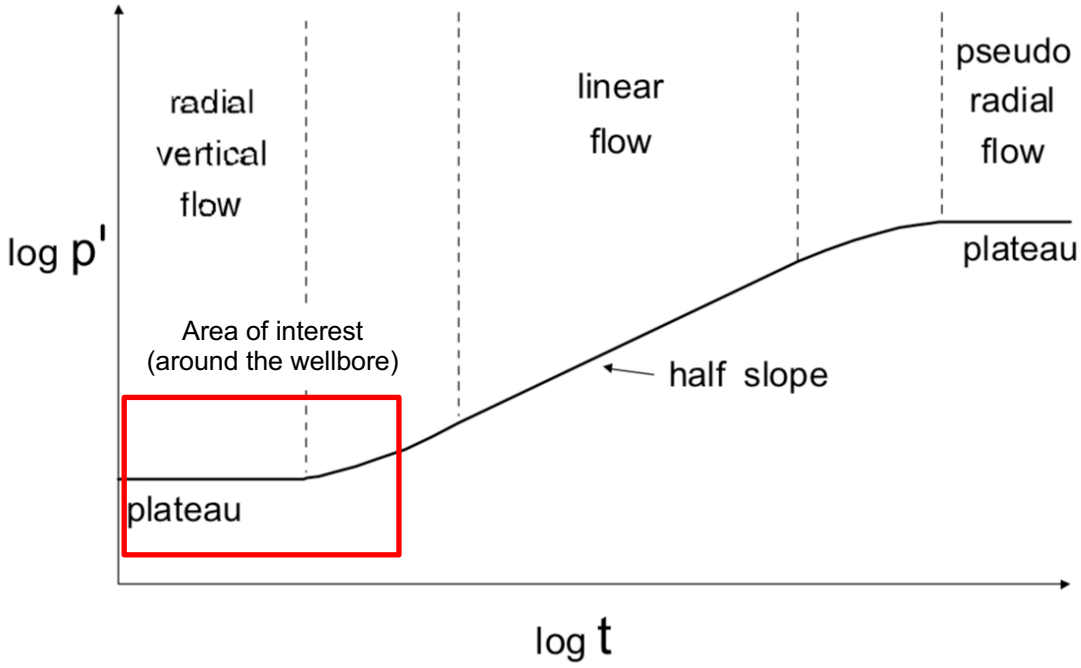

Figure 5.32—Pressure derivative of a typical horizontal well, showing three distinctive flow regimes.

Horizontal well flow regimes typically consist of an early radial, early linear flow and pseudo-radial flow (**Figure 5.33**). The early radial flow is similar to the radial flow of a vertical well; that is the flow is going towards the wellbore length in a radial direction. In the horizontal well case, however, the flow is covering the horizontal and vertical planes, in other words, it is flowing in the x and y direction, where both the vertical permeability (k_v) and horizontal permeability (k_h) governs the flow. As a result, one of the main parameters that can be estimated from this early radial flow is average horizontal and vertical permeability, or k_{bar}, which is defined as,

$$k_{bar} = \sqrt{k_h k_v} \tag{5.12}$$

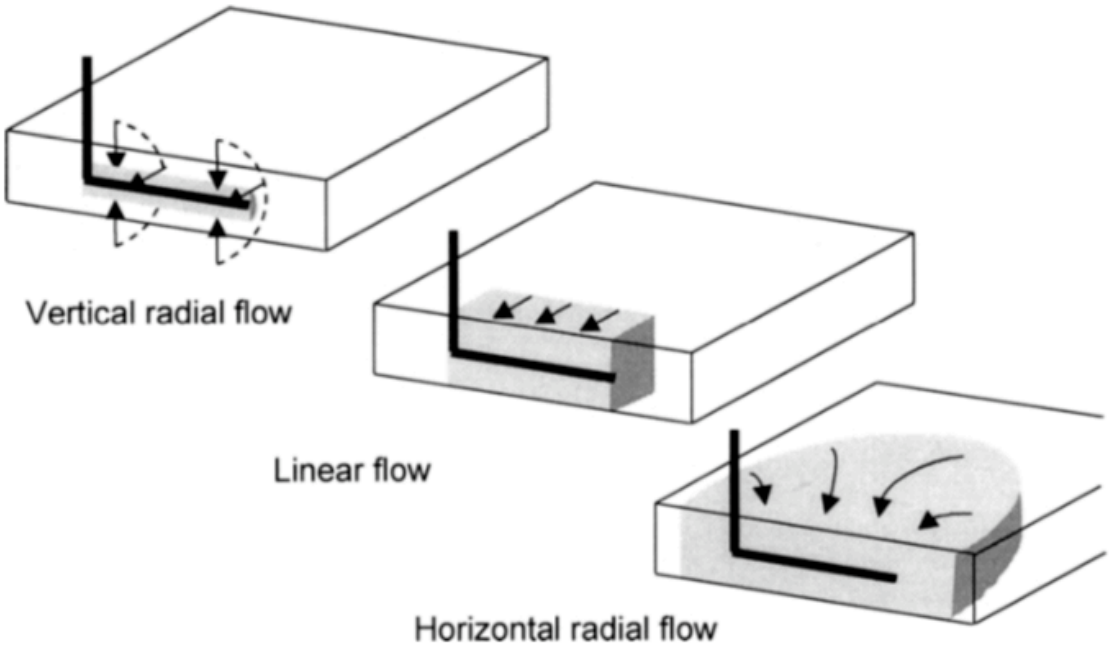

Figure 5.33—Flow regimes due to geometry for a horizontal well (Bourdet, 2002).

If the length of the horizontal well is much higher than the formation thickness, the linear flow regime may develop after the top and bottom boundaries have been felt. The linear flow can be used to estimate the effective horizontal section L_w and the furthest distance to a vertical boundary, D_z. Most importantly, is the late pseudo-radial flow regime, which represents the radial flow through the horizontal plane towards the well. The pseudo-radial flow occurs when the effect of the horizontal length on the overall flow diminishes to the point where the well can be assumed to represent a single point. From this late flow regime, the formation horizontal permeability, k_h, can be determined.

In this thesis's work and the context of two-phase flow (gas and condensate) around the wellbore, the near wellbore area is the area of interest, where the early radial flow regime occurs. The applicability of the suggested method would rely on the availability of k_v along with k_h in order to computer k_{bar}. However, as it has been shown in 5.6.1 above, since the solution relies on a specific segment of the pressure derivative data (which corresponds to the early radial flow in this case), the calculated relative permeability data will be limited

to that specific range of data, which ultimately constrain the use of such data. In other words, if k_v and k_h are available, the relative permeability as a function of pressure can be calculated for the pressure range corresponding to the early radial flow, but that could be of limited use.

To showcase such a scenario, a reservoir model was constructed using a Cartesian model, instead of a radial model, with local grid refinement (LGR) around the horizontal well (**Figure 5.34**). Several gridding sensitivities were investigated, and it has been found that the grid-block size in the vertical direction needed to be smaller than one foot to accurately capture the vertical permeability in the simulated well test data.

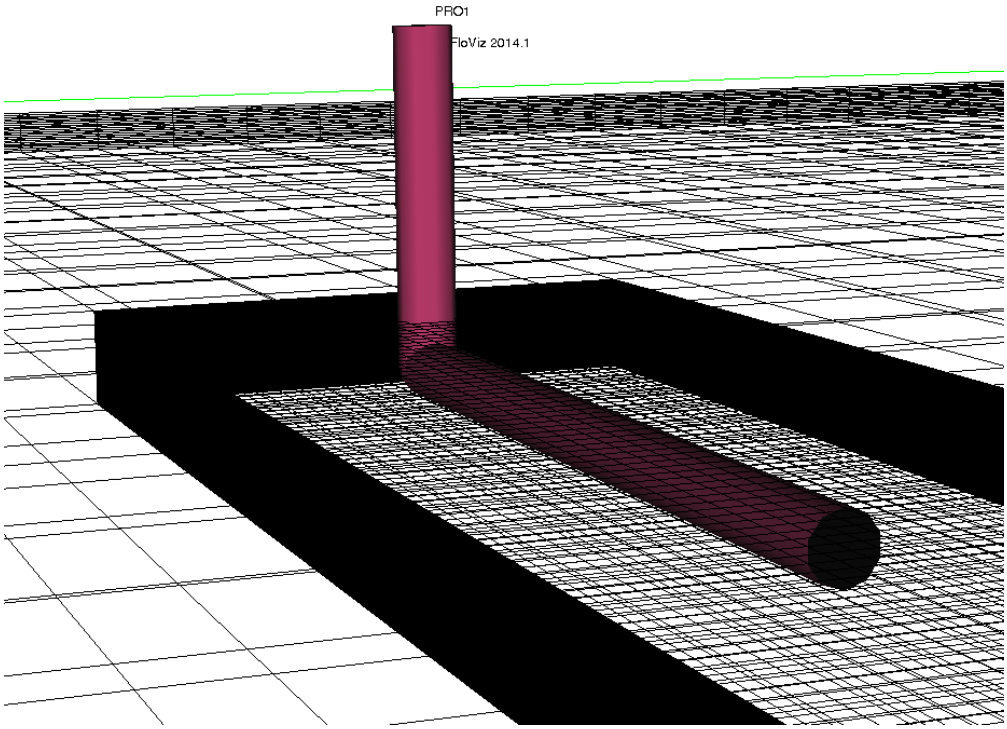

Figure 5.34—Cartesian reservoir model with LGR around the horizontal well.

In the vertical well scenario, the radial flow capacity is represented by kh, whereas in the horizontal scenario, $k_{bar}L_w$ represent the flow capacity in the radial direction around the wellbore, where L_{w} represent the length of the horizontal segment of the well. As a result, for the horizontal well case, the mobility equation (Equation 4.6) would change to,

$$\lambda_g = \frac{711\, q_g\, T}{\mu_g L_w\, p_p(p')} \tag{5.13}$$

where the thickness along the vertical well segment, h, is replaced by the length of the horizontal well segment, L_w. Subsequently, the relative permeability equations for gas and condensate (Equations 5.1, and 5.2, respectively) would change to include L_w instead of h, and k_{bar} instead of k_h,

$$k_{rg} = \frac{1}{5.615} \frac{m_T \mu_g (1-x)}{\alpha_1 k_{bar} L_w \rho_g r\left(\frac{\partial p}{\partial r}\right)} \tag{5.14}$$

$$k_{ro} = \frac{1}{5.615} \frac{m_T \mu_o x}{\alpha_1 k_{bar} L_w \rho_o r\left(\frac{\partial p}{\partial r}\right)} \tag{5.15}$$

A case was designed with a horizontal well of 900 feet set in the middle of the reservoir thickness. The vertical permeability, k_v was set at $0.1 \cdot k_h$, which is equal to 2.34 mD (for the 23.6 mD RC6 rock). The well test was then simulated and analysed. **Figure 5.35** shows the pressure derivative exhibiting the main three flow regimes. It is apparent that the condensate development affected the early radial flow regime, as the vertical permeability obtained from the analysis is 1 mD (57% less than actual value).

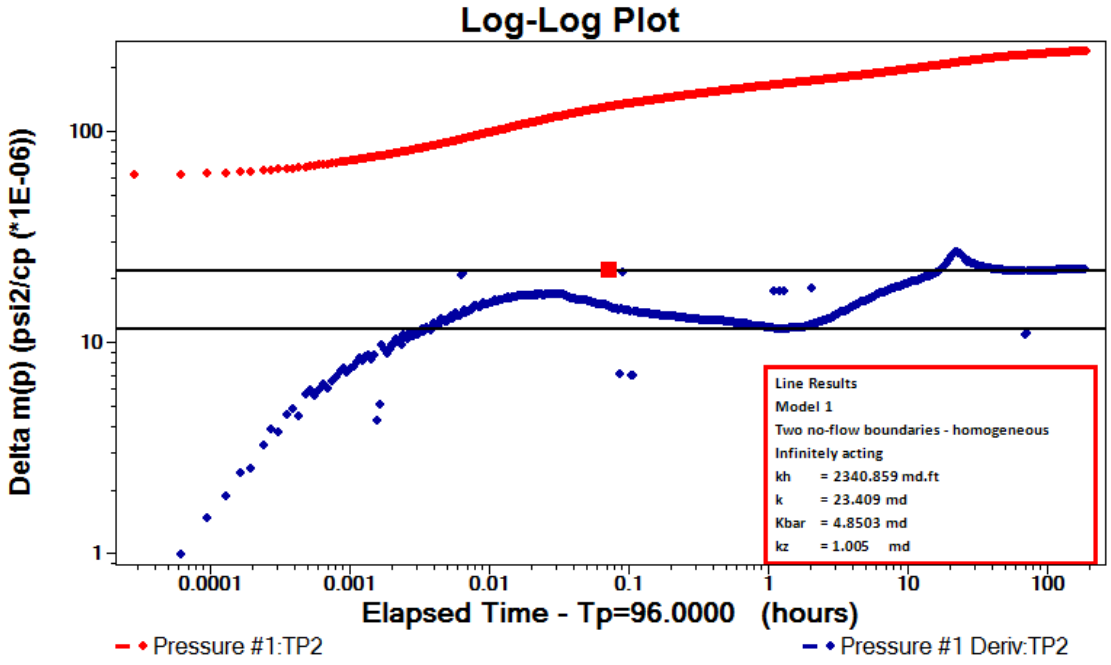

Figure 5.35—Pressure derivative of a simulated horizontal well.

The pressure derivative from well test data in the early radial flow is then used to calculate pressure versus radius and its gradient to compute relative permeability data using Equations 5.14 and 5.15 (**Figure 5.36**). The data points in Figure 5.36 were not compared with the output from the numerical simulation due to the Cartesian model and local grid refinements (LGR), required for the horizontal well model, that were used in this exercise. The ability to export relative permeability data points versus radial distance is not straightforward as in the radial model used in the previous exercises. However, the point of this example is to showcase the limitation in horizontal well applications, regardless of how close the results are to the numerical simulation output in this particular scenario.

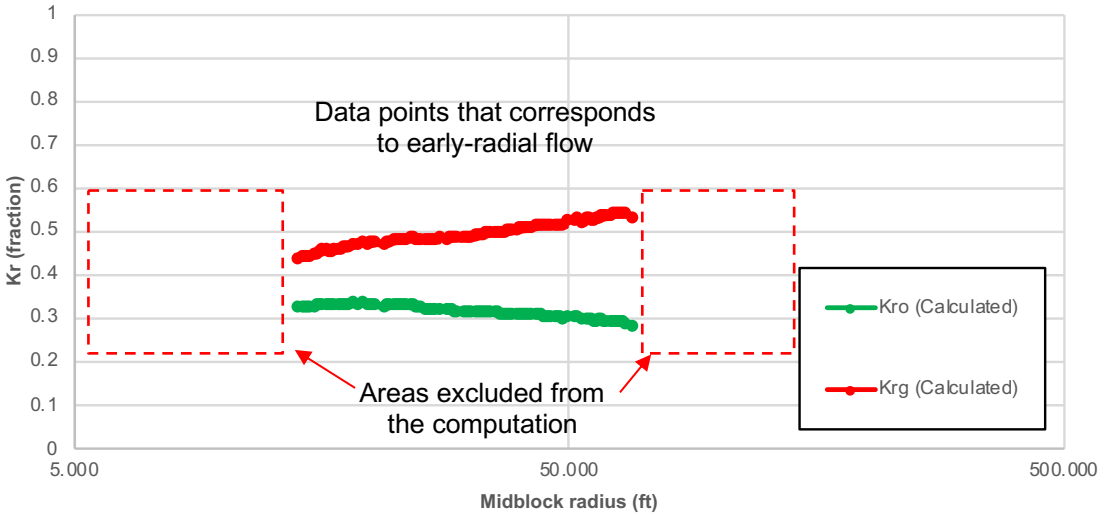

Figure 5.36—Analytically calculated relative permeability versus radius calculated from the early-radial flow in the well test data of a horizontal well.

As discussed above, only the early radial segment of the pressure derivative data can be used to compute the relative permeability, with uncertainty in the availability of k_v, to compute k_{bar}, the results show that such application can be of a limited use. In addition, the calculated relative permeability cannot be related to reservoir radial distance, since it is calculated from the early radial flow regime which corresponds to the radial flow around the horizontal section, and not along the horizontal plane of the reservoir.

5.7 Conclusion

This study evaluates the possibility of obtaining, analytically, relative permeability data affected by pressure and velocity assuming Darcy's law. The approach uses the pressure derivative with respect to distance obtained from the pressure versus radius profile, which in turn obtained from the pressure versus time during a well test operation. The calculations were verified by comparing the results with the output from a numerical simulation based on a single-layer single-well radial reservoir model. The results show adequate approximated results for analysis and engineering purposes and provides excellent insight of the two-phase flow conditions.

The calculated relative permeability data, in addition to two-phase pseudo-pressure calculations, could potentially have other applications such as tuning or verification of reservoir simulation results during a history matching process and when there is uncertainty in the input relative permeability data. This application is particularly important for the near wellbore velocity-dependent relative permeability values. These relative permeability data can be predicted by the simulator using the correlations which require core specific constants. However, these core specific constants are either unknown or need to be determined using demanding and costly experimentally measured data.

Below is a summary of the main findings of this chapter.

- Velocity-dependent relative permeabilities data can be calculated analytically from the well test data. The approach uses the pressure versus radius gradient obtained from the pressure versus radius profile, which in turn obtained from the pressure versus time during a well test operation.

- The analytical calculation of relative permeability using the approach described is a good approximation to the results expected from numerical simulation.

- The calculation of relative permeability relies on the proper smoothing of pressure derivative data which are liable to oscillate. Two main methods were described in this chapter. Using a fit function gives smoother data but using the built-in smoothing tools (e.g. PanSystem's) is more practical.

- Further sensitivity analysis investigation showed that at least some part of the data oscillation was generated from ECLIPSE numerical calculation, as the use of a different software to generate the data (e.g. Saphir) minimised the level of noise observed in the pressure versus shut-in time derivative for the single-phase black oil case.

- Although Saphir numerical model does not generate the same level of data oscillations, it lacks the capabilities required by the proposed method in this thesis. Specifically, its simulation option cannot generate two-phase gas-condensate pressure data with inertia and coupling effects, as done by ECLIPSE.

- It was shown that for the case considered, the available smoothing tool in PanSystem software is sufficient to carry on with the proposed techniques. These tools may not always be able to completely remove the oscillations, something which is done by the use of fit functions but are practically more attractive.

- When smoothing techniques that are available in well test software do not give good results, fit function techniques can be a desirable alternative method.

- Once relative permeability data as a function of pressure become available, two-phase pseudo-pressure can be calculated and utilised for any two-phase data analysis, such as production analysis (as will be described in Chapter 7).

- Series of simulations were repeated albeit with WBS. The results show

that the applicability of the proposed method is reliant on good well test pressure transient data that represent a radial flow. Effects such as WBS can minimise the data range of obtainable results.

- It has been shown that the procedure has a limited use in horizontal wells, where complex flow geometry influences the pressure transient data and uncertainty in the vertical permeability exists.

Chapter 6

Pressure Profile and Relative Permeability in Multi-Rate Testing

6.1 Introduction

In this chapter, an investigation is carried out into how the proposed method of calculating pressure profile and velocity-dependent relative permeability would respond in multi-rate test conditions (shorter test durations, and variable flow rates); with the aim of understanding the impact of multi-rate test parameters. This would help in the design of such tests in gas-condensate reservoirs, if the relative permeability calculation method, presented in Chapter 5, is to be used. However, first, and for clarification purposes, a brief description of key characteristics of multi-rate tests in gas reservoirs is given. This includes the benefits of this application and a summary of the past work that has been done in this area as part of the Gas Condensate Recovery team (HWU-GCR). Then, the model setup and design of the numerical simulations used to generate pressure versus data from the multi-rate scenarios required to calculate relative permeability following the proposed procedure are discussed, with the results of two different multi-rate scenarios presented at the end.

6.1.1 Multi-Rate Testing Background

Multi-rate testing is an important tool in gas reservoir engineering; it is commonly used to measure well production capabilities under specific conditions of reservoir and bottomhole flowing pressures and gas flowing rates. One of the most common productivity indicators obtained from such tests is the absolute open-flow, which is the maximum rate the well could flow. Another indicator is the reservoir inflow performance curve, which describes the relationship between surface production rate and bottomhole pressure. The inflow performance curves can be used to evaluate the well's deliverability potential under a verity of surface conditions, and as a production forecasting tool as well.

Several types of multi-rate test are used, the most common are step-rate, isochronal and modified isochronal tests. A step-rate test is conducted by producing the well at a series of different stabilised flow rates before shutting it in for a buildup test (**Figure 6.1**). It compromises of multiple drawdowns tests with varying constant rates followed by a single buildup at the end. The main aspect of this test is that it does not have intermediate shut-in periods between the flowing periods.

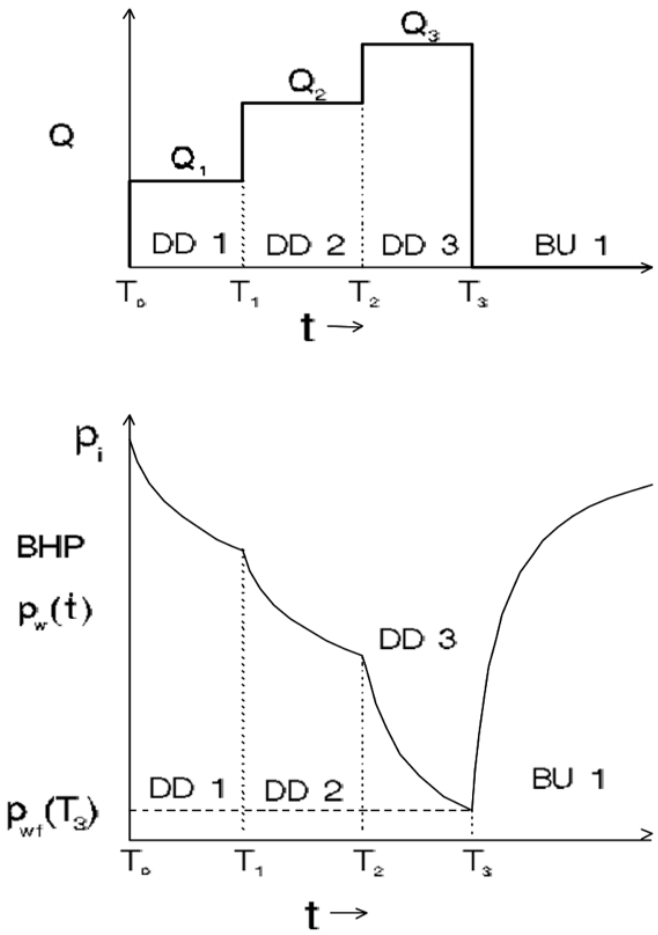

Figure 6.1—An example of the step-rate multi-rate test scheme.

An isochronal test is used to shorten test times in gas wells that take a long time to achieve stabilised rates. In an isochronal test, the well is flowing for equal periods of time at several different rates with intermediate buildup periods after each drawdown (**Figure 6.2**). The buildup periods are long enough allowing the pressure to build to the average reservoir pressure before the next flowing period starts. The idea in this method is that the formation pressure drop will be proportional to the production rate. It is based on the idea that the radius of investigation established during the flowing period is not a function of the flow rate, but a function of time. Hence, each flowing period, at different flow rates, are associated with the same drainage radius, which makes the data from each test period comparable with each other. That is, the pressure transient propagation in all the test duration is the same, and only flow rate is different. This type of test is used to estimate stabilised

deliverability characteristics without actually flowing the well for the time required to reach stabilisation. The isochronal test is more practical since less time is required to build up to reservoir pressure after short flow periods than to reach stabilised flow in a step-rate test.

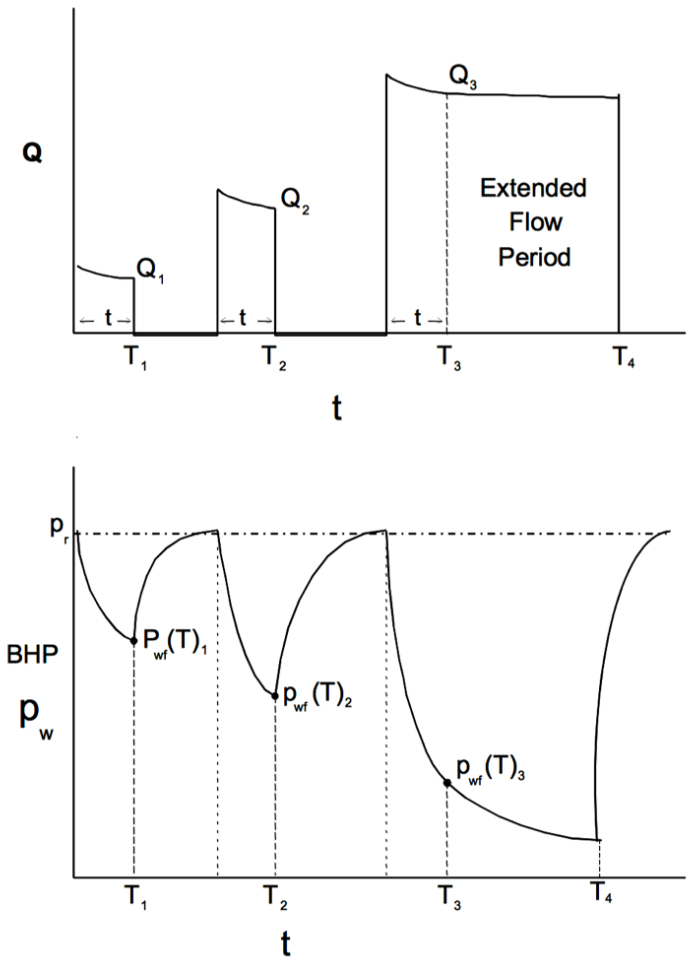

Figure 6.2—An example of the isochronal multi-rate test scheme.

The modified isochronal test is the same except that the drawdown and buildup periods have the same duration (**Figure 6.3**). The advantage of the modified isochronal test is that it requires shorter buildup test periods to obtain the same data as in the isochronal test. However, in this type of test, due to the equal and short durations of the shut-in periods, the pressure does not build up to average reservoir pressure after each flow period. Hence, the trade-off is that the modified isochronal test is generally less accurate than the isochronal test

because the duration of the buildup is shorter but as the duration of the buildup test increases, the accuracy of the modified isochronal test increases.

In any multi-rate test, the rate sequence can either have a forward scheme (flowing rate values increase with time), or backward scheme (the flowing rate values decrease with time).

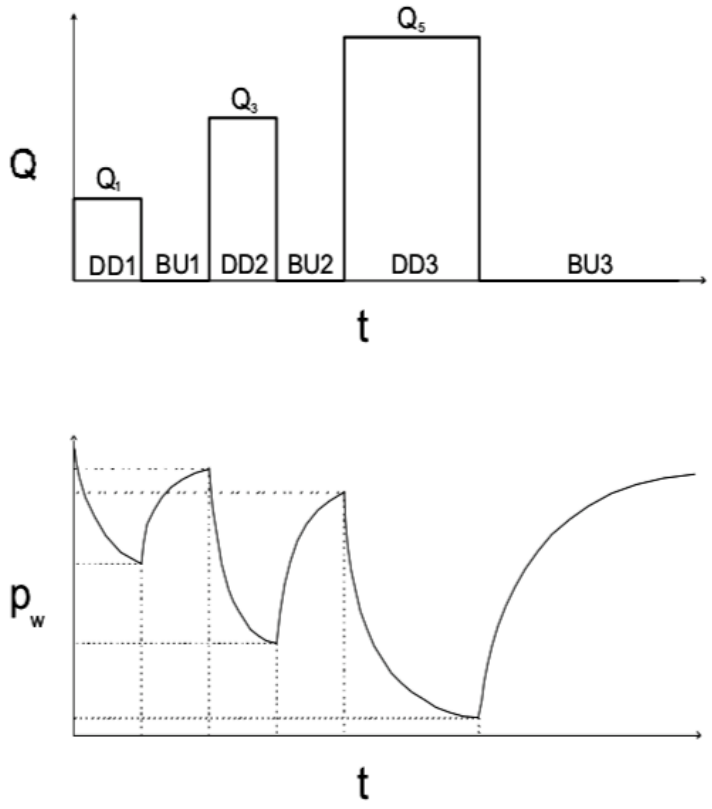

Figure 6.3—An example of the modified isochronal multi-rate test scheme.

6.1.2 Benefits

In the method that was proposed earlier in Chapter 5, velocity-dependent relative permeability could be analytically calculated for the test periods for which the pressure profile is generated. Here the main aim is to verify if the method works for multi-rate tests. In the first instance, calculating pressure versus radius profiles from well test data for a multi-rate test can give an insight into the pressure values at different radial distances at different rate values. Additionally, as a result of this exercise, different sets of relative permeability

data could be obtained at different flow rates. This is achieved by calculating relative permeability from multi-rate well test data, then compare the results with the numerical simulation output (taken into consideration velocity effects).

Another benefit of having relative permeability data calculated analytically at different rates from multi-rate tests is that they can potentially be used in a multi-regression package to generate core exponents of the correlations available in the literature and major reservoir simulators for expressing the coupling and inertial effects (e.g. VELDEP keyword in ECLIPSE). Currently, expensive and demanding lab-based measurements of different relative permeability curves at different flow rates are performed for simulation purposes. This approach will provide such data analytically.

6.1.3 Previous Work for Skin Estimation

The HWU-GCR team previously looked into multi-rate analysis using both step-rate and modified isochronal tests, with forward and backward schemes, albeit to some extent. Analysing the simulated well test data and comparing the two-phase skin, based on single-phase pseudo-pressure technique, it was noted that an increasing rate scheme is more consistent with skin estimation. That is, regardless of the flowing rate values, a low rate forward sequence (e.g. 5, 10 and 15MM scf/d) or a high rate forward sequence (e.g. 15, 30, 40MM scf/d), the same two-phase skin value for a specific flow rate was obtained. However, in the backward scheme, overestimation and inconsistencies of the two-phase skin value were observed.

The backward scheme is arguably more practical and more desired for operational reasons, such as if liquid hold-up in the production string is a problem, or if hydrate formation is probable, or for reasons like clean-up or sweeping out of water and mud from near wellbore region. Therefore, it was essential to further investigate the impact of the rate sequence especially in the context of using the proposed approach to calculate velocity-dependent relative permeability analytically.

In this thesis, the results show that there is no real preference on the type of flow rate scheme. That is, both forward and backward gave good results in terms of pressure versus radius profile and relative permeability. In fact, the results in section 6.3.2 show that backward scheme gave more consistent relative permeability data, which makes the "forward" scheme recommendation above specific to skin estimation rather than a general recommendation for multi-rate tests.

6.2 Model and Design

For this part of the work, synthetic data from the numerical simulations were used. The reservoir setup is similar to that used for the earlier constant-rate cases; reservoir Model 1 (Table 3.1). The same binary rich gas condensate fluid of C1 and C10 was considered (Table 3.7) using RC6 rock properties (Table 3.2). In this work, the isochronal tests were used for their ability to obtain buildup data after each flow rate, and for their accuracy as they have longer buildup periods compared to the modified-isochronal tests. Both forward (section 6.3.1) and backward (section 6.3.2) schemes were simulated and analysed.

The multi-rate test cases discussed below are designed to have a short duration– e.g. 50 hours for the whole test sequence (Table 6.1). The primary criterion for the duration of the drawdown is that they are short but long enough to go below the dew point, thus, the system allows the formation of condensate, and two-phase flow takes place around the wellbore under different gas flow rates. For the buildup periods, the duration is short as well, and the objective is to acquire enough well test data to understand the flow behaviour near the wellbore, which is the region where the coupling and inertia velocity effects are most important.

Case	Test Scheme	Flow Rates (MMscf/D)	Test Durations DD/BU (Hours)
1	Isochronal Forward	30, 40, 50	5/5, 5/10, 5/20
2	Isochronal Backward	50, 40, 30	5/5, 5/10, 5/20

Table 6.1—Multi-rate sequence and test duration configurations for the two considered cases.

6.3 Results

To reiterate, as discussed in section 5.5 above, that in the discussion of the analytically calculated relative permeabilities results below. The determination of having satisfactory results or a match are based on the comparison with the numerical simulation output where a maximum of ±0.1 margin of error is observed for both k_{rg} and k_{ro}.

6.3.1 Isochronal Forward Scheme

First, the isochronal forward multi-rate test is considered, referred to as Case 1. A simple three drawdowns and three buildups were designed as following: for each drawdown period, the production time is 5 hours, each followed by a buildup period of 5, 10, and 20 hours respectively (**Figure 6.4**). The production rate sequence for this set up is 30, 40 and 50 MMscf/D, respectively (Table 6.1). In all the three drawdown sequences, the pressure around the wellbore dropped below the dew point pressure.

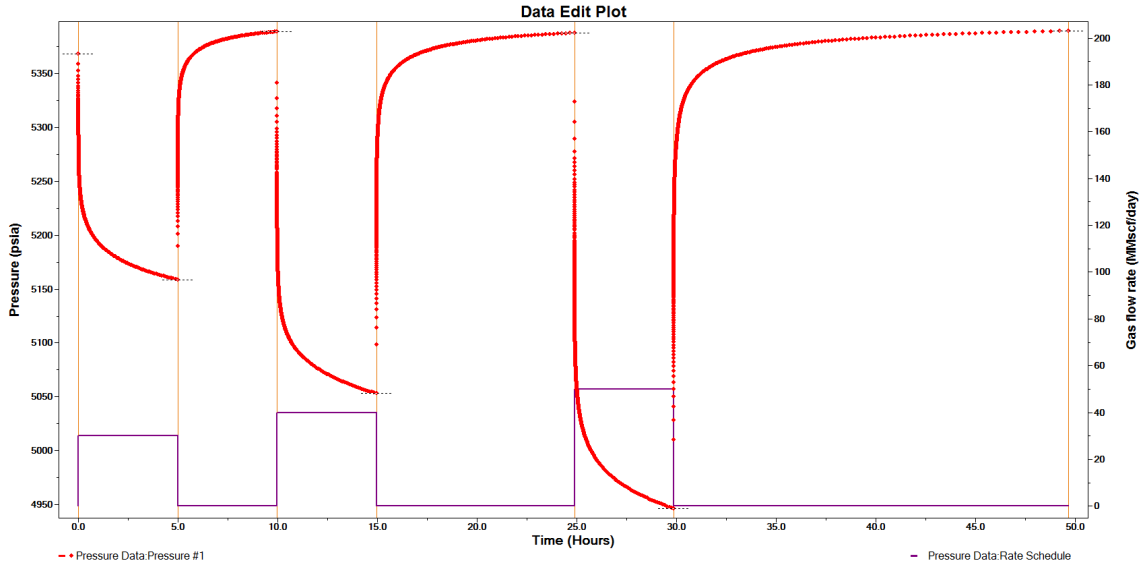

Figure 6.4—Case 1 Isochronal forward test design, pressure versus time, and rate schedule.

Pressure versus radius profiles for all the three buildup periods are calculated using the method described in Chapter 4 (**Figure 6.5, Figure 6.6,** and **Figure 6.7).** They all show a good agreement with the pressure versus radius profile from the numerical simulations. This proves the validity of using the probe radius concept to obtain pressure versus radius profile even for a multi-rate test scenario.

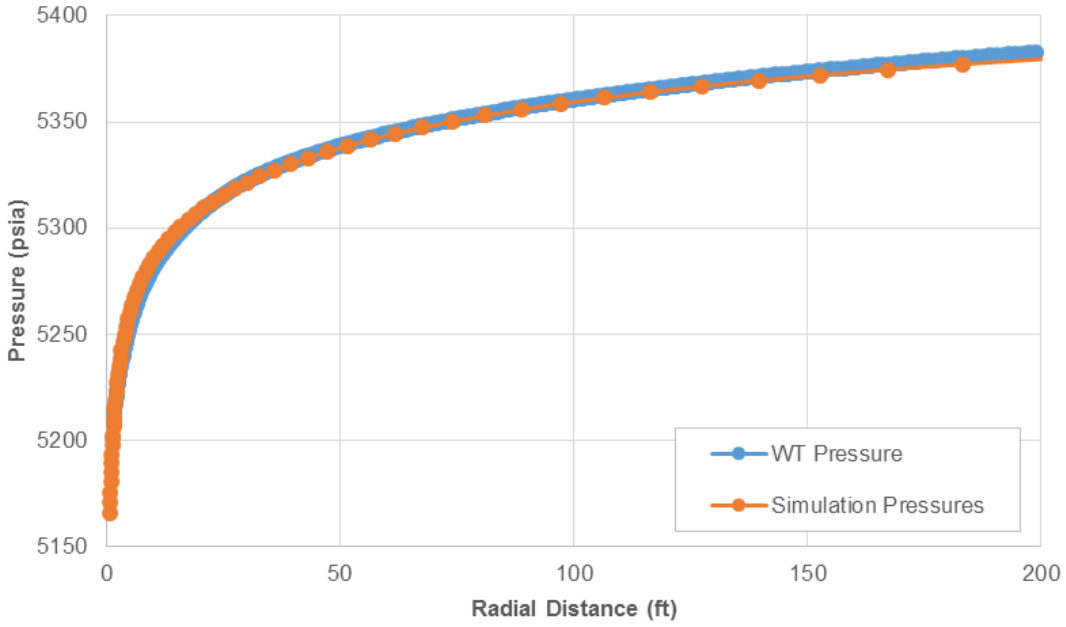

Figure 6.5—Comparison of pressure versus radius profile with the output from the numerical simulation for BU1, Case 1.

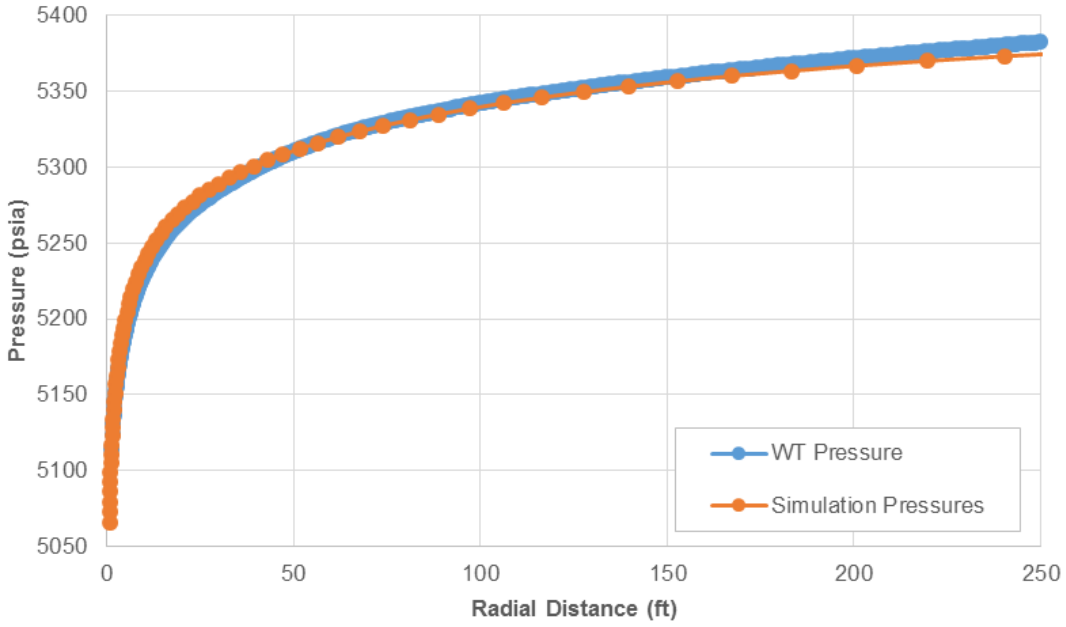

Figure 6.6—Comparison of pressure versus radius profile with the output from the numerical simulation for BU2, Case 1.

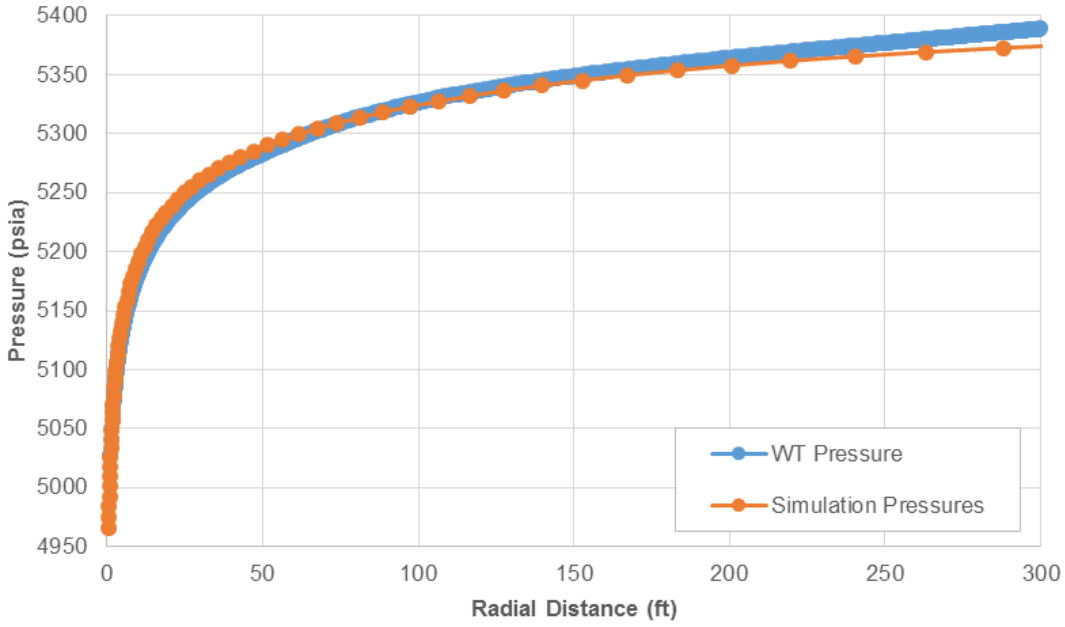

Figure 6.7—Comparison of pressure versus radius profile with the output from the numerical simulation for BU3, Case 1.

The relative permeability data were then calculated analytically using the pressure gradient for the first buildup. As shown in **Figure 6.8**, even when the test duration is short (5 hours) the calculated relative permeability data show a good trend. Following the same approach, the calculated relative permeability data for the second and third buildups are shown in **Figure 6.9** and **Figure 6.10**, respectively.

The overall trends in the relative permeability calculation for all the three buildup sequences show good matches with the relative permeability output from the numerical simulations. The relative permeability match in the second (Figure 6.9) and third (Figure 6.10) buildup are better than the first buildup (Figure 6.8). However, the discrepancy in the k_{ro} in terms of condensate bank extent from the third buildup (Figure 6.10) seems to be more pronounced compared to the first and second buildup (Figure 6.8 and Figure 6.9). Initially, it was suspected that the order or the magnitude of the rate sequence might be the cause of such a trend (i.e. forward versus backward schemes). Therefore,

this was further investigated by analysing the same rate values but using a backward scheme instead as discussed next.

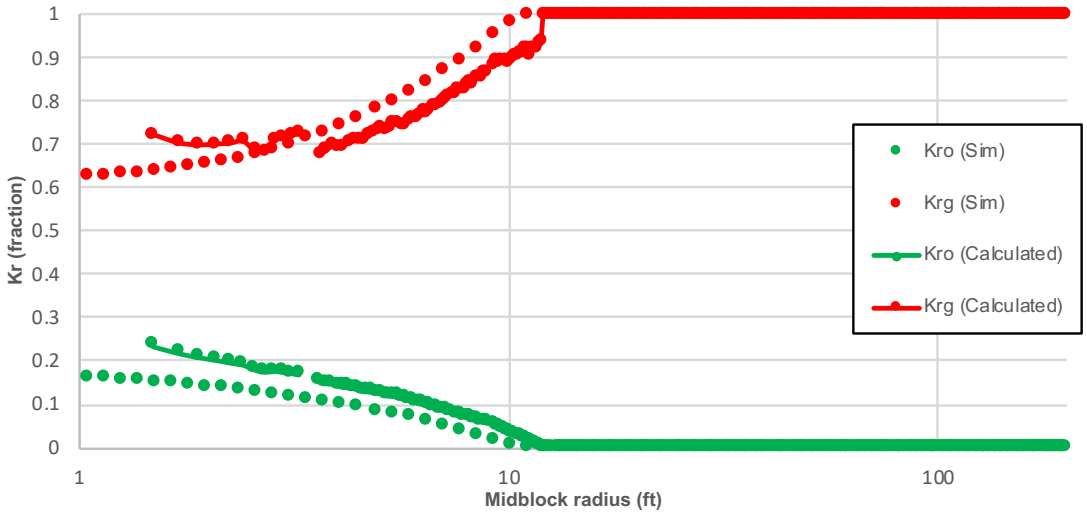

Figure 6.8—Analytically calculated relative permeability compared to output from the numerical simulation for BU1, Case 1.

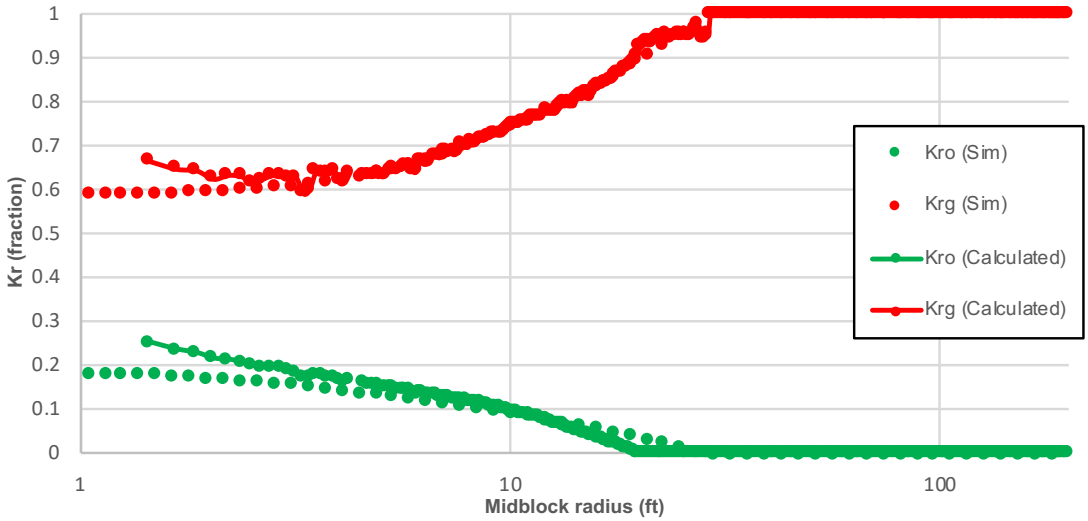

Figure 6.9—Analytically calculated relative permeability compared to output from the numerical simulation for BU2, Case 1.

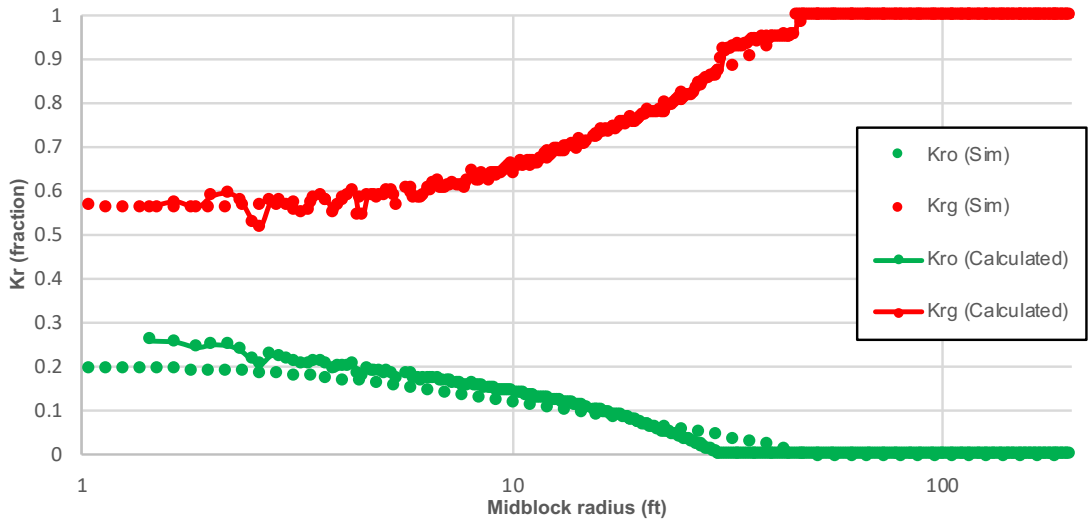

Figure 6.10—Analytically calculated relative permeability compared to output from the numerical simulation for BU3, Case 1.

6.3.2 Isochronal Backward Scheme

Case 2 was set up using a backward scheme with the same rate values but in the reverse order (Table 6.1). Gas flow rates values of 50, 40, and 30 MMscf/D were used for the first, second and third drawdown, respectively (**Figure 6.11**).

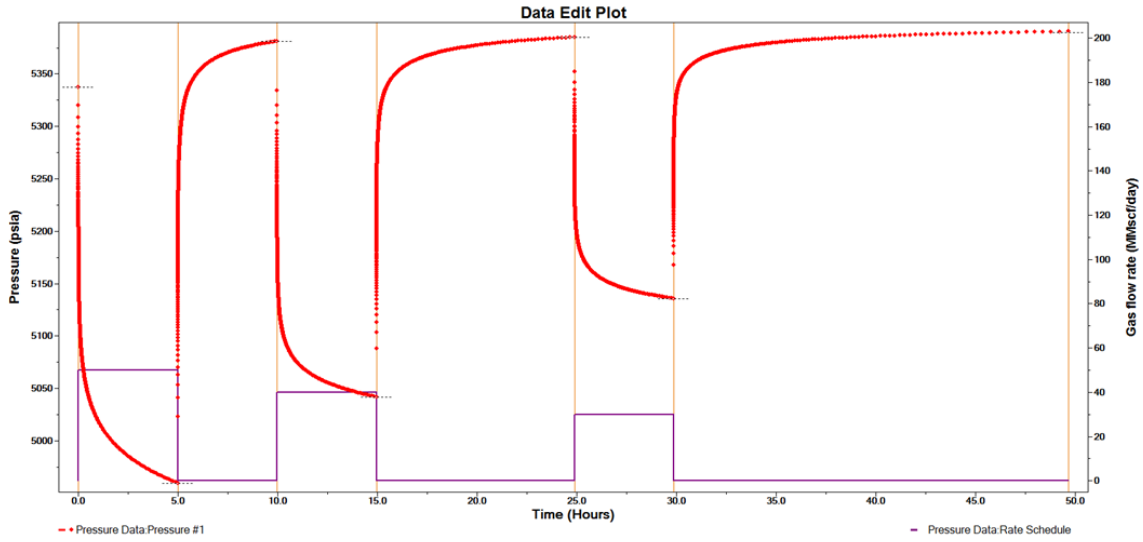

Figure 6.11—Case 6 test design, pressure versus time, and rate schedule.

The pressure versus radius profiles are calculated for the three consecutive buildups and plotted in **Figure 6.12, Figure 6.13** and **Figure 6.14**, respectively. In all the three pressure profiles, they show the same level of agreement compared to the numerical simulation output; similar to the results of the forward sequence test.

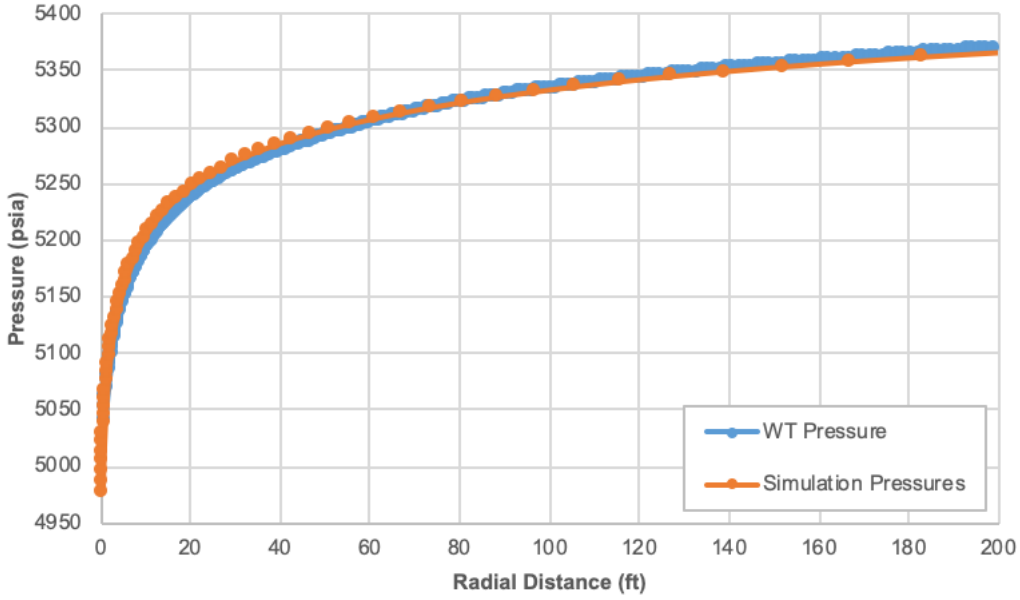

Figure 6.12—Comparison of pressure versus radius profile with the output from the numerical simulation for BU1, Case 2.

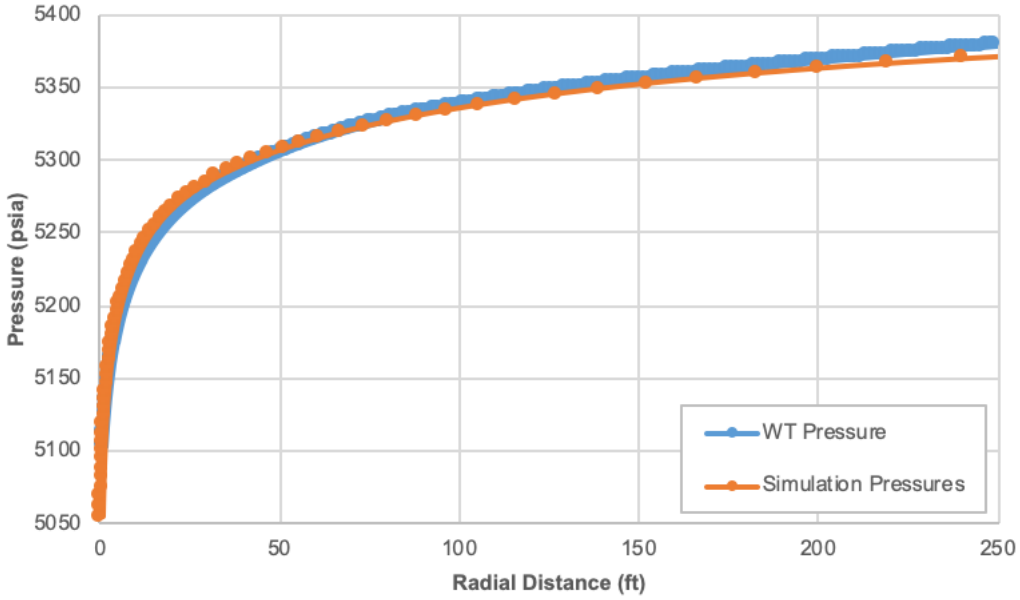

Figure 6.13—Comparison of pressure versus radius profile with the output from the numerical simulation for BU2, Case 2.

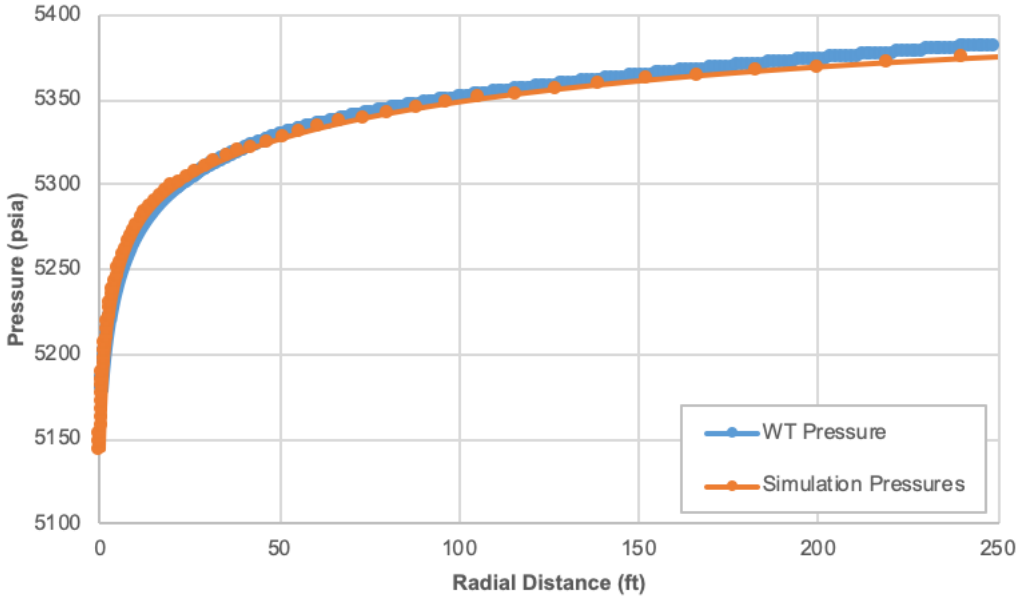

Figure 6.14—Comparison of pressure versus radius profile with the output from the numerical simulation for BU3, Case 2.

Then using the same approach, the velocity-dependent relative permeability data were calculated for the three buildup periods, it was noted that the k_{ro}

discrepancy in terms of condensate bank extent was still apparent for the buildup associated with the high flow rate (50 MMscf/D), which is the first buildup in this case (**Figure 6.15**). That is, the k_{ro} data at the end of the condensate bank does not match the simulation output. However, the overall trend of the calculated relative permeability for the all the three buildups show a good agreement with the numerical simulation output data (**Figure 6.15**, **Figure 6.16**, and **Figure 6.17**).

As for the third buildup (Figure 6.17) associated with a lower flow rate of 30 MMscf/D, the result show a better k_{ro} match, especially after about three feet, when compared with the numerical simulation data. Which is similar to the first buildup in Case 1. In fact, to some extent, the 30 MMscf/D for Case 2 (third buildup in the backward scheme, Figure 6.17) was showing a better relative permeability trend compared to the 30 MMscf/D for Case 1 (first buildup in the forward scheme, Figure 6.8).

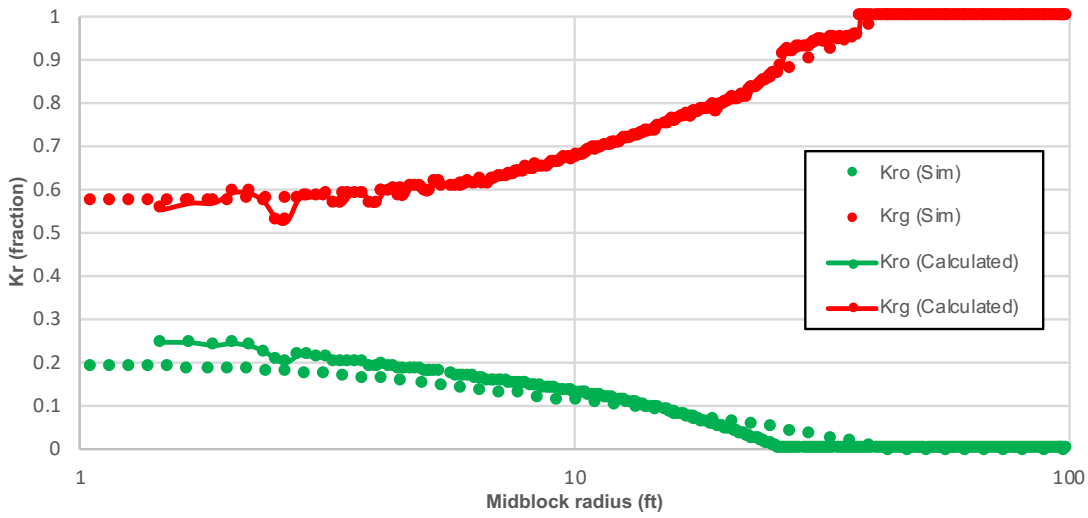

Figure 6.15—Analytically calculated relative permeability compared to output from the numerical simulation for BU1, Case 2.

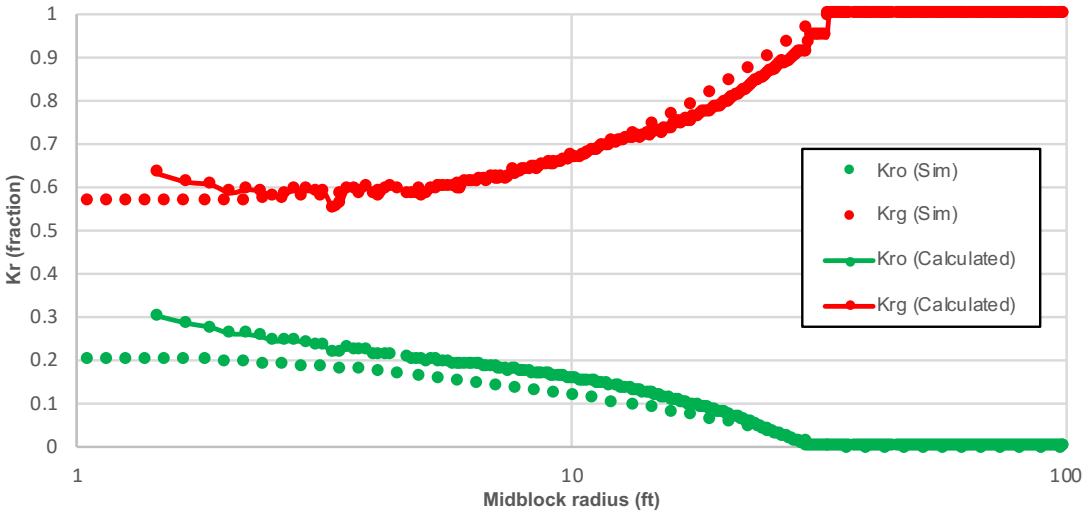

Figure 6.16—Analytically calculated relative permeability compared to output from the numerical simulation for BU2, Case 2.

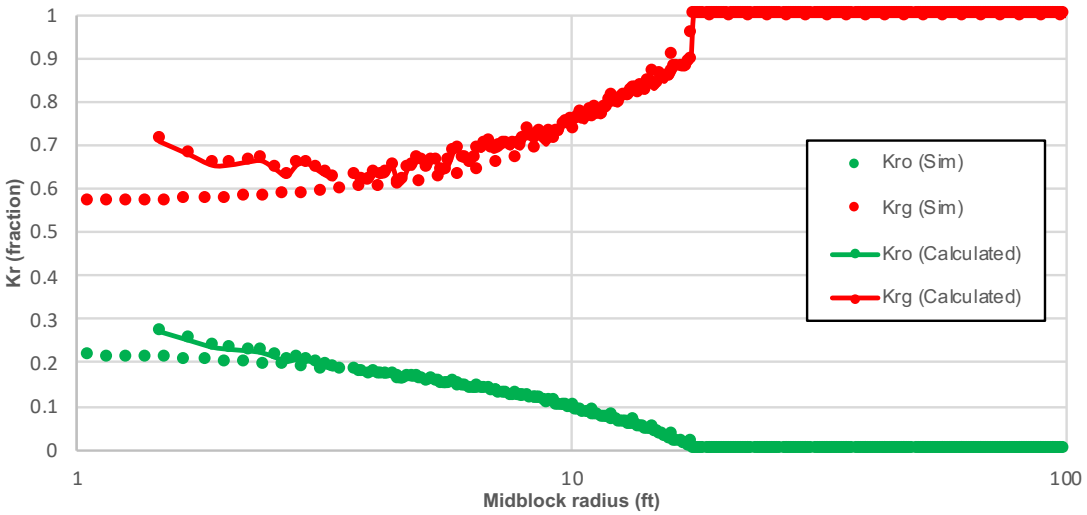

Figure 6.17—Analytically calculated relative permeability compared to output from the numerical simulation for BU3, Case 2.

6.3.3 Discussion

These results suggest that the value of the flow rate affects the relative permeability data calculated analytically. In other words, the higher the flow rate, the more deviation in the k_{ro} data points away from the wellbore (at the

end of the condensate bank) for the calculated relative permeability from the numerical simulation output. On the other hand, a lower flow rate (as low as 30 MMscf/D) produces a relative permeability trend that is in a good agreement with output data from the numerical simulations. However, it is also clear that the effect is not very significant, in the sense that the deviation is not too bad to the point that renders the analytical results to be obsolete. The source of the mismatch, especially at the beginning of the data is not clear and might need further investigation. However, this approximation of k_{rg} and k_{ro} have shown that such deviation does not affect the end results much. As it will be shown in Chapter 7, that the relative permeabilities calculated in Chapter 5 were used in the two-phase production data analysis that resulted in good permeability estimation.

Rate sequence also seems to play a minor role in the level of accuracy. The different rate sequence between the two tested cases, one being forward and the other being backward, have affected the overall results, albeit slightly, as well. In both cases, the resultant relative permeabilities data are satisfactory–i.e. can give good results when used in two-phase analysis techniques. There seems to be no clear advantage of one sequence scheme over the other.

6.4 Conclusion

The results presented above are practically appealing regarding the ability to calculate relative permeability analytically for multi-rate tests of short durations. It highlights how flow rate can influence the analytical approach of calculating relative permeability data, less so with the pressure versus radius profile. At the same time, it shows that any deviation from the actual data is not significant, specifically noting that such relative permeability data as a function of pressure are needed to be used (e.g. for two-phase pseudo-pressure calculations).

In addition, it confirms how the different design sequence can affect the results. As the backward scheme of the same flow rates gave better overall results

compared to the forward scheme. The earlier results by the HWU-GCR team had suggested that forward isochronal tests are better for gas condensate two-phase skin estimation. However, from the above findings, the backward scheme did give better results in terms of analytical relative permeability calculation for the rich gas condensate scenario. This is useful outcomes that need to be considered when designing multi-rate tests.

The calculated relative permeability data from multi-rate tests can potentially be used for other applications, such as two-phase production data analysis using pseudo-pressure and pseudo-time functions. Another potential benefit of having relative permeability data at different rates is that they can potentially be used to generate core exponents through multi-regression package of the correlations available in the literature and major reservoir simulators for expressing the coupling and inertial effects as an alternative to the expensive and demanding lab-based measurements of different relative permeability curves at different flow rates.

Chapter 7

Two-Phase Production Data Analysis using Velocity-Dependent Relative Permeability

7.1 Introduction

Production data analysis is a valuable tool for reservoir engineers to evaluate well performance and reservoir quality. Traditionally, decline curve analysis was used for production performance forecasting, but with the introduction of modern production analysis techniques, it also became possible to estimate reservoir parameters such as permeability, skin and drainage radius from production data. However, most available production analysis techniques rely on the assumption of single-phase Darcy flow, which is not very accurate if applied to two-phase gas-condensate systems. In other words, applying these single-phase-based techniques to two-phase gas-condensate reservoirs would give erroneous results, such as permeability estimation being lower than absolute permeability.

Johnson and Jamiolahmady (2016, 2017) used an equivalent-phase approach for production data analysis. The equivalent-phase concept was originally introduced for other applications by Jamiolahmady et al. (2007). Such a technique allows the single-phase based theory to be used for the multi-phase

conditions. They tested several scenarios to demonstrate under what conditions, an equivalent-phase approach is necessary to improve the analysis results for the two-phase gas-condensate production data. Their proposed method uses the Blasingame type-curves (Palacio & Blasingame 1993) for variable rate and pressure scenarios. In their approach, relative permeability data is needed for the calculation of the two-phase pseudo-pressure. The proposed method in Johnson and Jamiolahmady (2017) relies on the availability of base relative permeability data—which is assumed to have been obtained from a core lab experiment.

In this chapter, the goal is to suggest the use of the proposed analytical method of calculating relative permeability, as shown in Chapter 5, in the two-phase production data analysis. The technique proposed by Johnson and Jamiolahmady (2017) will be used to analyse the production data presented in this chapter. To demonstrate the applicability of the calculated relative permeability data, multiple cases of production data were analysed with varying rock qualities in section 7.5, and the applicability of relative permeability data were verified by obtaining a correct value for formation permeability in all the cases analysed here. In addition, one of the main findings in this chapter is an iterative procedure, using both well test and production data, to obtain the formation's absolute permeability (discussed in section 7.8). The iterative method is explained with three different cases to demonstrate and validate its applicability. The two-phase production data analysis sensitivity to velocity effects and production rate are also investigated.

7.2 Benefits

There are two direct benefits in applying the analytical velocity-dependent relative permeability calculation method, as described in Chapter 5, to production data analysis based on two-phase pseudo-pressure techniques.

The first is if velocity effects are assumed to be not significant, such as in very low permeability reservoirs, then using the method proposed by this thesis will

provide relative permeability data as a function of pressure that should represent the base relative permeability, thus, it removes the need to conduct a demanding and expensive core-flooding lab experiment to obtain base relative permeability data, which is a function of saturation. As a result, the lab-based relative permeability data will need to be correlated to pressure. One of the most common methods, to correlate the relative permeability data to pressure, proposed in the literature is by using the steady-state relationship between relative permeability as a function of saturation and reservoir properties (Jones & Raghavan 1988) as discussed earlier in sections 2.2.5 and 5.5.2.

On the other hand, if velocity effects are assumed to be significant, then utilising the proposed method becomes more important. As lab-based base relative permeability data, even if available, do not account for inertia and coupling, while the calculated relative permeability from well testing would inheritably capture velocity effects. That means, even if base relative permeability data as a function of saturation are available, using it for two-phase analysis would be insufficient, as the changes in relative permeability due to inertia and coupling are ignored. It has to be added that relative permeability affected by coupling and inertia can be measured in specialised lab like HW-GC lab, but they are costly and demanding.

Furthermore, the proposed method can also be beneficial when used in an iterative process to obtain formation permeability, when absolute permeability is unknown.

7.3 Method

The production analysis method used in this chapter is based on the work presented by Johnson and Jamiolahmady (2017). In their work, the focus was on low permeability reservoirs (below 0.1 mD), but the scope of this thesis covers higher permeability gas-condensate reservoirs. As a result, the equivalent-phase analysis technique proposed in their work will also be validated in this thesis for higher permeability gas-condensate reservoirs.

The production data is generated from a numerical simulation model, ECLIPSE, and then analysed based on the type-curve analysis technique as presented by Palacio and Blasingame (1993). However, it has to be added that the material balance pseudo-time (Equation 7.1) is based on the equivalent phase viscosity and compressibility that account for the presence of condensate phase. That is, the material balance pseudo-time in Palacio and Blasingame (1993) accounts only for single-phase gas flow. Johnson and Jamiolahmady (2016) proposed a modified pseudo-time function, $\bar{t}_{a,tp}$, using equivalent-phase approach to account for both phases, gas and condensate (Equation 7.1). The idea is that the equivalent phase allows the use of the single-phase type curves and related parameter estimation equations in the analysis of production data obtained under two-phase conditions.

$$\bar{t}_{a,tp} = \frac{\mu_{gi} c_{gi}}{q_g} \int_0^t \frac{q_g}{\mu_{tp}(\bar{p}) c_t(\bar{p})} dt \tag{7.1}$$

where μ_g and c_g are gas viscosity and compressibility at initial conditions, respectively. μ_{tp} and c_t are the equivalent-phase viscosity, and total compressibility at average reservoir pressure, $\bar{p}$, respectively.

The equivalent-phase viscosity (Equation 7.2) as described by Johnson and Jamiolahmady (2017) and Johnson (2018), which is based on the assumption that the mass flow rate of the equivalent phase is equal to the sum of the mass flow rates of the individual phases. It is only used when pressure is below dew point. Single-phase gas properties can be used when pressure is above dew point.

$$\mu_{tp} = \frac{1}{\left(\frac{k_{rg}}{\mu_g} + \frac{k_{ro}}{\mu_o}\right)} \tag{7.2}$$

and total compressibility is the combination of two-phase compressibility and formation compressibility,

$$C_t = C_{tp} + C_f \tag{7.3}$$

where two-phase compressibility is calculated using the equation defined by Stewart (2011),

$$C_{tp} = \frac{1}{v} \cdot \frac{\Delta v}{\Delta p} \tag{7.4}$$

The volume is based on the total volume of the mixture given by:

$$v = \frac{\upsilon}{\rho_g} + \frac{(1-\upsilon)}{\rho_o} \tag{7.5}$$

where v is the total molar volume and υ is the vapour mole fraction, which is obtained from a CCE test.

Then based on the type-curve analysis technique presented in Palacio and Blasingame (1993), the pseudo-pressure and rate function, $\left(\frac{q_g}{p_{pi}-p_{pwf}}\right)$ are calculated along with its integral and its derivative using Equations (7.6 and 7.7, respectively)

$$\left(\frac{q_g}{p_{pi}-p_{pwf}}\right)_i = \frac{1}{\bar{t}_a}\int_0^{\bar{t}_a} \frac{q_g}{p_{pi}-p_{pwf}} d\bar{t}_a \tag{7.6}$$

$$\left(\frac{q_g}{p_{pi}-p_{pwf}}\right)_{id} = \bar{t}_a \frac{d}{d\bar{t}_a}\left[\frac{1}{\bar{t}_a}\int_0^{\bar{t}_a} \frac{q_g}{p_{pi}-p_{pwf}} d\bar{t}_a\right] \tag{7.7}$$

where the pseudo-pressure drop is defined as:

$$\Delta p_p = 2\int_{p_{wf}}^{p_{dew}} \left(\rho_o \frac{k_{ro}}{\mu_o} + \rho_g \frac{k_{rg}}{\mu_g}\right) p dp + 2\int_{p_{dew}}^{p_i} \frac{p}{\mu(p)z(p)} dp \tag{7.8}$$

Once all the plotting functions are calculated, then a plot is constructed where the vertical axis functions, $\left(\frac{q_g}{p_{pi}-p_{pwf}}\right)$, $\left(\frac{q_g}{p_{pi}-p_{pwf}}\right)_i$, and $\left(\frac{q_g}{p_{pi}-p_{pwf}}\right)_{id}$ are plotted versus the horizontal axis of material balance pseudo-time $\bar{t}_{ca}$. The plot is then matched against the type-curve, and a match point is used to compute the formation parameters.

In this thesis, the primary focus is to quantify reservoir permeability, as the obtained formation permeability from the match point (Equation 7.9) is compared with the absolute permeability input to the numerical simulator,

$$k = 141.2\frac{B_{gi}\mu_{gi}}{h}\left[\ln\left(\frac{r_e}{r_w}\right) - \frac{1}{2}\right]\frac{\left[\left(\frac{q_g}{(p_{pi}-p_{pwf})}\right)_f\right]_{M.P.}}{(q_{Dd})_{M.P.}} \quad (7.9)$$

It has to be added that in the two-phase pseudo-pressure calculation the use of base relative permeability might not be a problem if velocity effects are negligible—e.g. in very tight reservoirs but, nevertheless, the calculation requires the base relative permeability to be available. However, for the reservoirs studied here, i.e. the gas-condensate reservoirs with higher reservoir permeability, velocity effects cannot be assumed negligible. Hence, using lab-measured base relative permeability data will not be helpful even if they are available.

This is where the method of calculating, analytically, the velocity-dependent relative permeability data that, was proposed in Chapter 5, comes into play. In other words, in this chapter, the relative permeability data is obtained for the reservoir in question using the proposed analytical method and then used in the two-phase pseudo-variables computations to analyse the production data. As a reminder, the analytically calculated relative permeability data are a function of pressure; hence, they can be directly used for the two-phase pseudo-variables computation as long as the pressure range of the test period is compatible with the pressure range prevailing for the production data.

7.4 Reservoir Model and Design

In this chapter, the numerical simulator ECLIPSE was utilised to study the application of analytically calculated relative permeability in production data analysis for a single well in a homogeneous radial system. The reservoir model used is Model 4 (Table 3.1), which is set to a single layer of 70 feet, and 100 grids in the radial direction. A distinct set of rocks were tested taking into consideration changes in porosity, permeability and base relative permeability behaviour. Three rocks were considered for this analysis, RC1 with two

permeability variations, RC6 and TC11 (Table 3.2). The same binary rich fluid was also used (Table 3.7).

The initial reservoir pressure was 5500 psi. Initially, the production data was designed to have a cap production at the beginning governed by a fixed BHP. The idea was to unify the flow rate in both the well test data and production data, at least for the early data points. However, this measure will not be necessary as will be shown later that the results are not too sensitive to flow rate; in other words, having different flow rates for the well test data and production data did not generate a significant error.

In order to conduct the analysis, few design considerations need to be acknowledged:

1. Production data are generated for scenarios whereby reservoir pressure drops below dew point pressure to create two-phase flow conditions. Otherwise, the single-phase approach can be applied.

2. On the other hand, the pressure buildup test must be within the range of the pressure values generated in (1) for the calculated $k_r(p)$ to be applicable.

3. At the same time, the pressure test must also be dropping below the dew-point to have the calculated relative permeability data for two-phase conditions.

4. For velocity effects to be considered, VELDEP keyword needs to be activated in both well test and production data numerical simulation. Having the keyword active in one will yield incompatible behaviour.

7.5 Results

Several cases were established (Table 7.1), and then further variations were analysed for verification and troubleshooting purposes, as they will be discussed

in detail in the next section. In this section, the results of each case will be discussed. In each case, the production and the well test conditions used to generate the data are explained, in addition to the type-curve match plot and the computed permeability.

Case #	Rock	Permeability (mD)	Inertia and Coupling
1	RC1	1	Inactive
2	RC1	10	Active
3	RC6	23.4	Active
4	TC11	11.1	Active

Table 7.1—Different cases used for two-phase production data analysis using the calculated relative permeability from well test data.

7.5.1 Case 1—Low Permeability and No Velocity Effects

As a start, since the work done by Johnson and Jamiolahmady (2017) is based on low permeability reservoirs, the RC1 rock with low permeability of 1 mD and reservoir Model 3 (Table 3.1) was considered, with no velocity effects (inertia and coupling are deactivated in the numerical simulator for both production data and well test data). The goal for this case was to verify if the suggested workflow concept works before adding other factors, such as velocity effects or higher permeability values. That is if the analytically calculated relative permeability from well test buildup can be used for two-phase pseudo-pressure in analysing the production data.

The procedure of this and the following exercises consists of the following steps: A well test buildup was simulated, and the pressure versus radius profile was calculated; then the pressure gradient was used to calculate relative permeability as a function of pressure analytically. Production data were also simulated and exported from the numerical simulator, then two-phase pseudo-time and pseudo-pressure were calculated using the relative permeability data obtained earlier. The pseudo-pressure and rate function $\left(\frac{q_g}{p_{pi}-p_{pwf}}\right)$, its integral

and its derivative were then calculated and plotted against Blasingame's type-curve (**Figure 7.1**).

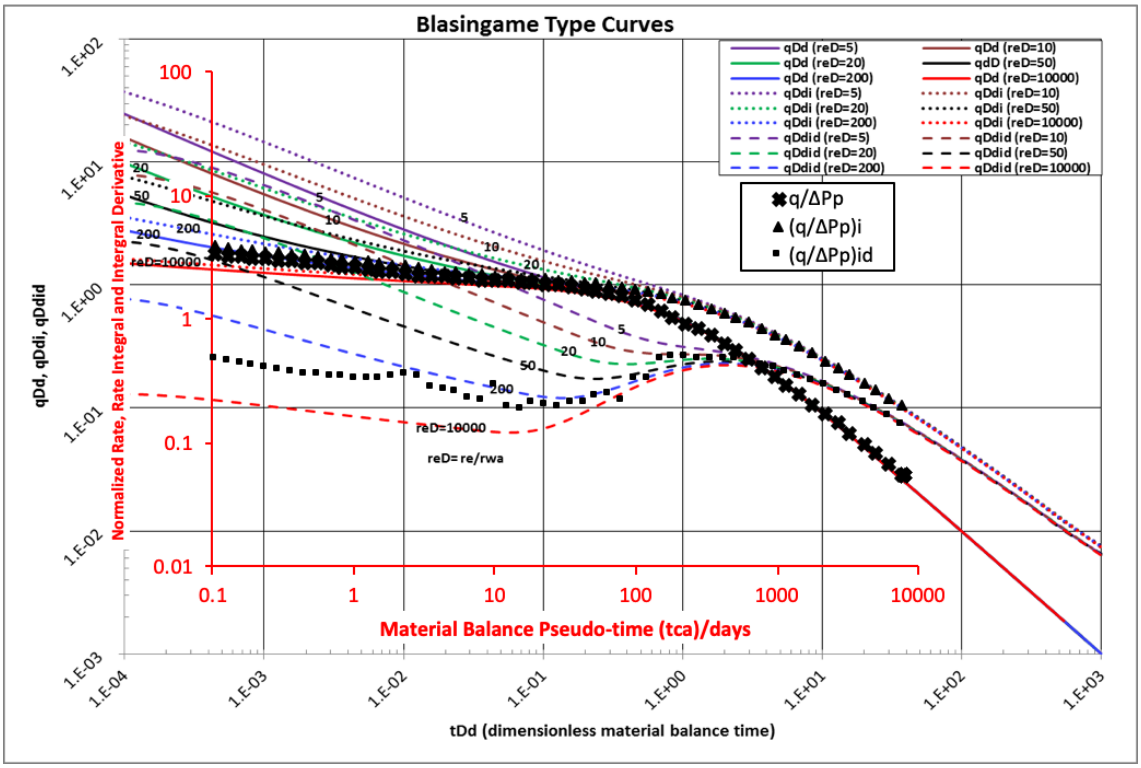

Figure 7.1—Type curve match for Case 1 without inertia and coupling.

From Figure 7.1, a match point was selected, and Equation 7.9 is used to calculate formation permeability. The permeability obtained for this case was 1.1 mD which corresponds very well with the original input value of 1 mD.

This case shows that the proposed approach of calculating relative permeability from well test data would sufficiently work in the two-phase pseudo-pressure to analyse production data, without the velocity effects, namely inertia and coupling which are important to consider, as will be shown in the next case.

7.5.2 Case 2—Higher Permeability with Velocity Effects

In this thesis, the argument is to honour velocity effects when it comes to gas-condensate reservoirs; thus, it is vital to consider it and show how it can affect the analysis outcome. As a result, for Case 2, the same rock, RC1, was used but the permeability was set to a higher value, 10 mD, but more importantly,

both inertia and coupling were active in the production data and the well test data simulations. Reservoir radius has been extended to 6000 ft, due to the formation relative high permeability (Model 4) to ensure sufficient production data are available for analysis.

Initially, the case was analysed without any velocity effect, to make sure that increasing the rock permeability does not introduce any analytical challenges to the workflow. That is, no velocity effects were introduced in both the simulated well test data used for the relative permeability calculation, and the simulated production data. By matching the data to the type curve for RC1, with 10 mD and no inertia and coupling, the results were good, with permeability estimated as 10.9 mD (**Figure 7.2**).

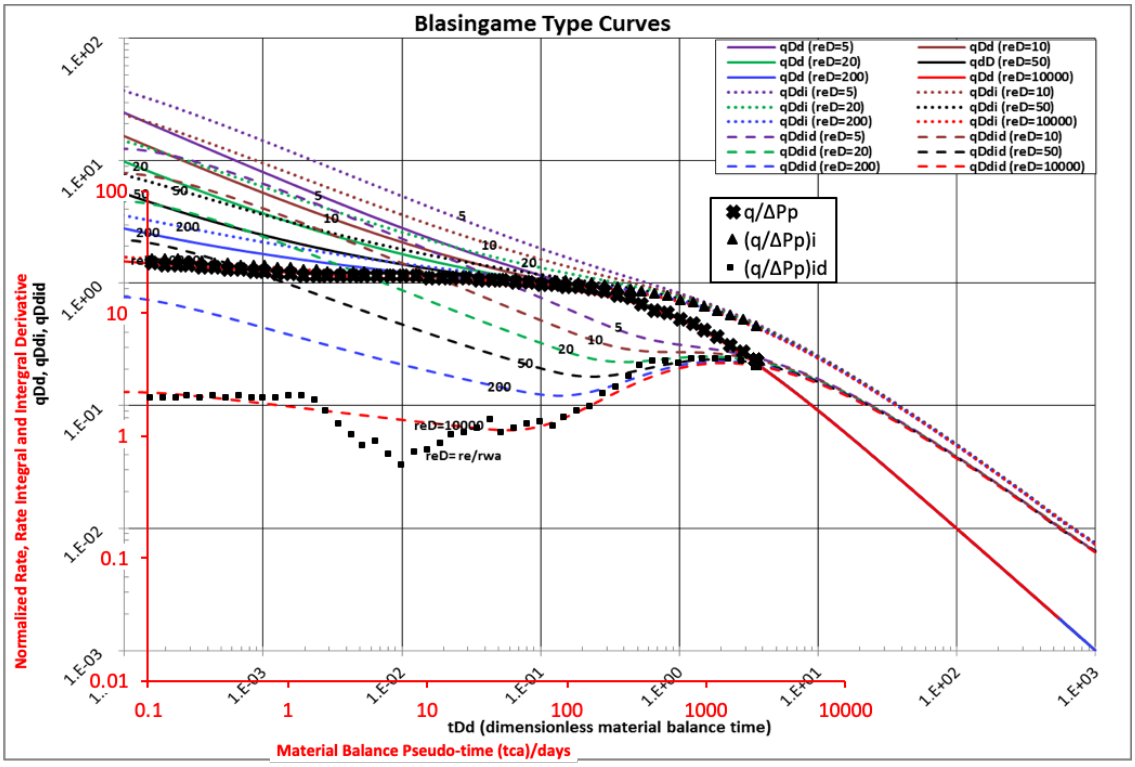

Figure 7.2—Type curve match for Case 1 without inertia and coupling.

After that, both inertia and coupling were activated, and the production data were re-analysed. Similar to the previous case, relative permeability data were calculated based on the well test buildup data and used to carry out the two-phase pseudo-time and pseudo-pressure calculations. **Figure 7.3** shows the

type curve match. With the match point coordinates, the permeability was calculated to be 10.3 mD which shows excellent agreement with the absolute permeability of 10 mD.

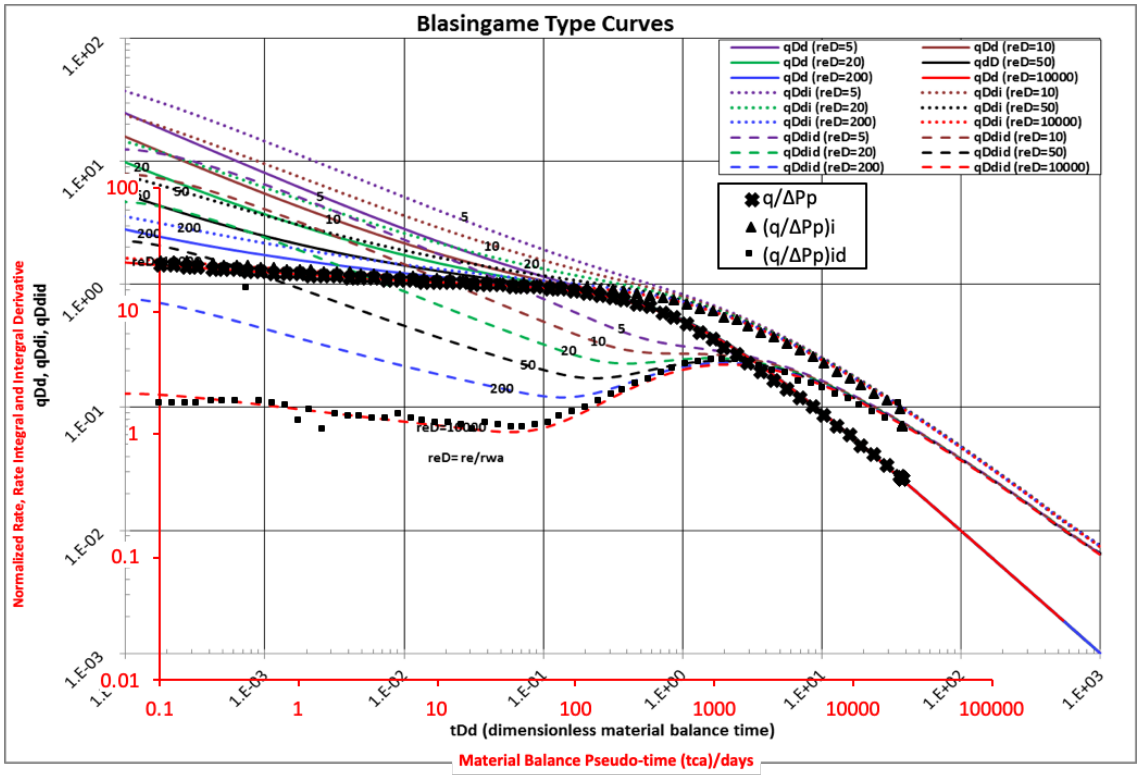

Figure 7.3—Type curve match for Case 2 with inertia and coupling.

It can be observed that velocity effects are apparent in the log-log pressure derivative data. The condensate region in the case where inertia and coupling are active have a lower flow capacity (**Figure 7.4**) of 1.83 mD compared to the case where inertia and coupling are inactive (**Figure 7.5**) whereby it was 7.9 mD, showing that positive coupling improved the relative permeability of the gas.

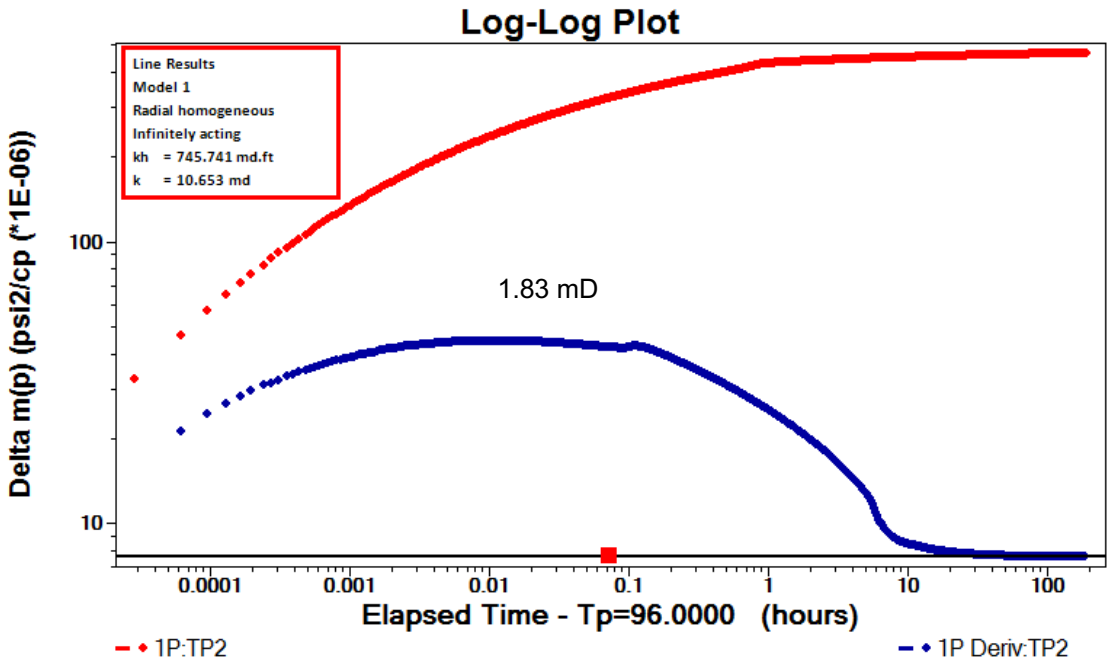

Figure 7.4—Single-phase transient pressure analysis for Case 2 without inertia and coupling used in relative permeability calculation.

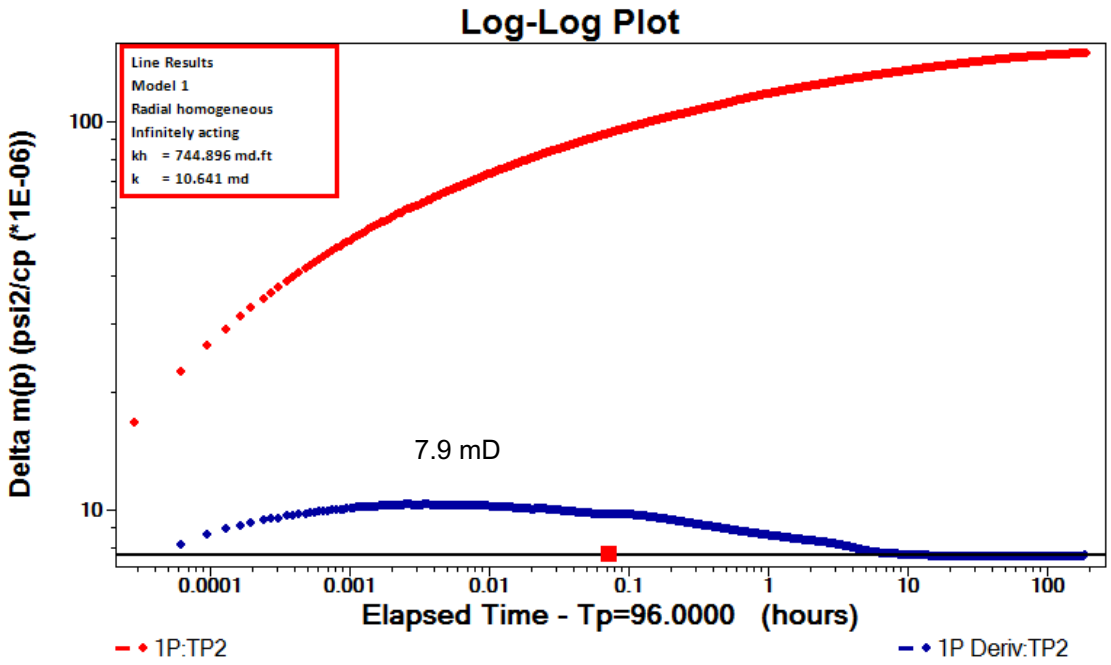

Figure 7.5—Single-phase transient pressure analysis for Case 2 with inertia and coupling used in relative permeability calculation.

7.5.3 Case 3—RC6, Different Rock with 23.4 mD and Velocity Effects

In this third case, the aim is to get similar excellent results for a much higher permeability rock of the RC6 with 23.4 mD (Table 3.2). Similar to Case 2, reservoir Model 4 (Table 3.1) was used to generate the pressure buildup data and the production data.

The pressure derivative data from the buildup were analysed, and the pressure versus radius profile was calculated, then relative permeability data as a function of pressure were computed for the given pressure range. The production data were then analysed using the type-curve technique (**Figure 7.6**), and a match was obtained. The formation permeability calculated from the match point was 23 mD which agrees very well with the input absolute permeability of 23.4 mD.

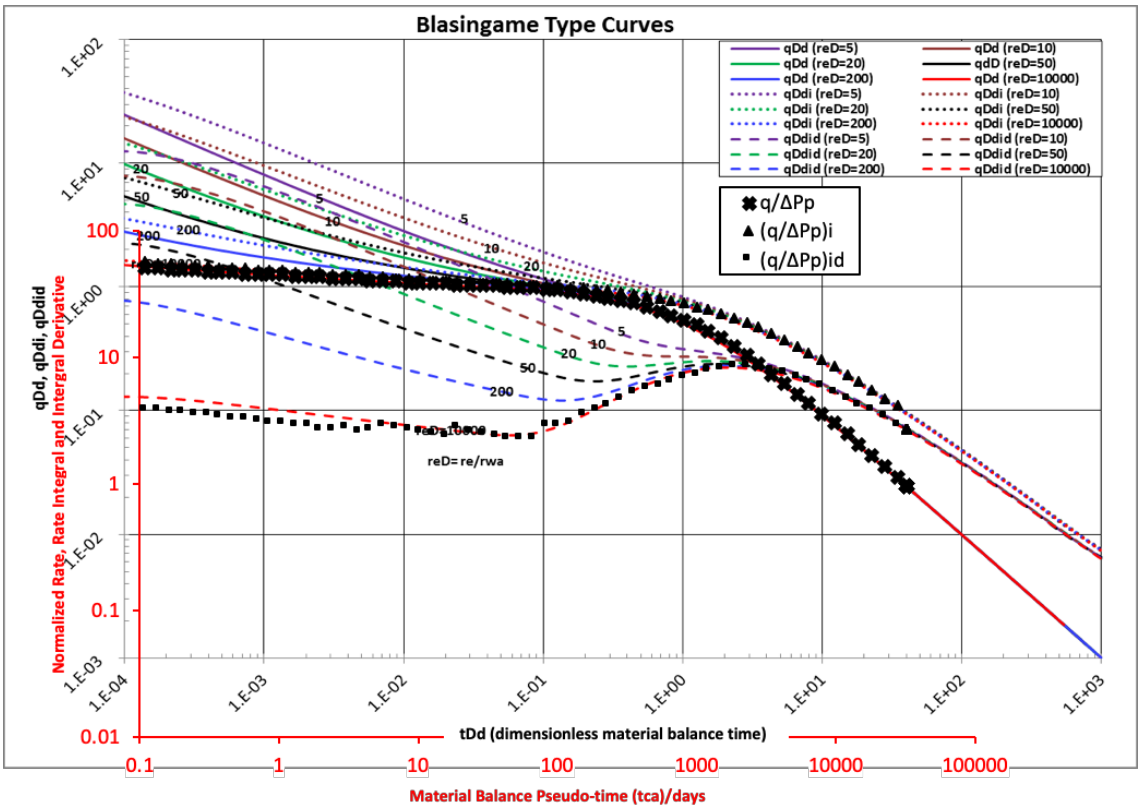

Figure 7.6—Type curve match for Case 3 with velocity effect active.

In both cases, Case 2 and Case 3, where velocity effects were considered, the results were excellent.

7.5.4 Case 4—TC11, Different Rock and Different Base k_r Behaviour, with Velocity Effects

For this case, a different rock, TC11 (Table 3.2) was considered. The choice for this rock is due to its distinct base relative permeability behaviour compared to the RC rocks studied earlier (Table 3.4).

The procedure is the same; that is, a new set of relative permeability data are calculated for a given pressure buildup test, and the corresponding two-phase pseudo-time and pseudo-pressure are calculated. The production data are then simulated and analysed using the two-phase approach with the calculated velocity-dependent relative permeability from the well test data. As noted, following this procedure, an excellent match was obtained in the type-cure analysis of the production data (**Figure 7.7**). Permeability calculated from the match point was 11.2 mD which agrees well with the absolute permeability input of 11.1 mD.

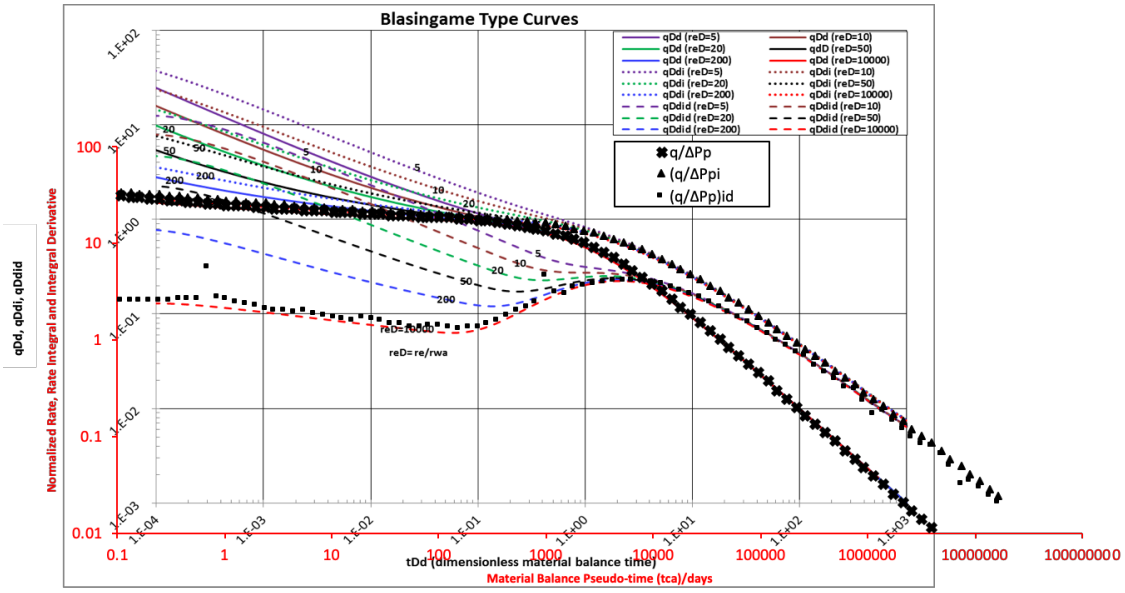

Figure 7.7—Type curve match for Case 4 with velocity effect active.

7.6 Sensitivity of Production Data Analysis to Velocity Effect

In this exercise, the aim is to showcase how sensitive the analysis results are when velocity effects are not considered in the relative permeability data. That is, when base relative permeability data, obtained from the lab, that do not take into account inertia and coupling are used in a gas-condensate production data that are affected by such velocity effects. Theoretically, the base relative permeability data would not be compatible in the sense that it lacks such an additional modifier due to the flow dynamics near the wellbore.

To investigate this, the TC11 rock of 11.1 mD was used, and the production data were generated with velocity effect (both inertia and coupling, denoted by IC) by activating the "VELDEP" keyword using the lab-obtained velocity parameters specific for TC11 rock. On the other hand, the well test pressure buildup data were simulated without velocity effects. In other words, no modification to the base relative permeability data used in the numerical simulator generating the well test data. The relative permeabilities as a function of pressure were then calculated and used to compute the two-phase pseudo-time and pseudo-pressure, and the production data were analysed using the type-curve technique. The resultant formation permeability is 16.3 mD, which is 47% more than the absolute permeability of 11.1 mD.

This result confirms that proper relative permeability data are essential in order to meaningfully analyse the production data using the proposed method presented in this thesis. In other words, when velocity effects are important, using lab-based relative permeability data is not sufficient, as it lacks the effect of velocity triggered under gas-condensate two-phase flow conditions; making it unreliable to predict reservoir parameters using the two-phase pseudo-pressure.

To further verify the role of inertia and coupling, the production data were analysed twice where only one velocity effect was active and considered in the

relative permeability data at a time. For example, inertia was set to be active and coupling inactive (IX) in the well test build up data used to calculate the relative permeability as a function of pressure. The relative permeability data were then used to analyse the two-phase production data (which has both inertia and coupling active, IC). This was followed up with another case where inertia was inactive, and coupling was active (XC) with the relative permeability data used, again, to re-analyse the production data.

In the first case, where only inertia was considered, the estimated formation permeability from the production data analysis was 16.3 mD which is far away from the absolute permeability of 11.1 mD. In fact, it is the same as if both velocity effects were not included in the analysis, whereas when only coupling was active, the estimated formation permeability from the production data analysis was 10.9 mD which is only 1.8% off the absolute permeability. In other words, the results where the coupling only was the active was very close to the case where both inertia and coupling were active. This again shows that, for the case considered, coupling has a much more dominant effect than inertia.

7.7 Sensitivity of Production Data Analysis to Flow Rate

In this section, an investigation on how vital the flow rate compatibility between the well test data and the production data is, given that the analysis method relies on relative permeability from well test buildup data. In other words, if velocity effects are important, what would happen to the analysis results if the flowing rates in the well test data where relative permeability is obtained are not the same as the flowing rates in the production data.

Rate sensitivity analysis was performed using the TC11 rock properties. As will be shown below, at various flow rates for the well test data, the production data analysis will always give reliable results, as long as velocity effects are taken into account in the calculation of the relative permeability. Three rate variations were tested (Table 7.2). In the first case, both the constant production flow rate in well test and cap production rate in the production data

analysis exercise was 10 MM scf/D— i.e. no discrepancy in flow rate between the two, at least for the period of fixed rate in the production data. This scenario resulted in a permeability estimate from the type-curve match to be 11.2 mD (as presented in section 7.5.4). In the second case, the gas flow rate for the well test exercise was set at 20 MM scf/D, which is double the cap rate of 10 MM scf/D for the production data analysis exercise. For this scenario, the permeability estimate from the production data analysis is 10.6 mD, which is not far off from the absolute permeability (11.1 mD). For the third case, the flow rate of the well test data was set at 50 MM scf/D, 5 times the cap flow rate of the production data analysis exercise; but again, the permeability can still be estimated within a reasonable error (10.6 mD).

	1	**2**	**3**
WTA rate (MM scf/D)	10	20	50
PDA cap rate (MM scf/D)	10	10	10
ΔQ	0	10	40
k estimation, PDA	11.2	10.6	10.6
Error vs. k(input) (%)	+1	-5	-5

Table 7.2—Variation in flow rate between production data analysis and well test data interpretation exercises.

The exercise was repeated using the same rock; however, this time, the absolute permeability was increased to 50 mD. Doing so, required higher gas flow rates. In other words, the cap flow rate for the production analysis was increased to 40MM scf/D, and the sensitivity of well test flow rate was checked against that number at four different variations (40, 55, 80, and 110MM scf/D). Analysing the production data again did not show any apparent trend, i.e. the agreement between estimated absolute permeability from production data analysis and input to simulator (Table 7.3).

	1	2	3	4
WTA rate (MM scf/D)	40	55	80	110
PDA cap rate (MM scf/D)	40	40	40	40
ΔQ	0	15	40	70
k estimation, PDA	48.44	48.44	48.44	48.44
Error vs. k(input) (%)	-3.1	-3.1	-3.1	-3.1

Table 7.3—Variation in flow rate between production data analysis and well test data for the same rock but with a higher permeability of 50 mD.

This shows that rate change is not important as long as velocity effects are considered in the relative permeability data. That is, regardless of what the flow rate is in the well test data, the permeability predictions are satisfactory.

7.8 Iteration Process to Obtain Absolute Permeability

7.8.1 Introduction

One of the main findings of this chapter is an iterative process to estimate reservoir permeability from well test data and production analysis. When the relative permeability as a function of pressure is calculated from the well test data, the assumption is that absolute permeability is available. Reservoir permeability can usually be obtained from a well test analysis of previous tests or nearby wells, or from other sources such as production logs and core analysis. However, here it is proposed to be estimated by an iterative process using both well test data and production data. This will be extremely helpful in the case where permeability is not available or if the value is uncertain.

7.8.2 Iteration Method

The premise of this technique is to utilise both well test and production data in an iterative process to converge to the correct permeability value. This

iterative process begins with the well test pressure transient analysis, to calculate relative permeability as a function of pressure, as presented in Chapter 5. At this stage, the relative permeability calculation needs to start with an initial guess of k value as an input. The starting point of the guessed absolute permeability value can either be higher or lower than the actual permeability, which is assumed to be unknown. It was found that starting with a higher value than the actual unknown value gives a faster convergence while starting at lower value takes longer to converge. In reality if permeability is unknown, it would be unknown if the initial input value is below or above, which is why both cases have been considered here.

The calculated relative permeabilities data are then used to calculate the two-phase pseudo-time and pseudo-pressure data which is used in the two-phase analysis of the production data. The estimated reservoir permeability from the type-curve match will likely be different from the absolute permeability used at the start of this first iteration. The new value computed from the production analysis is taken back to the first stage of relative permeability calculation, and a new set of relative permeability is generated based on the new permeability value of the first iteration. Production data is then re-analysed with the updated relative permeability data, and a new value of permeability is computed. This process is repeated until there is no significant change in the permeability obtained from the production data analysis in two subsequent iteration steps. The aim is to have a permeability value with an accuracy of ±5% compared to the absolute permeability.

A summary of the iteration workflow is presented below and in **Figure 7.8**:

- Start with an initial guess of k value as an initial input, called (k_i), for iteration #1 (it1), to calculate relative permeability data analytically from well test data.
- Use relative permeability data calculated analytically from it1 to analyse the production data.

- Compute k from the production data type-curve match, which is called k_{out}.
- Make $k_i = k_{out}$ to re-calculate the relative permeability data from the well test buildup; this is it2.
- Use the new relative permeability data from it2 to re-analyse the production data and compute a new permeability value, k_{out}.
- Repeat until there is no further improvement in the computed permeability from the two subsequent iterations; i.e. $k_{out} = k_i$.

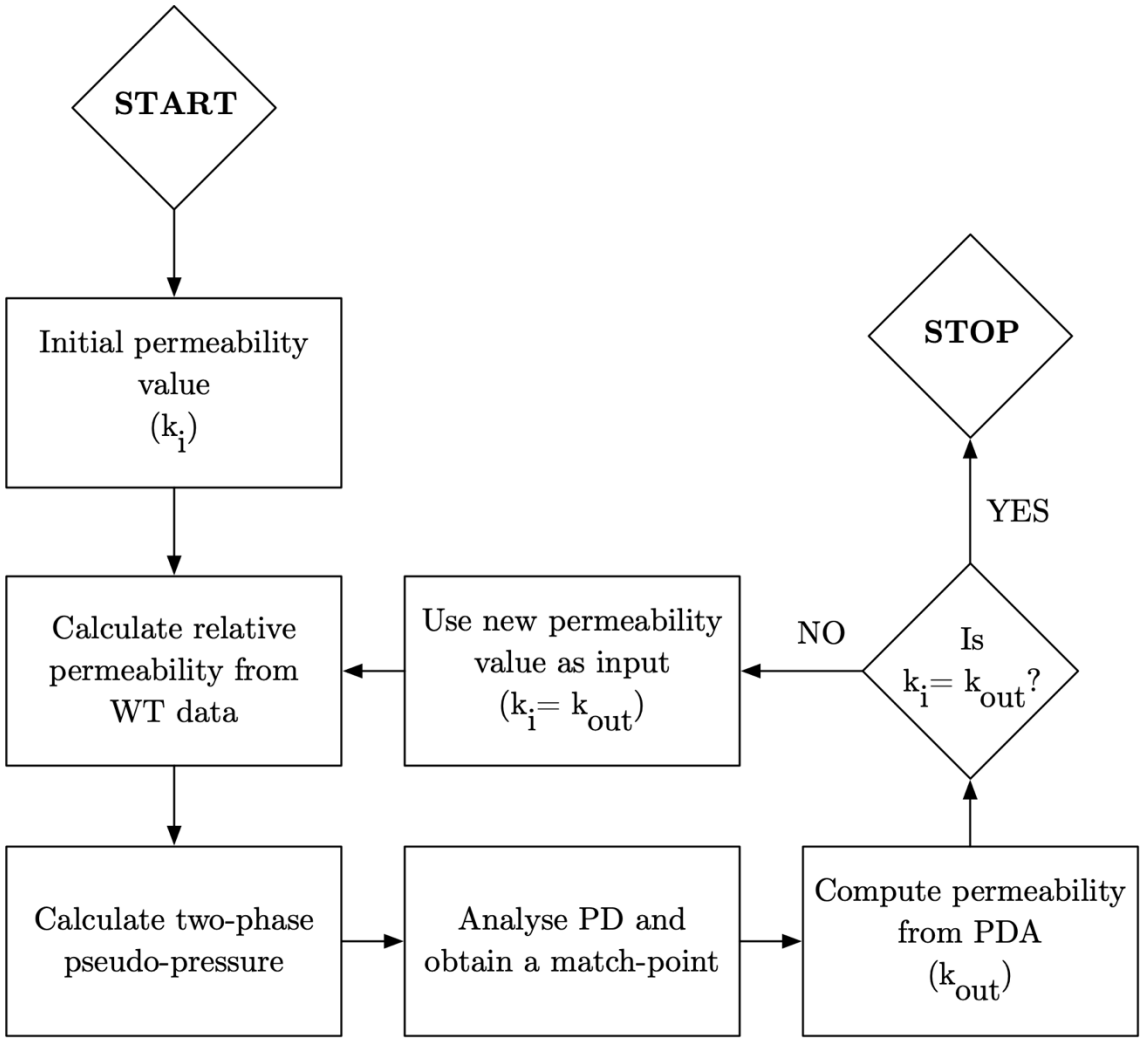

Figure 7.8—A visual map of the iteration process to obtain formation permeability.

7.8.3 Iteration Case 1

Case 1 is set-up with no velocity effects with the RC1 rock of 1 mD permeability. In this exercise, the assumption is that the absolute permeability value is unknown, and an initial input of 10 mD was used for iteration #1. Relative permeability data as a function of pressure was obtained and used to analyse the production data. Formation permeability was computed to be 4.8 mD from the first type-curve match. For iteration #2, a new set of relative permeability data was calculated based on 4.8 mD, instead of 10 mD, and the production data was re-analysed, and a permeability of 3.3 mD was computed in the second round of production data analysis.

It can be observed that the trend of permeability estimation is downward, towards the true absolute permeability value of 1 mD. Multiple iterations were run until there was no further improvement in the obtained permeability from production analysis–which was at iteration #13 for this case with an error of 4% compared to the absolute permeability used in the numerical simulator. Table 7.4 shows the progress of each iteration, with input permeability (for the analytical relative permeability calculation presented in Chapter 5) and output permeability (from the production data analysis using the equivalent-phase technique presented earlier in this chapter).

	Iteration	k(input) WTA	k(output) PDA
Start	it1	10	4.8
	it2	4.8	3.3
	it3	3.3	2.2
	it4	2.2	1.84
	it5	1.84	1.79
	it6	1.79	1.67
	it7	1.67	1.48
	it8	1.48	1.35
	it9	1.35	1.25
	it10	1.25	1.15
	it11	1.15	1.1
	it12	1.1	1.04
End	it13	1.04	1.04

Table 7.4—Progress of iteration to estimate reservoir permeability for Case 1.

7.8.4 Iteration Case 2

Next, to verify the iteration process, another case was considered, this time with a higher permeability rock, the RC6 (23.4 mD) and both velocity effects were active.

For extreme measures, the initial input was set at 100 mD, which resulted in k_{out} of 35.7 mD from the production analysis for iteration #1. The trend, again, was downward towards the actual value for RC6's absolute permeability. The same process was carried on for 6 iterations (Table 7.5) until there was no further change in the estimated permeability value from the production analysis, which was 23.6 mD, with an error of 0.9% compared to the absolute permeability.

	Iteration	k(input) WTA	k(output) PDA
Start	it1	100	35.7
	it2	35.7	30.3
	it3	30.3	26.6
	it4	26.6	24.2
	it5	24.2	23.6
End	it6	23.6	23.6

Table 7.5—Progress of iteration to estimate reservoir permeability for Case 2– using a high starting point.

In both previously mentioned cases, the starting point was a permeability value that is higher than the actual value. To verify that the procedure always works, a lower starting point needed to be tested too; that is an initial permeability value for iteration #1 that is lower than the absolute permeability. As a result, for the same rock, an initial permeability input of 0.1 mD (versus 100 mD) was used. The same iteration process was carried out by generating various relative permeability data to be used in the production data analysis, the fist iteration resulted in permeability output of 0.12 mD. This shows that the process, although taking an upward trend towards the real value of 23.4 mD, is much slower than when the initial input is higher than the actual value. After many more iterations (Table 7.6), no further improvements were obtained at iteration 17, with permeability value of 23.6 mD which agrees very well with the actual absolute permeability of 23.4 mD. Due to the slow iteration process with the upward trend, few iteration stops were jumped between iteration 8 and 9. That is, the author would arbitrary increase k(input) relative to what was obtained in iteration 8 in order to speed-up the iteration process. If the chosen value was higher than it should be, then the production data analysis would give a lower value, switching the convergence trend downward, instead of upward (as seen with the extra "Check" iteration at the end). Otherwise, the iteration would converge upward towards the absolute permeability. This step is not necessary as it was only used due to the slow iteration process. It is noted that

the increment in k(output) is very small, but still increasing with around 10-20% difference compared to the input value. In addition, the absolute permeability in this case is known, and this upward trend iteration was done to just verify if both iteration starting point (a higher initial point, and a lower initial point) would converge to give the right permeability value.

To further verify that this iteration process works well, as a checking point, a higher value was used after the iteration converged to 23.6 mD. A permeability of 28 mD used as an input that gave a permeability of 26.6 as an output, which indicates a downward direction is forced towards the true absolute permeability value.

	Iteration	**k(input) WTA**	**k(output) PDA**
Start	it1	0.1	0.121
	it2	0.121	0.14
	it3	0.14	0.16
	it4	0.16	0.18
	it5	0.18	0.2
	it6	0.2	0.24
	It7	0.24	0.28
	It8	0.28	0.30
	It9	10	11
	It10	11	13
	It11	13	14
	It12	14	15.14
	It13	15.14	17
	It14	17	18.2
	It15	18.2	20.6
	it16	20.6	23.6
End	It17	23.6	23.6

Table 7.6—Progress of iteration to estimate reservoir permeability for Case 2– using a low starting point.

7.8.5 Iteration Case 3

As the last case to test this method, Case 3 was set up using the TC11 rock (Table 3.2) with both inertia and coupling active. The initial input was 100 mD, and the same iteration process was followed until no further improvement in the permeability estimate from production data analysis was observed, which was at iteration #7 (Table 7.7) with permeability value of 11.5 mD (an error of 3% compared to absolute permeability of 11.1 mD).

	Iteration	**k(input)**	**k(output)**
		WTA	**PDA**
Start	it1	100	41.2
	it2	41.2	29.1
	it3	29.1	20.6
	it4	20.6	16.95
	it5	16.95	13.9
	it6	13.9	11.5
End	it7	11.5	11.5

Table 7.7—Progress of iteration to estimate reservoir permeability for Case 3 using a high starting point.

Again, for confirmation, the same case was tested with the initial starting point lower (0.1 mD) than the absolute permeability. Similar to Case 2, after many iterations (with few jumps in between some iteration to speed up the process, as explained earlier in 7.8.4) the upward convergence stops at 11.5 mD (Table 7.8).

	Iteration	k(input) WTA	k(output) PDA
Start	it1	0.1	0.14
	it2	0.14	0.18
	it3	0.18	0.23
	it4	0.23	0.3
	it5	0.3	0.38
	it6	0.38	0.51
	it7	0.51	0.73
	It8	0.73	1.03
	It9	1.03	1.33
	It10	1.33	1.82
	It11	9	10.3
	It12	10.3	11.5
End	it13	11.5	11.5

Table 7.8—Progress of iteration to estimate reservoir permeability for Case 3 using a low starting point.

7.8.6 Summary

The exercises above show that when well test and production data are available, using the right techniques of analytical relative permeability calculation (which captures velocity effects) as a function of pressure, and the equivalent-phase production data analysis, the value of absolute permeability can be determined through an iterative process.

It is recommended to start with a higher value, as a lower starting point can make the process very slow to converge. Since absolute permeability is assumed to be unknown, a higher starting point can only be deduced by observing the analytical relative permeability data. When the used permeability value is higher than absolute permeability, the resultant analytical relative permeability will be low (e.g. k_{rg} showing values lower than 1), whereas if a lower starting

point for permeability value is used, the analytical relative permeability will be very high (e.g. k_{rg} showing unrealistic values of more than 1).

7.8.7 Limitations

The presented method in this section relies on the availability of good quality well test and production data. Different sources of noise can disturb the pressure response in well test data and therefore affect the quality of calculated relative permeabilities. In addition, production data analysis requires accurate production rates, which are challenging to obtain in practice. Moreover, the iteration process could result in an error or incomplete production-decline match if the pressure range for the data set used from well test data is small, or incompatible with the pressure range available for the production data. On the other hand, this process can be long and inefficient when done manually; efforts to automate can be beneficial, and it will be suggested in the future work in section 8.2.

7.9 Conclusion

In this chapter, the application of calculating analytical relative permeability data from well test data is verified and tested on two-phase production data analysis techniques. In other words, such relative permeability data as a function of pressure proved to be a useful tool whenever two-phase pseudo-pressure calculation or relative permeability as a function of pressure is needed.

It has also been shown that when velocity effects are important, but neglected by using base relative permeability data, the production analysis will yield wrong results, and the single-phase approach cannot be reliable. When velocity effects in certain conditions (such as very low permeability rocks) are negligible, then the single-phase approaches might give satisfactory results. However, if the two-phase analysis approach is to be used even for cases where velocity effects are negligible, then the question becomes whether the relative permeability data are available in the first place. Therefore, it can be stated

that the analytical approach of calculating relative permeability data can still be useful, even if velocity effects are not important, in the case where lab-based relative permeability curves are not available.

It was also shown the effect of changing flow rate is not very significant as long as the coupling effect, which was more dominant than inertia for the tested ceases, is considered.

The findings also demonstrated how an iterative process utilising both analysis technique (analytical relative permeability from well test data, and equivalent-phase production analysis) could give an excellent approximation of the absolute permeability. That is, when absolute permeability is unknown, an initial guess of permeability is used to compute relative permeability analytically using the described method in Chapter 5. Then with relative permeability as a function of pressure, two-phase pseudo-pressure and pseudo-time are calculated to analyse the production data and obtain a match point. Which is then used to compute formation permeability. The computed permeability from the production analysis will be different than the initially input value, which is then used to re-calculate the relative permeability data based on this new value. This iterative process continues to converge, until it stops at a value very close to absolute permeability. This has been shown to work very quickly when the initial input of permeability value is higher than the actual permeability of the formation (as short as 6 iterations to a maximum of 13 iteration, depending on the starting point). But when a lower starting point for the initial input of permeability value is used, the iteration process takes much longer.

Chapter 8

Conclusions and Future Work

8.1 Conclusions

The work in this thesis has shown that a combination of analytical techniques can be used to construct a sound framework that can be used for better gas-condensate reservoir analysis by utilising well test data. More specifically the analytical approach to estimate relative permeability data as a function of velocity and pressure was shown to be an excellent tool for better gas-condensate reservoir characterisation. During this process, and in addition to the ability to calculate relative permeability data analytically, a pressure versus radius profile can be constructed which aids in estimating condensate bank extent. The thesis evaluated and emphasised on the roles of positive coupling and negative inertia in the two-phase flow conditions of gas-condensate systems as at the near wellbore the impact of high flow rates, and low IFT, which has been proven to be significant through this work and many others in the literature. That is, the thesis demonstrated that the proposed methods that account for the velocity effects (positive coupling and negative inertia), is a suitable tool for improved management of gas-condensate reservoirs. More importantly, the thesis showed and discussed one of the main applications of having relative permeability data as a function of pressure. That is, the ability to compute two-phase pseudo-pressure and analyse two-phase well test and production data. Such information is valuable and practical.

The thesis also discussed the difference between relative permeability data obtained through core-flooding lab experiments and those obtained analytically from dynamic well test data. That the well test data captures the actual mobility behaviour of both the gas and condensate phases, which would capture the effect of coupling and inertia. On the other hand, relative permeability data obtained in the conventional lab tests usually lacks such information, and to obtain such information, challenging and expensive lab experiments are required.

Several cases of single-phase and two-phase gas-condensate with varying rock properties, fluid richness, and unique base relative permeabilities were examined. The well test data were generated using numerical simulation which allowed the investigation of the individual or combined impact of relevant parameters to verify the reliability of the approach.

In Chapter 4, the simulated well test pressure transient data were analysed to construct pressure versus radius profile, where the calculated pressure profiles matched those obtained from the numerical simulator. The underlying concept used of this method and the calculation procedure were explained in Chapter 4. It also highlighted the benefits of the calculated pressure versus radius profile in condensate bank extent estimation and, later, in relative permeability calculation. It was shown that the method, originally developed for a liquid with small and constant compressibility can be extended to a two-phase gas-condensation system. The results of pressure versus radial distance were shown to work on different fluid richness (lean, moderate and rich gas condensate).

In Chapter 5, the pressure versus radius gradient was used to analytically compute velocity-dependent relative permeability data using steady-state assumption and Darcy's law. The analytical method was described, and an investigation of the numerical dispersion observed in the calculated relative permeability data was discussed. Several solutions to reduce data oscillation were examined and applied to the calculation presented in the thesis; at the end, it was recommended to use the smoothing tools available in well test data

along with unique, or common fit-functions. To validate the results, relative permeability with respect to radial distance, available as an output from the numerical simulator, was compared with the one obtained analytically from well test data. The overall trend matched the simulation output, and the results were considered to be satisfactory, and in some cases, excellent. Having velocity-dependent relative permeability data will help in both improving well test and production data analysis employing the two-phase pseudo-pressure approach as well as using such valuable data for other reservoir description and management purposes.

Chapter 5 also shed light on some of the challenges and limitation of the suggested approach. Wellbore storage (WBS) was considered to be a challenge for any well test data, and the work presented in this thesis is no different. In other words, when WBS was present, it affected the quality of the relative permeability data obtained, but it was still possible to end up with meaningful results, depending on the duration of the test and the quality of the remaining data. Few cases were analysed to demonstrate such a common wellbore behaviour. On the other hand, one of the limitations of the proposed methods in this thesis was shown to be its application in horizontal wells. Due to the complexity imposed by the well's geometry and the resultants different flow regimes, the suggested method of calculating pressure versus radius profile and relative permeability data can be of limited use when the well is horizontal. A case was examined to showcase the effect of flow regimes on the data and the overall approach, with a discussion on the reasons behind this limitation.

In Chapter 6, the reliability of the proposed technique was also examined for multi-rate testing which has shorter test times and variable flow rates compared to single-rate testing. Two different flow schemes were considered (forward and backward), and the results of pressure versus radius profile and relative permeability from all the buildup sequences were excellent for both schemes. At the same time, the results showed the effect of changing flow rate on the calculated relative permeability. In other words, the higher the flow rate, the more deviation in the k_{ro} data points away from the wellbore (at the end of

the condensate bank) for the calculated relative permeability from the numerical simulation output. On the other hand, a lower flow rate (as low as 30 MMscf/D) produced a relative permeability trend that is in a good agreement with output data from the numerical simulations. However, the effect is not very significant, and the analytical can still be meaningful even at higher flow rates. Not only flow rate values have an impact on the analytically calculated relative permeability data, but the rate sequence also seems to play a minor role in the level of accuracy. The different rate sequence between the two tested cases, one being forward and the other being backward, have affected the overall results, albeit slightly, as well. In both cases, the resultant relative permeability data were satisfactory, and no clear advantage of one sequence scheme over the other.

Chapter 7 showcased one of the main important applications of using velocity-dependent relative permeability data to improve production data analysis using an equivalent-phase approach where two-phase pseudo-pressure was used. In this application, reservoir permeability was calculated from production data, using relative permeability calculated in Chapter 5, which assumed that absolute permeability is known. The equivalent-phase approach, which utilises two-phase pseudo-pressure and two-phase pseudo-time, was explained and varying cases of different rock qualities were analysed, with different scenarios of velocity effects (i.e. in some cases they were activated, and in others deactivated). The results showed an excellent estimation of reservoir permeability when velocity effects are considered, and on the other hand, the permeability estimation is overestimated when the velocity effects are ignored. Furthermore, a new iterative procedure was shown to provide formation permeability when the absolute permeability input is unknown. The iterative procedure utilises both well test pressure transient data and production rate data. Multiple cases were used to demonstrate the capabilities of the iteration method, giving excellent results compared to the input absolute permeability.

8.2 Future Work

The findings presented in this thesis are practically attractive. The thesis discussed the theory of the proposed methods with analysis and validation using numerical simulation data of the two-phase gas-condensate reservoir. Applying the concepts and methods discussed within this thesis to a real field data would be the natural step forward. Field data comes with its own challenges and added complexities (for example: gauge quality, type of completion affecting the recorded data, heterogeneous reservoir quality). The aim is for this work to be of a practical benefit and ultimately applied to a field data.

On the other hand, further systematic sensitivity analysis can be examined, to define and understand what other limitations the suggested methods have–this could include a detailed quantification of flow rate effect and an introduction of other heterogeneities. In addition, the suggested workflow (as presented in Figure 5.1) could systematically be further developed for well test and production data analysis. Furthermore, an investigation on other applications for the analytically calculated relative permeability data is required—applications such as using various relative permeability data at different flow rates to predict core exponents, which can be used to modify other available real permeability curves. In addition to the possibility of using the relative permeabilities data for history matching purposes.

Another potential future work is the automatisation of the permeability estimation method using well test and production data through an iteration process (as proposed in section 7.8). This would be helpful to shorten the time required for the iteration to converge, especially when a lower starting point for k(input) is used.

Appendix A

Derivation of Relative Permeability Equation

Liquid flow is generally governed by Darcy's law. If a constant-rate production is assumed, then according to Darcy's law, the rate of flow from the formation in a radial system with flow in the radial direction only in written as:

$$qB = \frac{kA}{\mu}\frac{\partial \mathrm{p}}{\partial r} \tag{A-1}$$

The equation is then re-arranged to be in terms of k,

$$k = \frac{qB\mu}{A}\frac{\partial r}{\partial \mathrm{p}} \tag{A-2}$$

The surface area of a cylinder system is defined as the circumference of circle (for a radial reservoir) multiplied by reservoir thickness.

$$A = 2\pi rh \tag{A-3}$$

If the definition of area is substituted into Eq. A-2, it becomes:

$$k = \frac{qB\mu}{2\pi rh}\frac{\partial r}{\partial \mathrm{p}} \tag{A-4}$$

Where $\alpha_1 = 2\pi$ for SI unit system, and $\alpha_1 = 0.007082$ for oilfield unit system (see Nomenclature).

$$k = \frac{qB\mu}{\alpha_1 rh}\frac{\partial r}{\partial \mathrm{p}} \tag{A-5}$$

We can call this k, as k_{eff}:

$$k_{eff} = \frac{qB\mu}{\alpha_1 rh}\frac{\partial r}{\partial \mathrm{p}} \tag{A-6}$$

And since the definition of relative permeability, k_r is known to be:

$$k_r = \frac{k_{eff}}{k} \tag{A-7}$$

Then Eq. A-6 becomes:

$$k_r = \frac{qB\mu}{\alpha_1 krh}\frac{\partial r}{\partial \mathrm{p}} \tag{A-8}$$

Re-arranging the equation to look better:

$$k_r = \frac{qB\mu}{\alpha_1 kh\, r}\frac{\partial r}{\partial \mathrm{p}} \tag{A-9}$$

This is the general equation used for any unit system. Next, specific changes are made which represent the equation that is being used in this thesis for the type of data that is available in oilfield unit system.

Mass rate is defined as the following:

$$m_T = \rho(q \cdot B) \tag{A-10}$$

Or in terms of flow rate, q:

$$q = \frac{m_T}{B\rho} \tag{A-11}$$

Eq. A-11 is substituted in Eq. A-9 and divided by 5.615 to convert bbl to ft^3 (see Conversion Factors Table). This is needed to keep the unit of rate, q, consistent. Eq. A-9 then becomes:

$$k_r = \frac{1}{5.615}\frac{m_T B\mu}{\alpha_1 kh\, B\rho\, r}\frac{\partial r}{\partial \mathrm{p}} \tag{A-12}$$

Formation volume factor, B, will cancel each other and re-arrange:

$$k_r = \frac{1}{5.615}\frac{m_T \mu}{\alpha_1 kh\, \rho\, r\left(\frac{\partial p}{\partial r}\right)} \tag{A-13}$$

For the gas phase flowing together with the liquid phase, we multiply Eq. A-13 with the fractional flow of the flowing gas:

$$k_{rg} = \frac{1}{5.615}\frac{m_T \mu_g (1-x)}{\alpha_1 kh\, \rho_g r\left(\frac{\partial p}{\partial r}\right)} \tag{A-14}$$

And for the condensate phase, we multiply Eq. A-13 with the fractional flow of the flowing liquid:

$$k_{ro} = \frac{1}{5.615}\frac{m_T \mu_o x}{\alpha_1 kh\, \rho_o r\left(\frac{\partial p}{\partial r}\right)} \tag{A-15}$$

Eq. A-14, and Eq. A-15 are then used to calculate the relative permeability of gas and oil, respectively.

Conversion Factors

Unit	Multiplied by Approximate Conversion Factor	Equals to Unit
1 Darcy =	x 1000	mD
1 Day =	x 86000	secs
1 bbl =	x 5.615	ft3
1 m3 =	x 6.29	bbl
1 bbl =	x 158987.3	cm3
1 ft =	x 30.48	cm
1 atm =	x 14.7	psi

Appendix B

Snapshot sample of the calculation of pressure and relative permeabilities versus radius for Case-3 (RC6)–Figures 4.19 & 5.21

Pressure	Pseudo Pressure	Pansystem			Mobility	Equiv. Time	Probe Radius	m(p)	<Pdew Pressure	ΔP/Δr	Vap Viscosity			
psia	m(p)E-6	Δt (h)	Δm(p)	Δm(p)'					4838.938				krg	kro
4980	535.615503	0.0096746	68.3885789	9.0048337	344.205768	9.67E-03	12.945	566.216694	5100.6738	5.82316928	0.04071684		0.494076452	0.27228889
5000	540.808244	0.0099386	68.6336702	9.00004856	344.177029	9.94E-03	13.120	566.461785	5101.6758	5.53255431	0.04074189		0.513544858	0.28213381
5020	545.95453	0.0102122	68.8779054	8.98458527	344.558278	1.02E-02	13.307	566.70602	5102.6743	5.54141045	0.04076686		0.505968123	0.27710492
5040	551.055542	0.0104882	69.1214312	8.98638249	344.279171	1.05E-02	13.480	566.949546	5103.6699	5.60246279	0.04079175		0.4944531	0.26995605
5060	556.105788	0.0107738	69.3641254	8.98173078	344.248142	1.08E-02	13.662	567.19224	5104.6621	5.48969315	0.04081655		0.498328255	0.27122743
5080	561.106267	0.0110594	69.6061103	8.97706131	344.218628	1.11E-02	13.841	567.434225	5105.6514	5.43198153	0.04084128		0.497525213	0.26995159
5100	566.051881	0.011357	69.8473614	8.97235155	344.191513	1.14E-02	14.026	567.675476	5106.6377	5.2690521	0.04086594		0.506597532	0.27402441
5120	570.943923	0.0116666	70.0879031	8.9675342	344.16936	1.17E-02	14.215	567.916018	5107.6211	5.19286152	0.04089053		0.507612378	0.2737262
5140	575.778181	0.0119762	70.3278577	8.96026022	344.242291	1.20E-02	14.404	568.155972	5108.6021	5.15822228	0.04091505		0.504747371	0.27134268
5160	580.550141	0.0122954	70.5669563	8.9547414	344.248837	1.23E-02	14.595	568.395071	5109.5796	4.94583022	0.04093949		0.519979164	0.27867196
5180	585.26136	0.012629	70.8054678	8.94052225	344.591148	1.26E-02	14.799	568.633582	5110.5547	4.90838623	0.04096387		0.51715801	0.27630948
5200	589.902729	0.0129602	71.0433678	8.93515964	344.593421	1.30E-02	14.991	568.871482	5111.5273	4.91705959	0.04098818		0.510033014	0.27166774
5220	594.466293	0.0133034	71.2807052	8.92382667	344.826968	1.33E-02	15.194	569.10882	5112.4976	4.84146303	0.04101244		0.511526341	0.27162943
5240	598.949683	0.0136586	71.5172844	8.92274082	344.665725	1.37E-02	15.392	569.345399	5113.4648	4.8857782	0.04103662		0.500786611	0.26511447
5260	603.346248	0.0140114	71.7534232	8.91726958	344.674482	1.40E-02	15.589	569.581538	5114.4302	4.78474562	0.04106075		0.50529557	0.2666854
5280	607.640881	0.0143906	71.9889506	8.91677056	344.491808	1.44E-02	15.795	569.817065	5115.3931	5.85872329	0.04108483		0.407640863	0.21448975
5288.503	609.431409	0.0147674	72.2238664	9.00413333	340.950118	1.48E-02	15.918	570.051981	5116.3535	5.75956914	0.04110884		0.411794807	0.21601647
5300	611.837176	0.0151562	72.4581953	8.99668238	341.033803	1.52E-02	16.128	570.28631	5117.3115	4.57403298	0.04113279		0.512191885	0.26786613
5320	616.023898	0.015545	72.6921816	8.98822358	341.156398	1.55E-02	16.336	570.520296	5118.2681	4.47977733	0.0411567		0.516718575	0.26941318
5340	620.209743	0.0159578	72.9254342	8.980304	341.259583	1.60E-02	16.554	570.753549	5119.2217	4.40624017	0.04118054		0.518848956	0.26970448
5360	624.390443	0.0163706	73.1578177	8.97276949	341.334444	1.64E-02	16.769	570.985932	5120.1738	4.37849776	0.04120608		0.515904946	0.2673356
5380	628.56578	0.016793	73.3873724	8.96038714	341.530632	1.68E-02	16.988	571.215487	5121.1235	4.37876384	0.04123932		0.50976979	0.2632145
5400	632.739984	0.0172274	73.6165888	8.95800357	341.346783	1.72E-02	17.202	571.444703	5122.0718	4.34937404	0.04127251		0.507406838	0.2610606
5420	636.913231	0.0176738	73.8452008	8.95038661	341.363482	1.77E-02	17.424	571.673315	5123.0176	4.260654	0.04130562		0.511947732	0.26245958
5440	641.085296	0.0181322	74.0734503	8.94595511	341.259524	1.81E-02	17.646	571.901565	5123.9619	4.12107248	0.04133867		0.523215779	0.26728235
5460	645.256157	0.0186026	74.3012406	8.93017434	341.59002	1.86E-02	17.882	572.129355	5124.9043	4.0441466	0.04137165		0.526713393	0.26811306
5480	649.421622	0.0190826	74.5285474	8.92273832	341.602925	1.91E-02	18.111	572.356662	5125.8447	4.15854619	0.04140456		0.506290816	0.25680265
5500	653.581676	0.0195746	74.7555158	8.92494016	341.247783	1.96E-02	18.334	572.58363	5126.7837	4.06307088	0.04143743		0.512465598	0.25901248
5520	657.740673	0.0200786	74.9820008	8.9132402	341.425506	2.01E-02	18.573	572.810115	5127.7207	3.88583917	0.04147022		0.529515726	0.26668159
5540	661.898395	0.0205922	75.2081474	8.8999622	341.665096	2.06E-02	18.816	573.036262	5128.6563	3.86360286	0.04150297		0.526272863	0.2641095
5560	666.054817	0.0211202	75.4337864	8.89152961	341.720113	2.11E-02	19.057	573.2619 01	5129.5898	3.88448639	0.04153564		0.517383439	0.25872971
5580	670.20992	0.0216578	75.6591111	8.88624933	341.65479	2.17E-02	19.296	573.487226	5130.522	3.85829116	0.04156827		0.515001719	0.25662781
5600	674.363681	0.0222074	75.8840492	8.87888679	341.670379	2.22E-02	19.540	573.712164	5131.4526	3.74851655	0.04160084		0.524041419	0.26020936
5620	678.51608	0.0227786	76.1086488	8.86942454	341.767705	2.28E-02	19.792	573.936763	5132.3818	3.71012494	0.04163336		0.523277273	0.25891196
5640	682.663019	0.0233498	76.33291	8.86117767	341.819169	2.33E-02	20.040	574.161025	5133.3096	3.71565516	0.04166584		0.516588768	0.25469994
5660	686.804486	0.023945	76.5567845	8.85677173	341.723343	2.39E-02	20.291	574.384899	5134.2358	3.60912861	0.04169825		0.525826627	0.25833967
5680	690.944548	0.0245522	76.7803206	8.84441903	341.935192	2.45E-02	20.553	574.608435	5135.1606	3.53903076	0.04173062		0.52997654	0.25946005
5700	695.083185	0.025181	77.00351 83	8.8385828	341.896189	2.52E-02	20.813	574.8331633	5136.084	3.5123682	0.04176294		0.527887963	0.25752632
5720	699.220376	0.0258218	77.2264501	8.82997612	341.965118	2.58E-02	21.078	575.054565	5137.0063	3.46999642	0.04179522		0.52817591	0.25675838

References

Afidick, D., Kaczorowski, N.J. & Bette, S., 1994. Production Performance of a Retrograde Gas Reservoir: A Case Study of the Arun Field. Presented at the *SPE Asia Pacific Oil and Gas Conference*. 7-10 November, Melbourne, Australia: Society of Petroleum Engineers.SPE-28749-MS http://dx.doi.org/10.2118/28749-MS.

Agarwal, R.G., 1980. A New Method To Account For Producing Time Effects When Drawdown Type Curves Are Used To Analyze Pressure Buildup And Other Test Data. Presented at the *SPE Annual Technical Conference and Exhibition*. Dallas, Texas: Society of Petroleum Engineers.SPE 9289 http://dx.doi.org/10.2118/9289-MS.

Al-Hussainy, R., Ramey, H.J. & Crawford, P.B., 1966. The Flow of Real Gases Through Porous Media. *Journal of Petroleum Technology*, 18(05), pp.624–636. http://dx.doi.org/10.2118/1243-A-PA.

Ali, J.K., McGauley, P.J. & Wilson, C.J., 1997. Experimental Studies and Modelling of Gas Condensate Flow Near the Wellbore. Presented at the *Latin American and Caribbean Petroleum Engineering Conference*. Society of Petroleum Engineers. http://dx.doi.org/10.2118/39053-MS.

Bang, V.S.S., Ayyalasomayajula, P.S., Kumar, V., et al., 2006. Relative Permeability of Gas/Condensate Fluids: A General Correlation. Presented at the *SPE Annual Technical Conference and Exhibition*. Society of Petroleum Engineers. http://dx.doi.org/10.2118/102741-MS.

Bardon, C. & Longeron, D.G., 1980. Influence of Very Low Interfacial Tensions

on Relative Permeability. *Society of Petroleum Engineers Journal*, 20(05), pp.391–401. http://dx.doi.org/10.2118/7609-PA.

Barnum, R.S., Brinkman, F.P., Richardson, T.W., et al., 1995. Gas Condensate Reservoir Behaviour: Productivity and Recovery Reduction Due to Condensation. Presented at the *SPE Annual Technical Conference and Exhibition*. Society of Petroleum Engineers. http://dx.doi.org/10.2118/30767-MS.

Becker, M.D., Zhang, M. & Ayala H, L.F., 2016. On the pressure-saturation path in infinite-acting unconventional liquid-rich gas reservoirs. *Journal of Natural Gas Science and Engineering*, 35, pp.97–113. http://dx.doi.org/10.1016/J.JNGSE.2016.08.007.

Behmanesh, H., Hamdi, H. & Clarkson, C.R., 2013. Production Data Analysis of Liquid Rich Shale Gas Condensate Reservoirs. *SPE Unconventional Resources Conference Canada*. http://dx.doi.org/10.2118/167160-MS.

Blom, S.M.P., Hagoort, J. & Soetekouw, D.P.N., 2000. Relative Permeability at Near-Critical Conditions. *SPE Journal*, 5(02), pp.172–181. http://dx.doi.org/10.2118/62874-PA.

Bourdet, D., 2002. *Well Test Analysis: The Use of Advanced Interpretation Models*, Elsevier.

Bourdet, D., Ayoub, J.A. & Pirard, Y.M., 1989. Use of Pressure Derivative in Well Test Interpretation. *SPE Formation Evaluation*, 4(02), pp.293–302. http://dx.doi.org/10.2118/12777-PA.

Briones, M., Zambrano, J.A. & Zerpa, C., 2002. Study of Gas-Condensate Well Productivity in Santa Barbara Field, Venezuela, by Well Test Analysis.

Presented at the *SPE Annual Technical Conference and Exhibition*. Society of Petroleum Engineers. http://dx.doi.org/10.2118/77538-MS.

Burdine, N.T., 1953. Relative Permeability Calculations From Pore Size Distribution Data. *Journal of Petroleum Technology*, 5(03), pp.71–78. http://dx.doi.org/10.2118/225-G.

Carvajal, G.A., Arreaza, E., Gonzalez, C., et al., 2007. The Effect of Positive Coupling and Negative Inertia on Deliverability of Gas Condensate Wells. Presented at the *EUROPEC/EAGE Conference and Exhibition*. Society of Petroleum Engineers. http://dx.doi.org/10.2118/107138-MS.

Chen, H.L., Wilson, S.D. & Monger-McClure, T.G., 1995. Determination of Relative Permeability and Recovery for North Sea Gas Condensate Reservoirs. Presented at the *SPE Annual Technical Conference and Exhibition*. Society of Petroleum Engineers. http://dx.doi.org/10.2118/30769-MS.

Chopra, A.K. & Carter, R.D., 1986. Proof of the Two-Phase Steady-State Theory for Flow Through Porous Media. *SPE Formation Evaluation*, 1(06), pp.603–608. http://dx.doi.org/10.2118/14472-PA.

Corbett, P.W.M., Geiger, S., Borges, L., et al., 2012. The Third Porosity System. *Petroleum Geoscience*, 18(1), pp.73–81. http://dx.doi.org/10.1144/1354-079311-010.

Corey, A.T., 1954. The Interrelation Between Gas and Oil Relative Permeabilities.

Corey, A.T. & Brooks, R.H., 1966. Properties of Porous Media Affecting Fluid Flow. *Journal of the Irrigation and Drainage Division*, 92(2), pp.61–90.

Coskuner, G., 1999. Performance Prediction In Gas Condensate Reservoirs. *Journal of Canadian Petroleum Technology*, 38(08). http://dx.doi.org/10.2118/99-08-DA.

Dandekar, A.Y., 2013. *Petroleum Reservoir Rock and Fluid Properties*, CRC Press.

Danesh, A., Henderson, G.D., Krinis, D., et al., 1988. Experimental Investigation of Retrograde Condensation in Porous Media at Reservoir Conditions. Presented at the *SPE Annual Technical Conference and Exhibition*. Society of Petroleum Engineers. http://dx.doi.org/10.2118/18316-MS.

Danesh, A., Khazam, M., Henderson, G.D., et al., 1994. Gas Condensate Recovery Studies. Presented at the *DTI Improved Oil Recovery and Research Dissemination Seminar*.

Danesh, A., 1998. *PVT and Phase Behaviour of Petroleum Reservoir Fluids*, Elsevier.

Danesh, A., Henderson, G.D. & Peden, J.M., 1991. Experimental Investigation of Critical Condensate Saturation and Its Dependence on Interstitial Water Saturation in Water-Wet Rocks. *SPE Reservoir Engineering*, 6(03), pp.336–342. http://dx.doi.org/10.2118/19695-PA.

Fan, L., Harris, B. & Jamaluddin, A., 2005. Understanding gas-condensate reservoirs. *Oilfield Review*, (Winter 2005/2006), pp.14–27.

Fetkovich, M.D., Guerrero, E.T., Fetkovich, M.J., et al., 1986. Oil and Gas Relative Permeabilities Determined From Rate-Time Performance Data. Presented at the *SPE Annual Technical Conference and Exhibition*. Society of Petroleum Engineers. http://dx.doi.org/10.2118/15431-MS.

Fevang, Ø. & Whitson, C.H., 1996. Modeling Gas-Condensate Well Deliverability. *SPE Reservoir Engineering*, 11(04), pp.221–230. http://dx.doi.org/10.2118/30714-PA.

Forchheimer, P., 1914. *Hydraulik*, Leipzik and Berlin: B. G. Teubner.

Fussell, D.D., 1973. Single-Well Performance Predictions for Gas Condensate Reservoirs. *Journal of Petroleum Technology*, 25(07), pp.860–870. http://dx.doi.org/10.2118/4072-PA.

Ghahri, P., Jamiolahmady, M. & Sohrabi, M., 2011. Gas Condensate Flow Around Deviated And Horizontal Wells. *Proceedings of SPE EUROPEC/EAGE Annual Conference and Exhibition*, (May), pp.23–26. http://dx.doi.org/10.2118/143577-MS.

Ghahri, P., Jamiolahmady, M. & Sohrabi, M., 2010. Impact of Velocity and Interfacial Tension on the Performance of Horizontal Wells in Gas Condensate Reservoirs. Presented at the *COMSOL*.

Gringarten, A.C., Bourdet, D.P., Landel, P.A., et al., 1979. A Comparison Between Different Skin And Wellbore Storage Type-Curves For Early-Time Transient Analysis. Presented at the *SPE Annual Technical Conference and Exhibition*. Society of Petroleum Engineers. http://dx.doi.org/10.2118/8205-MS.

Gringarten, A.C., Bozorgzadeh, M., Hashemi, A., et al., 2006. Well Test Analysis in Lean Gas Condensate Reservoirs: Theory and Practice. Presented at the *SPE Russian Oil and Gas Technical Conference and Exhibition*. Society of Petroleum Engineers. http://dx.doi.org/10.2118/100993-MS.

Henderson, G.D., Danesh, A., Al-Kharusi, B., et al., 2000. Generating reliable gas

condensate relative permeability data used to develop a correlation with capillary number. *Journal of Petroleum Science and Engineering*, 25(1), pp.79–91. http://dx.doi.org/10.1016/S0920-4105(00)00004-8.

Henderson, G.D., Danesh, A., Tehrani, D.H., et al., 1998. Measurement and Correlation of Gas Condensate Relative Permeability by the Steady-State Method. *SPE Reservoir Evaluation & Engineering*, 1(02), pp.134–140. http://dx.doi.org/10.2118/30770-PA.

Henderson, G.D., Danesh, A., Tehrani, D.H., et al., 1997. The Effect of Velocity and Interfacial Tension on Relative Permeability of Gas Condensate Fluids in the Wellbore Region. *Journal of Petroleum Science and Engineering*, 17(3–4), pp.265–273. http://dx.doi.org/10.1016/S0920-4105(96)00048-4.

Henderson, G.D., Danesh, A., Tehrani, D.H., et al., 2000. The Relative Significance of Positive Coupling and Inertial Effects on Gas Condensate Relative Permeabilities at High Velocity. Presented at the *SPE Annual Technical Conference and Exhibition*. Society of Petroleum Engineers. http://dx.doi.org/10.2118/62933-MS.

Henderson, G.D., Danesh, A. & Tehrani, D.H., 2001. Effect of Positive Rate Sensitivity and Inertia on Gas Condensate Permeability at High Velocity. *Petroleum Geoscience*, 7(1), pp.45–50. http://dx.doi.org/10.1144/petgeo.7.1.45.

Hernandez-G., H., Samaniego, F. & Camacho-V., R.G., 1993. Gas Condensate Well Testing Under the Influence of High-Velocity Flow. Presented at the *SPE Annual Technical Conference and Exhibition*. Society of Petroleum Engineers. http://dx.doi.org/10.2118/26666-MS.

Horner, D.R., 1951. Pressure Build-up in Wells.

Huerta Quinones, V.A., Lanchimba, A.F. & Porlles, J.W., 2012. Modeling Condensate Banking Phenomena in Lean Gas Condensate Reservoirs. Presented at the *SPE Latin America and Caribbean Petroleum Engineering Conference*. Society of Petroleum Engineers. http://dx.doi.org/10.2118/153388-MS.

Institute of Petroleum Engineering, 2018. Gas Condensate Recovery (GCR) Project.

International Energy Agency, 2018. *Global Energy & CO 2 Status Report*,

International Energy Agency, 2017. World Energy Outlook 2017.

Al Ismail, M. & Horne, R.N., 2010. Pressure Buildup Test Analysis of a Gas Condensate Well in the Middle East. Presented at the *SPE Annual Technical Conference and Exhibition*. Society of Petroleum Engineers. http://dx.doi.org/10.2118/134671-MS.

Jamiolahmady, M., Sohrabi, M., Ireland, S., et al., 2009. A generalized correlation for predicting gas–condensate relative permeability at near wellbore conditions. *Journal of Petroleum Science and Engineering*, 66(3), pp.98–110. http://dx.doi.org/10.1016/j.petrol.2009.02.001.

Jamiolahmady, M., Danesh, A., Tehrani, D.H., et al., 2000. A Mechanistic Model of Gas-Condensate Flow in Pores. *Transport in Porous Media*, 41(1), pp.17–46. http://dx.doi.org/10.1023/A:1006645515791.

Jamiolahmady, M., Danesh, A., Sohrabi, M., et al., 2007. Gas-Condensate Flow in Perforated Regions. *SPE Journal*, 12(01), pp.89–99. http://dx.doi.org/10.2118/94072-PA.

Jamiolahmady, M., Danesh, A. & Tehrani, D., 2003. Positive Effect of Flow

Velocity on Gas – Condensate Relative Permeability : Network Modelling and Comparison with Experimental Results. *Transport in Porous Media*, pp.159–183.

Jamiolahmady, M., Mahdiyar, H. & Sohrabi, M., 2010. High Velocity Flow in and Around Long Perforation Tunnels. *Transport in Porous Media*, 84(2), pp.457–469. http://dx.doi.org/10.1007/s11242-009-9514-y.

Johnson, C. & Jamiolahmady, M., 2015. Decline Curve Analysis for Low Permeability Gas Condensate Reservoirs - Effect of Fluid Richness, Inertia and Coupling. Presented at the *77th EAGE Conference & Exhibition 2015 – Workshops programme IFEMA Madrid, Spain*. pp. 1–4. http://dx.doi.org/10.3997/2214-4609.201413475.

Johnson, C. & Jamiolahmady, M., 2016. Decline Curve Analysis for Two-phase Flow in Tight Gas Condensate Reservoirs. Presented at the *78th EAGE Conference & Exhibition 2016 Vienna, Austria*.

Johnson, C. & Jamiolahmady, M., 2017. Production Data Analysis Using Type Curves in Gas Condensate Reservoirs - Impact of Degree of Undersaturation. Presented at the *EAGE Conference & Exhibition*.

Jones, J.R. & Raghavan, R., 1988. Interpretation of Flowing Well Response in Gas-Condensate Wells (includes associated papers 19014 and 19216). *SPE Formation Evaluation*, 3(03), pp.578–594. http://dx.doi.org/10.2118/14204-PA.

Jones, J.R., Vo, D.T. & Raghavan, R., 1989. Interpretation of Pressure-Buildup Responses in Gas-Condensate Wells. *SPE Formation Evaluation*, 4(01), pp.93–104. http://dx.doi.org/10.2118/15535-PA.

Kumar, V., Pope, G.A. & Sharma, M.M., 2006. Improving the Gas and Condensate Relative Permeability Using Chemical Treatments. Presented at the *SPE Gas Technology Symposium*. Society of Petroleum Engineers. http://dx.doi.org/10.2118/100529-MS.

Lee, J. (W. J. & Wattenbarger, R.A., 1996. *Gas Reservoir Engineering*, Henry L. Doherty Memorial Fund of AIME, Society of Petroleum Engineers.

Li, K. & Horne, R.N., 2006. Comparison of methods to calculate relative permeability from capillary pressure in consolidated water-wet porous media. *Water Resources Research*, 42(6), pp.1–9. http://dx.doi.org/10.1029/2005WR004482.

Li, Y., Hu, Y., Li, B., et al., 2009. Deliverability of wells in carbonate gas condensate reservoirs and the capillary number effect. *Petroleum Science*, 6(1), pp.51–56. http://dx.doi.org/10.1007/s12182-009-0009-9.

Mahdiyar, H. & Jamiolahmady, M., 2014. Optimization of hydraulic fracture geometry in gas condensate reservoirs. *Fuel*, 119, pp.27–37. http://dx.doi.org/10.1016/J.FUEL.2013.11.015.

Marhaendrajana, T., Kaczorowski, N.J. & Blasingame, T.A., 1999. Analysis and Interpretation of Well Test Performance at Arun Field, Indonesia. Presented at the *SPE Annual Technical Conference and Exhibition*. Society of Petroleum Engineers. http://dx.doi.org/10.2118/56487-MS.

Matthews, C.S., 1961. Analysis of Pressure Build- Up and Flow Test Data.

Mazloom, J., Kelly, R.T., Mahani, H., et al., 2005. A New Two Phase Pseudo Pressure Approach for the Interpretation of Gas Condensate Well Test in the Naturally Fracture Reservoir. Presented at the *SPE/EAGE Annual*

Conference.

Mokhtari, R., Varzandeh, F. & Rahimpour, M.R., 2013. Well productivity in an Iranian gas-condensate reservoir: A case study. *Journal of Natural Gas Science and Engineering*, 14, pp.66–76. http://dx.doi.org/10.1016/J.JNGSE.2013.05.006.

Mott, R.E., Cable, A.S. & Spearing, M.C., 2000. Measurements of Relative Permeabilities for Calculating Gas-Condensate Well Deliverability. *SPE Reservoir Evaluation & Engineering*, 3(06), pp.473–479. http://dx.doi.org/10.2118/68050-PA.

Muskat, M., 1938. *The Flow of Homogeneous Fluids Through Porous Media*,

O'Dell & Miller, 1967. Successfully Cycling a Low-Permeability, High-Yield Gas Condensate Reservoir. *Journal of Petroleum Technology*, 19(01), pp.41–47. http://dx.doi.org/10.2118/1495-PA.

Osorio, R., Stewart, G., Danesh, A., et al., 2005. Estimation of Long Term Gas Condensate Well Productivity Using Pressure Transient Data. Presented at the *SPE/EAGE Annual Conference*.

Palacio, J.C. & Blasingame, T.A., 1993. Decline-Curve Analysis Using Type Curves -- Analysis of Gas Well Production Data. Presented at the *SPE Joint Rocky Mountain Regional and Low Permeability Reservoirs Symposium, Denver, CO*.

Peaceman, D.W., 1978. Interpretation of Well-Block Pressures in Numerical Reservoir Simulation. Presented at the *SPE Annual Technical Conference and Exhibition*.

Purcell, W.R., 1949. Capillary Pressures - Their Measurement Using Mercury and

the Calculation of Permeability Therefrom. *Journal of Petroleum Technology*, 1(02), pp.39–48. http://dx.doi.org/10.2118/949039-G.

Raghavan, R., Chu, W.C. & Jones, J.R., 1999. Practical Considerations in the Analysis of Gas-Condensate Well Tests. *SPE Reservoir Evaluation & Engineering*, 2(03), pp.288–295. http://dx.doi.org/10.2118/56837-PA.

Raghavan, R. & Jones, J.R., 1996. Depletion Performance of Gas-Condensate Reservoirs. *Journal of Petroleum Technology*, 48(08), pp.725–731. http://dx.doi.org/10.2118/36352-JPT.

Rahimzadeh, A., Bazargan, M., Darvishi, R., et al., 2016. Condensate blockage study in gas condensate reservoir. *Journal of Natural Gas Science and Engineering*, 33, pp.634–643. http://dx.doi.org/10.1016/j.jngse.2016.05.048.

Ramey, H.J., 1992. Advances in Practical Well-Test Analysis. *Spe*.

Saleh, A.M. & Stewart, G., 1992. Interpretation of Gas Condensate Well Tests With Field Examples. Presented at the *67th Annual Technical Conference and Exhibition*.

Smits, R.M.M., van der Post, N. & al Shaidi, S.M., 2001. Accurate Prediction of Well Requirements in Gas Condensate Fields. Presented at the *SPE Middle East Oil Show*. Society of Petroleum Engineers. http://dx.doi.org/10.2118/68173-MS.

Stewart, G., 2011. *Well Test Design & Analysis*, PennWell Corporation.

Stewart, G. & Jamiolahmady, M., 2016. *Well Test Analysis G11WT*, Heriot-Watt University.

Taghizadeh Sarvestani, M., Rashidi, F. & Mousavi Dehghani, S.A., 2016. A

production data analysis model for gas/condensate reservoirs. *Journal of Petroleum Science and Engineering*, 141, pp.52–69. http://dx.doi.org/10.1016/J.PETROL.2016.01.016.

Terry, R.E. & Rogers, J.B., 2014. *Applied Petroleum Reservoir Engineering* 3rd ed., Prentice Hall.

Thomas, F.B., Bennion, D.B. & Andersen, G., 2009. Gas Condensate Reservoir Performance. *Journal of Canadian Petroleum Technology*, 48(07), pp.18–24. http://dx.doi.org/10.2118/09-07-18.

Thompson, L.G., Niu, J. & Reynolds, A.C., 1993. Well Testing for Gas Condensate Reservoirs. Presented at the *SPE Asia Pacific Oil and Gas Conference*. pp. 445–456.SPE-25371-MS

Wheaton, R.J. & Zhang, H.R., 2000. Condensate Banking Dynamics in Gas Condensate Fields: Compositional Changes and Condensate Accumulation Around Production Wells. Presented at the *SPE Annual Technical Conference and Exhibition*. Society of Petroleum Engineers. http://dx.doi.org/10.2118/62930-MS.

Whitson, C.H., Brulé, M.R. & Society of Petroleum Engineers of AIME., 2000. *Phase Behavior*, Henry L. Doherty Memorial Fund of AIME, Society of Petroleum Engineers.

Xu, S. & Lee, W.J., 1999. Two-Phase Well Test Analysis of Gas Condensate Reservoirs. Presented at the *SPE Annual Technical Conference and Exhibition*. Society of Petroleum Engineers. http://dx.doi.org/10.2118/56483-MS.